Separation and Purification Technology 376 (2025) 134157

Contents lists available at ScienceDirect

Separation and Purification Technology

journal homepage: www.elsevier.com/locate/seppur

MOF- & COF-integrated composite separators/membranes: innovations for sustainable and high-performance redox flow batteries

Iqra Shaheen [a], Wei-Hao Chiu [b], Shih-Hsuan Chen [a], Kun-Mu Lee [a,b,c,d,*]

[a] Department of Chemical and Materials Engineering, Chang Gung University, Taoyuan 33302, Taiwan
[b] Center for Sustainability and Energy Technologies, Chang Gung University, Taoyuan 33302, Taiwan
[c] College of Environment and Resources, Ming Chi University of Technology, New Taipei City 24301, Taiwan
[d] Division of Neonatology, Department of Pediatrics, Chang Gung Memorial Hospital, Linkou, Taoyuan 33305, Taiwan

ARTICLE INFO

Editor: S Deng

Keywords:
Covalent organic framework (COF)
Metal–organic framework (MOF)
Ion exchange membrane
MOF/COF separator/membrane
Ion permeability/selectivity
Non-ionic/ porous membranes
Pore channels

ABSTRACT

Advancements in membrane engineering are perceived as the primary concern for leading redox flow batteries (RFBs) to large-scale energy storage technology. Separators/Membranes that offer balanced trade-offs between permeability and selectivity, with controlled wettability, solvent resistance, and robustness, have emerged as promising materials for separation in RFBs. Traditional ion exchange membranes (IEMs), like Nafion, are prone to high permeability to active species and high costs, which limit their commercial viability and the overall performance of RFBs. Over the past decade, the development of non-ionic/porous membranes has garnered tremendous research attention due to their industrial-level properties, including porosity and flexibility, as well as advancements in fabrication methods and the principle of operation, such as size-based sieving effects. In this context, recent research has focused on intrinsic porous materials, such as covalent organic frameworks (COFs) and metal–organic frameworks (MOFs), for membrane fabrication due to their modifiability in pore channels, ion selectivity, and design flexibility. However, this technology is still in its early stages. This review summarizes recent advances in MOF/COF separators for RFBs, providing insights into existing challenges (e.g., desired pore size, processability, or scaling) and fundamental strategies (such as functional side chain modification) to achieve targeted functionality. Apart from the intrinsic features of frameworks, optimized structural properties (e.g., pore size) and performance evaluation are crucial to improve the quality of the separator, which are discussed in detail. This review provides valuable insights and can guide future research directions for designing next-generation MOF/COF separators in RFBs.

1. Introduction

With the desire for living standards and the continuous advancement of science and technology, people are paying more attention to health and environmental protection. Therefore, rapid and green energy production has attracted great interest. According to recent studies, global energy consumption is around 20,000 TWh annually, and each year it appreciates at a rate of 3 % [1]. Fossil fuels are always considered a primary source of electric energy, as two-thirds of electricity is produced by this category of non-renewable energy, which not only takes

Abbreviations: AEMs, Anion exchange membranes; AIEMs, Amphoteric ion exchange membranes; CEMs, Cation exchange membranes; CE, Coulombic efficiency; COF, Covalent Organic Framework; CuBTC, Copper (II)-benzene-1,3,5-tricarboxylate; Cys-COF, Zwitterionic Covalent Organic Framework; DS, Degree of sulfonation; EE, Energy efficiency; EVs, Electric vehicles; GO, Graphene oxide; HMN, Nanohybrid; HoP, Hot pressing method; HRFBs, Hybrid redox flow batteries; iCONs, Ionic Covalent Organic nanosheet; IEC, Ion exchange capacity; IEMs, Ion exchange membranes; IUPAC, International Union of Pure and Applied Chemistry; LIBs, Lithium-ion batteries; MOF, Metal Organic Framework; NARFBs, Non-aqueous redox flow batteries; NIMs, Non ion-selective membranes; PBI, Polybenzimidazole; pCTF, Piperazine Covalent Triazine Framework; PDA, Polydopamine; PE, Polyethylene; PEM, Proton exchange membrane; PFSA, Perfluorinated sulfonic acid; PMs, Porous membranes; PP, Polypropylene; PS, Pore size; PTFE, Polytetrafluoroethylene; PVDF, Polyvinylidene fluoride; PWA, Phosphotungstic acid; QPM, Quaternized poly (2,6-dimethylphenylene oxide); RFBs, Redox flow batteries; SCOFs, Sulfonated Covalent Organic Frameworks; SIBs, Sodium-ion batteries; SPEEK, Sulfonated poly ether ether ketone; SPI, Sulfonated polyimide; SR, Swelling ratio; UPS, Uninterruptible power supplies; VE, Voltage efficiency; VRFBs, Vanadium redox flow battery; WU, Water uptake.

* Corresponding author at: Department of Chemical and Materials Engineering, Chang Gung University, Taoyuan 33302, Taiwan.
E-mail address: kmlee@mail.cgu.edu.tw (K.-M. Lee).

https://doi.org/10.1016/j.seppur.2025.134157
Received 30 April 2025; Received in revised form 12 June 2025; Accepted 27 June 2025
Available online 29 June 2025
1383-5866/© 2025 Published by Elsevier B.V.

millions of years for geological production mechanisms but also is responsible for environmental degradation by releasing greenhouse gases [2]. The extraction and consumption of fossil fuels intensively contribute to the rise of carbon dioxide levels in the environment, which rapidly reached 280–401 ppm in December 2015 and play a pivotal and threatening role in global warming [3]. According to the Mauna Loa monthly mean data from the "NOAA Global Monitoring Laboratory" (Boulder, Colorado, USA), carbon dioxide levels exceeded 424 ppm in May 2023, so ultimately, fossil fuels are declared as the central cause of environmental pollution and climate changes are pushing the world towards the alarming situation and provoke the need of replacement of this kind of non-renewable energy sources with renewable energy sources [4]. Energy systems with zero carbon emissions, such as solar, wind, hydroelectricity, and geothermal energy, are promising candidates for minimizing environmental risks and have gained considerable attention from researchers over the past decade [5]. They utilize renewable sources to generate power for both domestic and industrial levels. Specific geographic parameters constrain geothermal energy and hydroelectricity, such as the need for tectonic activity, a high geothermal gradient, and hydrothermal resources for geothermal power plants. In contrast, consistent and abundant water availability, suitable topography, and geological stability are essential for hydroelectric power plants [6,7]. Therefore, in the future, solar energy and wind energy power plants will be efficient alternatives to electricity generation [8].

In the past decade, a significant number of power plant projects have been started all over the world. Still, they were mostly considered unreliable sources due to the limited time and suitable climate, leading them towards interrupted or fluctuating power production sources and highlighting the need for energy storage devices [9,10]. For energy storage and uninterrupted energy supply, Lead-acid batteries [11], Redox flow batteries (RFBs) [12], fuel cells [13], Lithium-ion batteries (LIBs) [14], and Sodium-ion batteries (SIBs) [15] are commonly used. All storage devices have limitations, with advantages and disadvantages based on their performance and demand. For example, lead-acid batteries are cost-effective and capable of providing high currents, but they have short lifespans and are heavy. In contrast, LIBs are lightweight but have flammability issues and are expensive [16]. In the era of electrification of industries based on manufacturing units and transportation, energy storage device performance must be evaluated on the basis of scalability, affordability, safety, durability, recyclability, and environmental friendliness; among all of them, RFBs are the most sustainable and efficient for large-scale applications based on their performance and design flexibility [17]. RFBs are a practical solution for storing fluctuating renewable energies on a large scale. It features a flexible design that enhances storage capacity to an industrial level [18]. In RFBs, electrical energy is generated by the chemical reactions of elements in an electrolyte solution [19]. RFBs utilize separate tanks for catholyte and anolyte, enabling independent scaling of energy and power. These electrolytes are pumped into an electrochemical cell (stack) that is divided by a membrane, where they undergo redox reactions, altering their oxidation states to provide electrons [20]. The number of cell stacks built into the RFB determines output power. On the other hand, the volume of electrolytes determines the discharging duration and energy capacity, as each cell can be designed separately, allowing for independent scaling of energy and power. Hence, increasing the number of cell stacks to increase output or increasing electrolyte volume by enlarging electrolytic tanks to extend the charging and discharging time with the same output makes it feasible for large-scale production [21,22]. The membrane, which functions as a separator for the half-cell compartments, is a key design parameter to evaluate RFB performance, as its chemical stability, ion exchange capacity, ionic selectivity, and proton conductivity directly affect battery efficiency [23]. The key role of this membrane is to maintain electro-neutrality by allowing protons to pass through while blocking the penetration of active species to prevent short circuits. Such a membrane also accounts for a significant portion of the overall system's manufacturing cost and considerably impacts performance. Therefore, a lower membrane cost is also preferable to decrease the total system costs [24]. RFBs also encounter a few drawbacks, including relatively lower energy density and higher manufacturing costs compared to conventional batteries. To address these problems of stable, affordable, and high-energy–density RFBs, various systems have been proposed, such as zinc-bromine system [25], vanadium-cerium system [26], zinc-polyiodide system [27], all vanadium redox flow system [28] and some metal-free systems, such as quinone-based system [29], viologen-based system [30], polysulfide/polyiodide systems [31,32], The configuration details of these RFBs are given in Table 1.

In the 1980 s, Skyllas-Kazacos and his co-workers designed the first vanadium redox flow battery (VRFB)[33]. The VRFBs have unique advantages due to a single active element, vanadium (V), with various oxidation states (V^{2+}, V^{3+}, V^{4+}, V^{5+}), a long cycle life (10 k–20 k cycles, >10 years), safety (non-flammable electrolyte), scalability, and environmentally friendliness, introduce it as the most commercially advanced type of RFB to date [34].

VRFBs primarily consist of two electrodes (carbon-based fibers, e.g., carbon felt or carbon cloth), a polymer-based membrane, two pumps, and two separate electrolyte tanks [35]. The selection of electrodes is guided by key criteria, including oxidation stability, design flexibility, high electrical conductivity, and economic feasibility. Carbon-based materials are considered the most favorable materials to date [36]. The redox pairs of active vanadium species, at valence states VO_2^+/VO^{2+} and V^{3+}/V^{2+}, function as the respective redox couples in the positive and negative electrolytes of the cell. The supporting electrolytes comprise acidic solutions, such as H_2SO_4, HCl, or their mixtures in varying concentration ratios, which affect the mechanical strength of the membrane and, consequently, the battery's performance. The membrane is designed to prevent vanadium ion crossover and short circuits while promoting proton (H^+) flow to complete the circuit [37]. The schematic structure and working flow of VRFBs are illustrated in Fig. 1.

During charging, tetravalent vanadium, found as VO^{2+} ions, is oxidized at the positive electrode to pentavalent vanadium as VO_2^+ ions. At the same time, trivalent ions V^{3+} are reduced to bivalent ions V^{2+} at the negative electrode. Protons and electrons flow across the membrane and the external circuit, respectively, to maintain the system's electroneutrality [38]. This mechanism occurs in reverse during the discharge mode of the VRFBs. The cathodic and anodic reactions can be represented as follows.

In charging mode:

Positive electrode: $VO^{2+} + H_2O \rightarrow VO_2^+ + 2H^+ + e^-$ $E^o_{Cathode} = 0.99\,V$

Negative electrode: $V^{3+} + e^- \rightarrow V^{2+}$ $E^o_{anode} = -0.26\,V$

In discharging mode:

Positive electrode: $VO_2^+ + 2H^+ + e^- \rightarrow VO^{2+} + H_2O$ $E^o_{Cathode} = 0.99\,V$

Negative electrode: $V^{2+} \rightarrow V^{3+} + e^-$ $E^o_{anode} = -0.26\,V$

Cell potential calculation:

$E_{cell} = E^o_{Cathod} - E^o_{anode}$

$E_{cell} = 0.99V - (-0.26V) = 1.25V$

Current research is primarily motivated by the development of high-performance membranes with high proton conductivity and low permeability to active species, as proton conductivity across a membrane significantly impacts the power of the cell or battery. The membrane's capacity to repel vanadium ion penetration is also a vital characteristic, as their crossover would trigger self-discharge and lower cell capacity, ultimately degrading device performance [39]. Electrochemical performance is also important to evaluate in terms of capacity retention rate, voltage efficiency (VE), energy efficiency (EE), and coulombic efficiency (CE) [40]. Water uptake and swelling ratio also need to be taken into account when considering the cost and

Table 1
Overview of different RFB systems proposed by various groups.

System	Redox Pairs	Electrode type	Membrane Type	Key Advantages	Challenges	Reference
Zinc-Bromine (Zn-Br_2)	Zn/Zn^{2+}, Br_2/Br^-	Carbon-electrodes	Sulfonated Teflon IEM (Nafion_125),microporous (Celgard_3400)	• High energy densitypolarization • Cost-effective • Low electrode • Thermal stability	• High self-discharge rate • Bromine crossover • Dendrite formation	[25]
Vanadium-Cerium (V-Ce)	V^{2+}/V^{3+}, Ce^{3+}/Ce^{4+}	Carbon Rods	Nylon (CEM)	• High efficiency cost materials • Improved stability • Abundant and low	• Ce solubility issues • Electrode degradation • Vanadium side reactions • Membrane cost • Membrane crossover	[26]
Zinc-Polyiodide (Zn-I_2)	Zn/Zn^{2+}, I^-/I_3^-	Graphite felts (GFs) electrodes	Nafion-based (CEM)	• High energy density • Ambipolar and • Bifunctional electrolyte • Reduced dendrite formation	• Iodide crossover • Membrane degradation • Conductivity issues • Scalability • Long-term stability	[27]
All-Vanadium Based	V^{2+}/V^{3+}, V^{4+}/V^{5+}	Carbon felt	Ion-selective or microporous membrane	• High energy efficiency • No cross-contamination • Long cycle life • Scalable capacity • Low self-discharge • Stable electrolyte • Predictable service life	• Membrane resistance • Electrolyte stability • Requires air-tight storage • Heat generation • Requiring cooling solutions • Cost considerations	[28]
Quinone-Based (Organic RFBs)	Benzoquinone/ hydroquinone	Carbon electrodes	Nafion −N212, − N115, −N117(CEM)	• Non-flammable in alkaline media • Non-corrosive • Metal-free • High solubility & stability	• Capacity fade • Quinone solubility • Side reactions • Trade-off issues • Optimization requirement	[29]
Viologen-Bromine (Neutral Aqueous RFBs)	Viologen/V°, Br_2/ Br^-	Carbon electrode (W.E) ,Graphite electrode (C.E)	Porous polyolefin membrane (CEM)	• High solubility • High efficiency • Stable performance • Prevention of Br crossover	• Bromine volatility • Crossover issue • Membrane optimization • Complexation issue	[30]
Polysulfide-Polyiodide (PS/I_2)	S_4^{2-}/S_2^{2-}, I^-/I_3^-	Graphite felt	Nafion and Charge-Reinforced Ion-Selective (CRIS)	• High energy density • Low cost • Self-discharge suppression • Membrane selectivity	• Crossover issues • Power density limitation • Membrane fouling • Electrolyte instability	[31,32]

performance of a membrane [41]. In general, an ideal membrane should provide a combination of low cost (initial investment and maintenance costs), high conductivity, high proton selectivity, and minimal vanadium ion permeation, along with both good mechanical and chemical stability [42].

In recent years, non-ionic porous membranes that depend on pore size screening have gained significant interest in the field of RFBs due to their simplicity, low cost, and mechanical stability [85]. Most commercial membranes are made of polymeric materials due to their excellent manufacturability into viable membrane structures and the variety of polymers. However, polymers offer some limitations due to their bad thermal and chemical strength, low selectivity, and durability. However, inorganic membranes exhibit higher stability and porosity, but the available range of pore sizes (PS) is restricted, offering small surface areas [43]. As separator membranes, the porosity of the material is a key factor when exploring new nanostructured materials for advanced functional membranes [44]. Therefore, covalent organic frameworks (COFs) and metal–organic frameworks (MOFs) are introduced as the most advanced materials to prepare membranes [45,46]. They exhibit considerable potential for their application as membranes in RFBs, attributable to their modifiability in pore channels, ion selectivity, and design flexibility. However, comprehensive and critical analyses focusing on the use of COF and MOF materials for advancement in membrane technology are still lacking. Therefore, this article is a mainly summary of recent research about MOF/COF-based materials to serve as proposed ideal candidates (membranes) in RFBs. In the first section, we discuss parameters for optimizing membranes in detail, followed by a discussion on existing COF and MOF-based membranes. We also analyzed the current challenges and opportunities that lie ahead in this area for practical implementation, with a vision to creating a roadmap for future research endeavors.

2. Evaluation criteria of membrane

In RFBs, the membrane properties directly affect the performance, efficiency, and strength of the battery, making it the backbone of the battery system [47]. This not only facilitates energy conversion and maintains electrical circuit continuity through proton transport but also prevents short circuits by controlling the cross-contamination of active species (vanadium ions) between the half-cells [48]. This dual function is critical to maintain; however, for the energy conversion efficiency and capacity retention of RFBs, the optimal performance of membranes is essential and requires a standard evaluation of critical design parameters along with systematic characterization [49]. The schematic of membrane evaluation criteria for a VRFB (a type of RFB) is shown in Fig. 2.

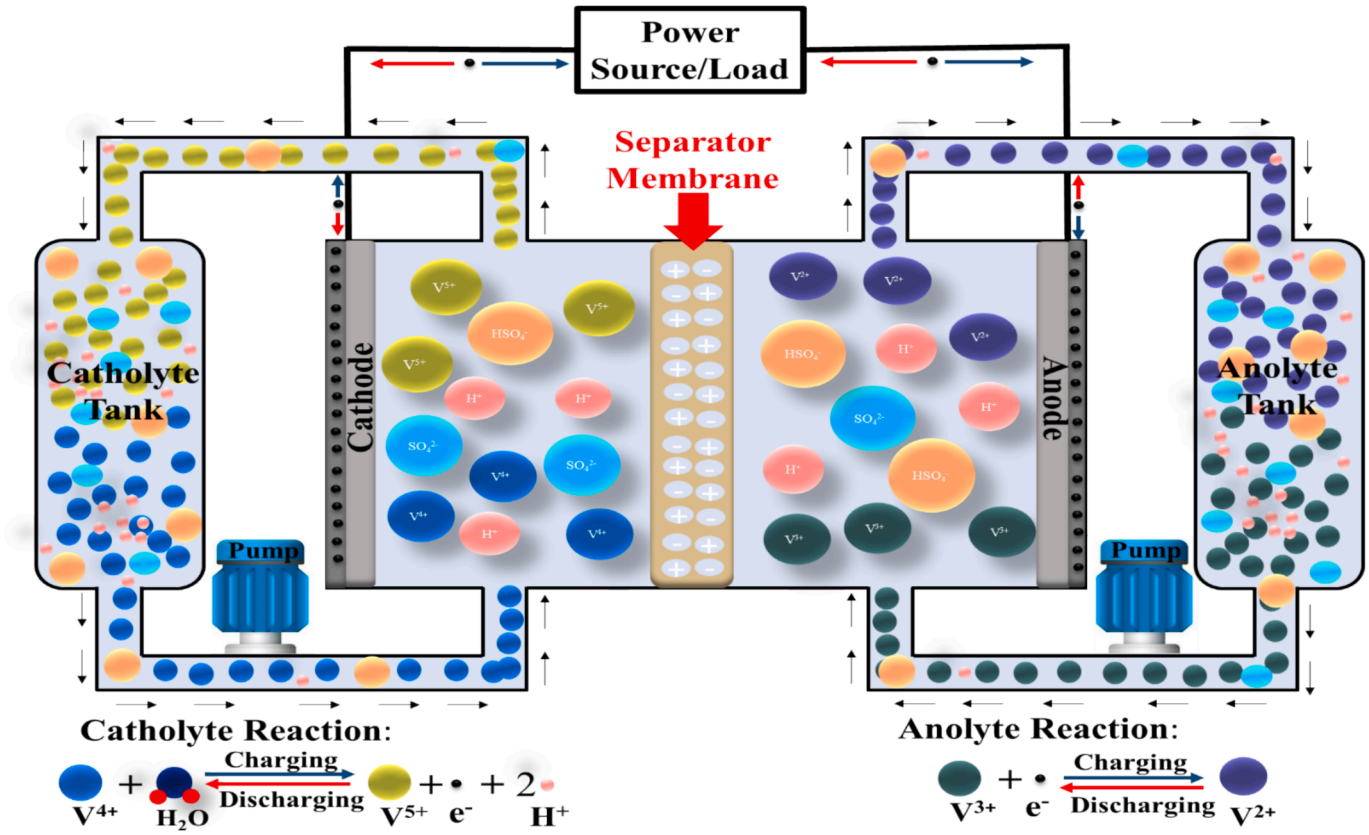

Fig. 1. The schematic structure and working flow of VRFBs.

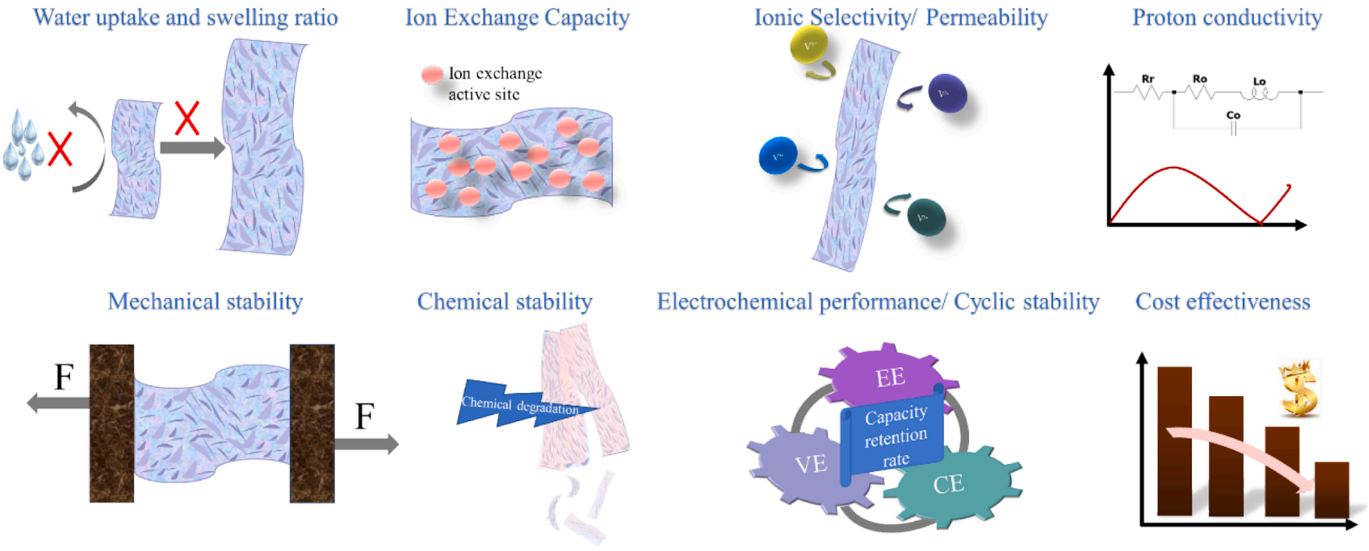

Fig. 2. Schematic of evaluation criteria of membranes for VRFBs.

After evaluating the standard criteria, high-performance redox flow batteries must include several key factors: high ionic conductivity, minimal crossover of active species, low solvent uptake, strong mechanical and chemical stability, and economic feasibility for large-scale implementation [50,51]. This section summarizes the key indicators and testing methods of the membrane.

2.1. Water uptake, swelling ratio, and water transport measurements

To ensure the resilience of membranes in electrolytes, it is essential to consider their hydration behavior by estimating the water uptake (WU) and swelling ratio (SR). This behavior acts as an ion-selective barrier, and the preference for a hydrophilic or hydrophobic membrane depends on the type of RFBs, their operating environment, and specific requirements [52]. WU and SR can be calculated by the percentage increase in weight or volume and the linear dimension (e.g., thickness or length) of the membrane, respectively, when immersed in the electrolyte during operational mode [53]. The low SR of a membrane offers advantages in terms of better mechanical and dimensional stability in aqueous solutions, but at the expense of ionic conductivity and

an increase in the internal resistance of the battery [54]. A high SR can facilitate hydrate ion-conducting pathways, enhancing ionic conductivity. However, excessive water absorption can cause membrane deformation or disintegration due to excessive expansion, decreasing efficiency through high penetration of active species, and compromising ion selectivity and framework stability over time [55]. An optimal SR must balance ionic conductivity, mechanical stability, and selectivity. Pretreatment strategies (e.g., pre-swelling in an alkaline medium or introducing new materials, such as cross-linked membranes) can optimize membrane properties, balance conductivity, and swelling to mitigate capacity degradation and maintain dimensional stability [56,57]. These factors can be calculated by using the following equations.

$$Wateruptake(WU) = \frac{W_{wet} - W_{dry}}{W_{dry}} \times 100\% (1)$$

$$Swellingratio(SR) = \frac{L_{wet} - L_{dry}}{L_{dry}} \times 100\% (2)$$

where W_{wet} and L_{wet} represent the weight and length of the wet membranes, respectively, while W_{dry} and L_{dry} denote the corresponding parameters of the dry membranes. The mechanism of water transport in the membrane can be explored by using the method proposed in [58]. The schematic for testing the water transport VRFB membrane is illustrated in Fig. 3. A test cell consists of two half-cells separated by a tight testing membrane. The half-cells were filled with catholyte (1.5 mol/L V^{4+}/V^{5+} + 3.0 mol/L H_2SO_4) and anolyte (1.5 mol/L V^{2+}/V^{3+} + 3.0 mol/L H_2SO_4) solutions at a 50 % state of charge (SOC). A transparent tube (with a calibration bar) is connected to each half-cell to measure any changes in the electrolyte. The volume of water transported through the membrane is determined by the change in electrolyte level (same initial level halfway up the tubes) after a specific duration.

2.2. Ion exchange capacity (IEC) of membranes

To maintain voltage efficiency during the charging and discharging phases, the passage of charge carriers through the membrane is essential, as it reduces ohmic and energy losses to ensure overall battery functionality. However, there is also the possibility of an undesired exchange of active species, such as V^{n+} [59]. IEC is a quantitative measurement of the charged nature attributed to the incorporation of functional groups within the membrane's structure. These functional groups can regulate the membrane potential to facilitate ion transfer with the surrounding electrolyte [60]. Therefore, it is important to optimize or quantify the IEC value to control the trade-off between proton conductivity and the crossover of active species through the membrane. A low IEC means fewer proton-conducting sites, reducing proton conductivity and increasing ohmic resistance, which raises ohmic losses and decreases voltage efficiency (VE). However, low IEC membranes generally show better mechanical stability and restrict vanadium ion crossover effectively. Conversely, a high IEC increases ion-exchange sites, enhancing proton conductivity and reducing ohmic resistance, which lowers losses and improves voltage efficiency. However, excessively high IEC may cause membrane swelling, reduce mechanical strength, and raise vanadium ion permeability if not controlled properly. Essentially, IEC depends on the availability of functional groups and helps in estimating the current densities that the membrane can sustain. IEC is defined as the ratio of the number-of moles of exchangeable ions to the dry weight of the membrane [61]. The IEC value of membranes can be practically calculated through the back-titration method [62,63] using the following equation 3.

$$IEC\left(\frac{mole}{g}\right) = \frac{M_{titrant} \times V_{titrant}}{W_{dry}} (3)$$

where $M_{titrant}$ and $V_{titrant}$ denote the molarity and volume of the titrant solution used, respectively, the evaluation of IEC and titrant depends on the ion exchange membrane. For cation exchange membranes (CEMs), a basic titrant (e.g., sodium carbonate (Na_2CO_3) or sodium hydroxide (NaOH)) is commonly used after replacing the proton (H^+) with another cation [64]. In comparison, anion exchange membranes (AEMs) first use acid (hydrochloric acid (HCl) or nitric acid (HNO_3)) to displace hydroxide ions (OH^-) with other anions. After that, KOH is used to determine the IEC [65].

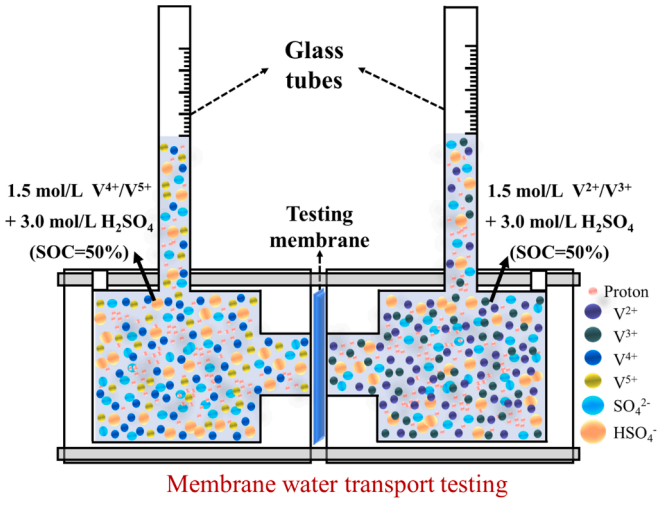

Fig. 3. Schematic of water transport testing proposed by Mohammadi et al.

2.3. Ionic Selectivity/ permeability

A membrane's ability to provide high ionic selectivity and optimize permeability is crucial for battery performance. Generally, it focuses on how easily or at what rate desired ions can diffuse through the membrane per unit area while blocking undesired ions based on their charge nature and size. During the operation of redox flow batteries, self-discharge and capacity fade occur due to the establishment of osmotic pressure and the electric field, which facilitates the diffusion of active species across ion-selective membranes [66,67]. High ion selectivity is highly desirable, particularly for estimating the lifespan in asymmetric RFBs, such as alkaline zinc-iron [68], polysulfide-based [32,69], and organic-based RFB systems [70]. In contrast, low ion selectivity significantly affects the long-term operation of the battery due to the accumulation of undesired ions (with low diffusivity) at the electrolyte-membrane interface, while some ions (with high diffusivity) block pores or channels. This phenomenon, known as membrane fouling, ultimately leads to energy losses due to an increase in the internal resistance of the battery. For example, in VRFBs, the Nafion membrane faces low ion selectivity caused by fouling, as trivalent (V^{3+}) and pentavalent (VO_2^+) vanadium ions deposit on the electrolyte-membrane interface because of their low diffusivity. In contrast, bivalent (V^{2+}) and tetravalent (VO^{2+}) vanadium ions enter the channel due to their high diffusivity and accumulate within it [59].

Membrane ionic permeability can be calculated using various methods, typically involving two tanks separated by a membrane resembling an H-shaped diffusive cell [71,72]. This method quantifies the diffusion concentration of active ions based on UV–vis absorption results measured through UV–visible spectroscopy. In the initial step, osmotic pressure is maintained across the membrane by filling the first tank with a vanadyl sulfate solution ($VOSO_4$) and the second tank with a magnesium sulfate solution ($MgSO_4$), both at the same molar concentration. Additionally, continuous magnetic stirring is required on both sides during testing to avoid uneven ion distribution or ion accumulation on the membrane [73]. Typically, the ion permeability of the membrane is assessed by the concentration gradient of tetravalent vanadium ions (VO^{2+}). Initially, there are no VO^{2+} ions on the $MgSO_4$ side; however, over time, they diffuse through the membrane and can be detected in the $MgSO_4$ solution (second tank). The migration rate of VO^{2+} ions from the first tank to the second tank helps to assess the quantitative reliability of the membrane using a UV–visible spectrophotometry technique. Generally, the ion permeability can be calculated using the following equation [74,75]

$P = \frac{L \times V}{S \times (C_O - C_t)} \frac{\partial C_t}{\partial t}$(4)where A and L are membrane dimensional parameters, representing the effective area and thickness of the membrane, respectively, V represents the volume of the second tank solution ($MgSO_4$), while C_0 and C_t are the initial concentration (in the $VOSO_4$ side) and concentration at any time t (in the $MgSO_4$ side) of VO^{2+} ions, respectively. The $\frac{\partial C_t}{\partial t}$ term is temporal concentration change, defined as the rate of change of VO^{2+} ion concentration in the $MgSO_4$ solution tank. The pictorial illustration of an H-type osmotic cell for measuring ionic selectivity/ permeability is shown in Fig. 4.

2.4. Proton conductivity

Innovation in proton conductivity is a critical frontier in the energy sector, as it directly influences voltage losses and energy efficiency in RFBs [76,77]. During the operational process of RFBs, protons migrate through the membrane via two mechanisms that may occur concurrently or individually [78]. The first mechanism is the Vehicle mechanism, in which proton diffusion depends on the proton-rich solvent (e.g., water molecules). These protons are physically transported along or in the form of hydrated ion clusters (H_3O^+ or other protonated species). The second mechanism is the Grotthuss mechanism, which involves protons "hopping" between water molecules and relies on the continuous formation and breaking of the hydrogen bonding network for proton transfer without any bulk ion movements [79]. The schematic representations of both mechanisms are shown in Fig. 5(a) and 5(b). The availability of water and the behavior of membrane hydration are important to both mechanisms and, ultimately, to proton conduction.

The membrane conductivity is typically determined using a specially designed conductivity cell, which consists of two chambers filled with identical electrolyte solutions, separated by a test membrane [80]. For a more realistic evaluation, it is recommended to utilize the same electrolyte composition and cell configuration as those employed in conventional RFBs [81,82]. DC resistances (with and without the test membrane) can be measured using traditional electronic multimeters or electrochemical impedance spectroscopy (EIS) [83,84]. Proton conductivity (σ) can be calculated using equation 5 below [85].

$\sigma = \frac{L}{A.(R_1 - R_2)}$(5)where A and L are membrane dimensions, representing the effective area and thickness of the membrane respectively, the term ($R_1 - R_2$) denoted for the specific resistance contributed by the membrane to the entire conductivity cell system (intrinsic resistance), as R_1 and R_2 represent the overall system resistances with and without the membrane respectively.

Proton conductivity is directly related to voltage and energy efficiency when evaluating the overall performance of RFBs. High proton conductivity minimizes ion transport resistance, thereby reducing energy losses by lowering the system's internal resistance, which leads to improvements in both voltage and energy efficiency [86,87]. Conversely, low proton conductivity can regulate reaction rates, especially under conditions of high current density, by restricting proton transport. This limitation may decrease the battery's power output, but it simultaneously improves overall cell stability by controlling undesired side reactions [88]. Therefore, selecting a membrane with suitable proton conductivity is essential to minimize ohmic losses and enhance power density in RFBs.

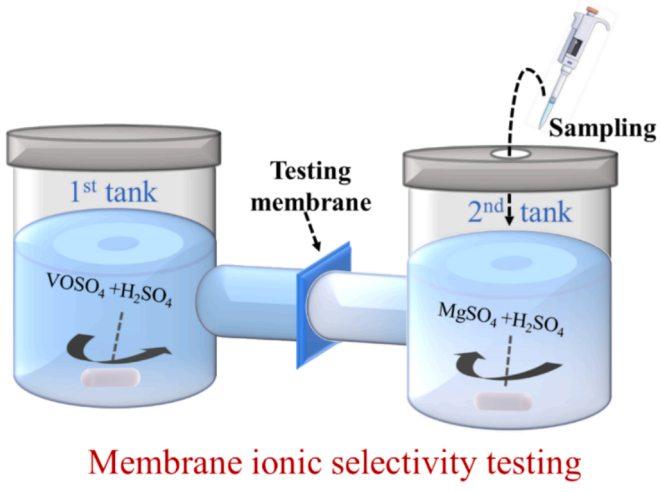

Fig. 4. Schematic illustration of H-type osmotic cell for measuring ion selectivity/ permeability.

2.5. Mechanical stability

Membrane strength, or sustainability against fluctuating internal battery pressure arising from thermal expansion, chemical reactions, electrolyte flow, etc., is referred to as mechanical stability. The excellent mechanical strength of a membrane is imperative for the long-term operation and durability of batteries, particularly in solid mixed redox flow battery systems (solid mixed-RFBs) [89]. In zinc-based hybrid redox flow batteries (HRFBs), sufficient blockage of zinc dendrites is essential to overcome the risk of short circuits and battery failure, which requires adequate mechanical stability of the membrane [55,90]. However, brittle or improperly molded membranes frequently suffer from breakage and mechanical failure as they endure various compressive forces or stresses exerted by other encapsulated components (e.g., electrodes) during the cell or battery assembly process.

The mechanical characteristics are generally evaluated using tensile testing machines to determine the elastic modulus and tensile strength of the membrane, which provides its dimensional stability against applied tensile stress. For the more realistic evaluation of Nafion membrane tensile strength, multiple tests are conducted on both wet and dry samples under different conditions [91,92]. Tensile strength (T) is calculated using the following equation 6 [93]

$T = \frac{F_{max}}{W \times L}$(6)where F_{max} Correspond to the maximum force or tensile stress applied to the testing sample. W and L represent the membrane dimensions, the width and thickness of the testing sample, respectively. High tensile strength is crucial to ensure the membrane can withstand and meet operational standards. Notably, several factors, including fabrication methods, solvent selection, processing conditions, and drying temperature, can significantly diversify tensile strength and optimize the membrane's mechanical behavior [94].

2.6. Chemical stability

Since RFBs operate in strong acidic or alkaline mediums, their internal structural components are immersed in highly corrosive oxidizing and reducing agents, which can potentially cause side chemical reactions inside the cell [95,96]. As membranes also have direct interactions with a degrading environment that requires long-term stability and functionality, they must exhibit exceptional chemical stability. A membrane with insufficient sustainability may suffer structural damage (such as breakage) from the surrounding medium, which can lead to direct contact between the anolyte and catholyte, resulting in battery cell failure due to a short circuit [97]. Major factors related to membrane withstand in chemically degradable environments, such as stable molecular design/structures, resilience to acidic and alkaline medium, chemical-water resistance, mechanical and thermal durability, and an optimal ion exchange capacity, are also essential [70]. The chemical stability of a membrane is primarily evaluated using the ex-situ method, where it is soaked in an oxidizing reagent, such as an acid solution enriched with VO_2^+ ions (at a known concentration of active species), for a specific duration. During this process, it undergoes a transition in oxidation state, resulting in a noticeable color change. After prolonged immersion, its structural integrity, along with any significant

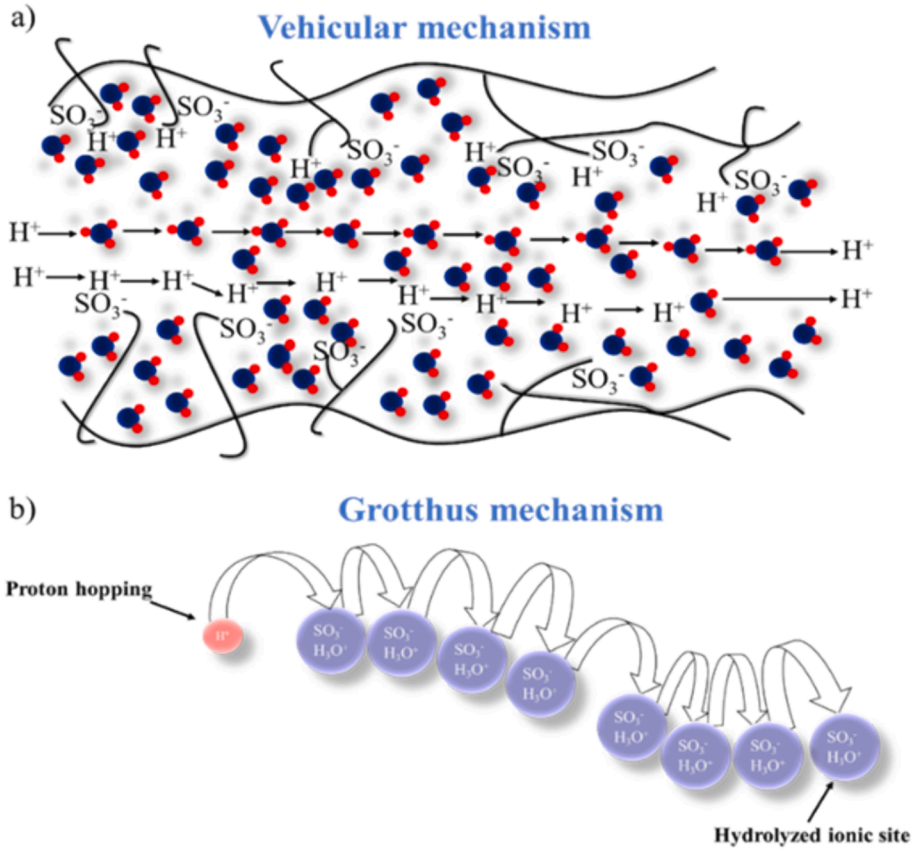

Fig. 5. Schematic representation of proton conduction mechanism through the separator.

compositional or color variations and ion concentrations, helps in assessing its chemical durability [98,99].

2.7. Electrochemical performance/ cyclic stability

The cell efficiency of RFBs is primarily assessed by their electrochemical performance, including charge–discharge capacity and voltage profile [100]. Coulombic efficiency (CE), voltage efficiency (VE), and energy efficiency (EE) are key metrics for evaluating the electrochemical behavior of batteries, particularly in rechargeable batteries. An ideal membrane should offer high and stable charge–discharge capacity, low charging voltage but high discharging voltage, and maximum energy efficiency with minimal losses [101].

Efficiency refers to the percentage of an input that is converted into output. CE is the fraction of usable output charge ($Q_{discharge}$) relative to the total input charge (Q_{charge}). It quantifies how effectively a battery can utilize charges (stored during the charge cycle) during discharge, reflecting the membrane's ability to block the crossover of active species [102]. CE decreases directly affect battery capacity due to side reactions triggered by the exchange of active species (such as V^{n+}), through the membrane. [103]. It can be calculated by following the equation

$$CE = \frac{Q_{discharge}}{Q_{charge}} \times 100\% \quad (7)$$

VE is the average fraction of the output voltage ($V^{(avg)}_{discharge}$) relative to the total input voltage ($V^{(avg)}_{charge}$). It quantifies how effectively a battery can convert input voltage to output voltage during the discharging cycle, reflecting its internal resistance and the membrane's ability to conduct ions [104]. It evaluates overpotential losses during charge–discharge phases, which are directly influenced by the membrane's ion conductivity, electrolyte composition, and the battery's internal resistance [105]. It can be calculated by following the equation.

$$VE = \frac{V^{(avg)}_{discharge}}{V^{(avg)}_{charge}} \times 100\% \quad (8)$$

EE in the battery can be expressed as the product of CE and VE, as shown below.

$$EE = CE \times VE \quad (9)$$

EE is comparably higher at lower current densities due to reduced overall losses (ohmic losses and overpotential) but declines as current density increases [80]. Losses in a battery soar at higher current density conditions and significantly impact its cyclic stability, which is the biggest challenge for its practical application. Therefore, it is essential to monitor self-discharge and other losses of a battery through the aforementioned rate capability tests (CE, VE, and EE) for a more accurate evaluation of the battery [106]

2.8. Cost-effectiveness

RFBs are getting attention for their cost-effectiveness and large-scale implementation, particularly in renewable energy storage. Cost dynamics are influenced by electrolyte cost, stack cost (the physical structure of the battery), and electrolyte exchange cost (the cost of battery maintenance) [107]. The membrane consumes a handsome fraction of the overall system's manufacturing cost [108]. For example, the cost of the ion-selective membrane for VRFB is estimated to be around 20 % (> USD $ 200/kWh) of the capital cost [109]. In the iron-chromium redox flow battery (Fe-Cr RFB), the membrane cost is estimated to be 38 % of the overall system cost [110]. Thus, a lower membrane cost is preferable to reduce the total cost of the RFB system; therefore, optimizing cost-effective and sustainable ion-selective membranes is essential for broader implementation [111,112]. Minke et al. claimed that the price of widely used Nafion-117 would not drop below $ 62 m^{-2}, given that the estimated costs for input materials and production are $ 35 m^{-2} and $ 27 m^{-2}, respectively. Therefore, considering

additional operational costs and potential profits, the estimated price for Nafion-117 ranges from $500 to $ 1000 m^{-2} [113]. These findings highlight the significance of utilizing more affordable materials for RFB membranes, potentially enhancing cost-effectiveness. Emerging organic frameworks appear less costly and widely accessible and represent promising alternatives for improving or replacing Nafion in the future.

3. Classification of membranes in RFBs

Over the past fifty years, various membranes/separators have garnered significant attention in advancing RFBs, especially in facilitating their transition from the laboratory to industry [114]. The RFB membrane is also referred to as a separator because of its functional nature, as it prevents the mixing of electrolyte solutions and thus controls the reactions between the cell compartments [115]. The development of preparation technology and the manufacturing of optimized membranes used in RFBs for optimal operation is an ongoing research area. Various groups propose different membranes for specific applications across diverse operating modes, such as energy-efficient operation, high current densities, or low self-discharge operation [116]. These modes primarily depend on the chemical and mechanical properties of the membrane and can be controlled by modifying the material's structure or tuning its morphology. Separator membranes can be classified based on membrane structure design (ion-exchange membranes (IEMs) [117–120], non ion-selective membranes/porous membranes (NIMs/PMs) [121–126]), membrane material type (fluorinated polymers e.g., Nafion [119]; hydrocarbon-based polymers, e.g., sulfonated poly(ether ether ketone)(SPEEK)) [127]; inorganic/composite membranes e.g., zirconium phosphate $Zr(HPO_4)_2$ [128]), or membrane purpose/functionality (proton conducting [129], anion conducting [130], or selective for specific chemistries [131]) in RFBs.

3.1. Ion exchange membranes (IEMs)

IEMs are widely used membranes in RFBs due to their unique selectivity feature, which permits the flow of specific ions while blocking other species through the presence of charged groups (either cation or anion-selective) [117]. Their charged nature facilitates the transport of ions while repelling co-ions, thereby maintaining charge balance and preventing electrolyte crossover [132]. We studied some reported AEMs to evaluate their performance and summarized them in Table 2. Based on the type of charged ion selectivity, IEMs for RFBs can be further classified into cation exchange membranes (CEMs), anion exchange membranes (AEMs), and amphoteric ion exchange membranes (AIEMs). A schematic of the ion exchange process through different IEMs in VRFB is shown in Fig. 6.

3.1.1. Cation exchange membranes (CEMs)

CEMs only permit the flow of positively charged ions, while repelling negatively charged ions, as they contain functional groups with a negative charge, such as sulfonate ($-SO_3^-$), carboxylate ($-COO^-$), and phosphonate ($-PO_3^-$), which dissociate H^+ [2,133]. Proton transport in

Table 2
A brief overview of the performance evaluation of different CEMs, AEMs. and AIEMs.

Year	Membrane Name	Water Uptake/ Swelling Ratio (%)	Proton Conductivity (S cm^{-1})	Ion Permeability (cm^2 min^{-1})	Ion Selectivity (S min cm^{-3})	Current Density ($mAcm^{-2}$)	EE/CE/VE (%)	Reference
CEM								
2014	SPEEK/GO@ PTFE	41.6/11.1	0.0146	7.6×10^{-7}	1.92×10^4	80	84/96.9/ 86.7	[147]
2015	SPEEK/MWCNTs-OH	–/-	0.010	3.2×10^{-7}	–	60	80/99.4/-	[148]
2018	SPAEK/$Ce_2Zr_2O_7$-2 %	52/6.2	0.084	1.27×10^{-5}	67.4×10^6	40	82.1/99.3/ 82.6	[149]
2018	SPEEK/PANi-GO-2	23.4/6.3	0.025	15×10^{-7}	1.8×10^4	30	81.7/98.5/ 82	[150]
2020	trPTFE/SP50	38/11	0.047	4.6×10^{-7}	–	80	77/96.5/80	[151]
2022	SPEEK/FCB-3	18.52/9.84	–	0.8×10^{-7}	1.185×10^6	120	83.46/ 99.49/-	[152]
2022	SC-bSPI-14	25.7 /15.1	0.00278	1×10^{-7}	2.78×10^5	140	82.9/97.6/ 72	[153]
2022	S/O-bPn-1.5 %	43.7/20.3	0.000053	1.56×10^{-7}	3.41×10^5	100	88/99/89	[154]
AEM								
2017	CAPSU-2.5	60/11.4	–	0.272×10^{-7}	–	50	86/100/86	[155]
2019	HPSf-Im-CD30%	25.5/7.5	0.100	–	23.04×10^4	120	79/98/80	[156]
2019	C6QPSF	10/-	0.017	24×10^{-7}	3.5×10^5	120	87/98.5/85	[157]
2019	QPPP-2	22/33	0.006	2.12×10^{-4}	–	80	86/99/87	[158]
2022	PCrPI-10	24.7/14.8	–	–	–	100	80/99.6	[159]
2022	PTP-QA	4/14	0.017	1.9×10^{-5}	2.6×10^5	100	90/99/90	[160]
2022	CMVI-C3	27.1/21.7	0.0081	1.97×10^{-7}	68×10^4	120	78.2/98.8/ 80.5	[161]
AIEM								
2009	DMAEMA-St/PVDF-26.1 %	<30/-	0.046	0.7×10^{-7}	–	–	–/-/-	[162]
2014	SPEEK/PEI (S/P-3)	32.9/16.9	0.073	2.868×10^{-6}	–	50	86.9/97.7/ 88.9	[163]
2015	SPI/PEI-rGO-2	44.2/7.1	0.0062	11×10^{-7}	0.4×10^4	40	75.6/95/-	[164]
2015	S/Q-15	39.97/-	0.04737	1.30×10^{-7}	36.35×10^4	50	88.45/96.1/ 92.04	[165]
2017	S/GO-NH_2-2	29.59/-	0.038	2.04×10^{-7}	19.14×10^4	50	89.5/97.2/ 92.1	[166]
2018	SPEEK-PBI-(15 %)	43.63/15.74	–	–	–	80	89.8/98.5/ 91.1	[167]
2018	Nafion-g-PSSA	26.38/7.18	0.0638	13.6×10^{-7}	–	40	89.6/96.2/ 94.0	[168]

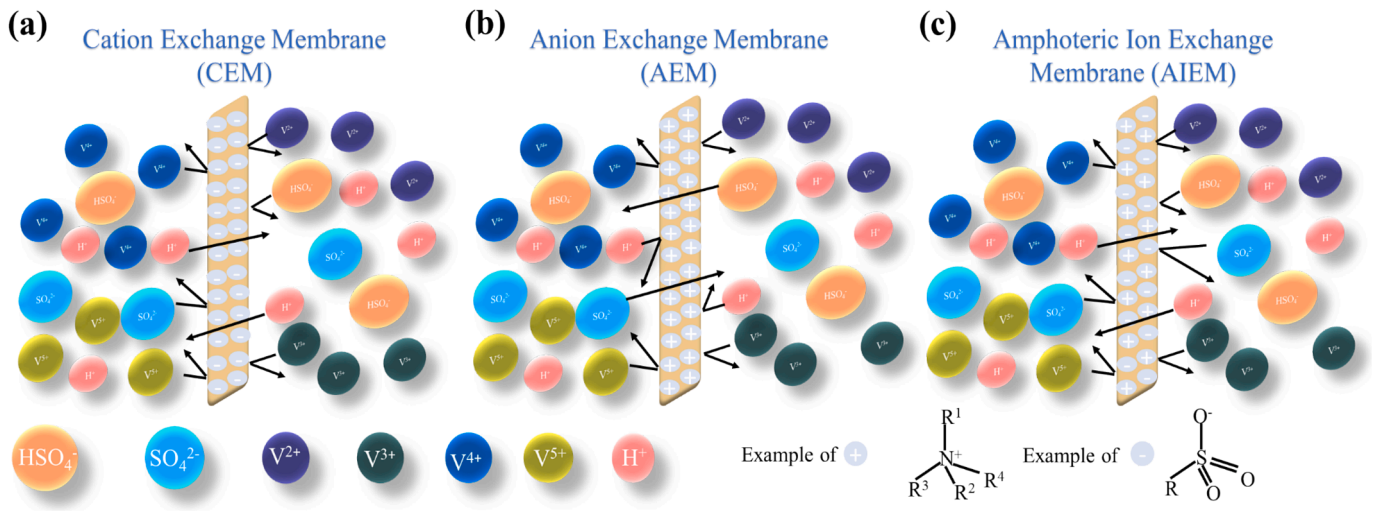

Fig. 6. Schematic of the ion exchange process of a) CEM, b) AEM, and c) AIEM in VRFB (one of the RFBs).

CEM membranes is governed by the Grotthus mechanism and the Vehicular mechanism, primarily preventing the crossover of active species and thereby controlling capacity fade, which is the main challenge. Despite the advantages of high ion selectivity and excellent chemical and thermal stability, there are limitations and drawbacks, including high costs (particularly for Nafion) [134], contamination on the membrane (surface fouling) [135], and degradation over time [136,137].

3.1.2. Anion exchange membranes (AEMs)

AEMs only support the flow of negatively charged ions while blocking positively charged ions, as they contain positively charged functional groups in a polymer matrix, such as quaternary ammonium ($-NR_4^+$), imidazolium ($-C_3H_3N_2R^+$), and phosphonium groups ($-PR_4^+$), where R represents generic alkyl or aryl groups, which facilitate anion transport [106,138]. It significantly reduces the Active species crossover issue but simultaneously limits proton conductivity, resulting in a lower VE. AEMs utilize the Donnan exclusion to block the crossing of cationic active species. It has the potential advantage of a low exchange rate of active species and lower cost compared to CEMs [139,140]. However, its use for long-term applications is challenged by issues such as chemical instability, swelling, and degradation.

3.1.3. Amphoteric ion exchange membranes (AIEMs)

AIEMs are the third and most advanced IEM-based membranes, introduced by Sollner in 1932. They contain both positively and negatively charged functional groups [141], such as sulfonate ($-SO_3^-$) and quaternary ammonium ($-NR_3^+$) groups embedded in the same polymer matrix [117,142]. They not only offer high proton conductivity but also exhibit low permeability of active species based on their pH-dependent behavior [143]. They permit the exchange of both cations and anions, depending on the types of ions and pH conditions. At high pH values, they act as AEMs due to the removal of protons from the cationic group (deprotonation). In contrast, at low pH, they act more like CEMs due to the addition of protons from an anionic group (protonation), and at near-neutral pH, they support both cation and anion exchange through them [144]. However, because the permeability of active species and proton conductivity are inherently conflicting parameters, the performance scale will depend on the proportion of these two functional groups. AEMs encounter challenges related to their high production costs, fouling, and swelling when operating in varying pH conditions, which reduce their stability and limit their widespread adoption [145]. The preparation process of the membrane, particularly the distribution of both ion-exchange groups, is complex and expensive. Researchers are exploring crosslinking and advanced materials to mitigate these issues [141,146]. However, AIEMs are highly promising as separators in various fields, including purification, fuel cells, batteries, biotechnology, and electrodialysis, because of their dual functionality.

3.2. Non-ionic selective membranes/ porous membranes (NIMs/PMs)

Non-ionic selective membranes primarily operate through a size-based sieving effect, similar to that of porous membranes, which is attributed to their principle of operation. NIMs/PMs differ from IEMs in that they don't mainly rely on functional groups for ion transport. Instead, they are governed by the pore size exclusion effect, as well as the structure and surface properties of the membrane material [169]. Although they offer lower costs and resistance, they may suffer from trade-offs between conductivity and crossover, which causes electrolyte imbalance, self-reaction, and capacity degradation, ultimately affecting overall battery performance. To effectively block active species without degrading proton conductivity, it is crucial to maintain a hydrophilic pore structure with an adjustable pore size [170]. According to the International Union of Pure and Applied Chemistry (IUPAC), porous solids are classified as microporous, mesoporous, and macroporous with PS less than 2 nm, 2–50 nm, and greater than 50 nm, respectively [171,172]. Filtration membranes are classified into nanofiltration membranes, ultrafiltration membranes, and microfiltration membranes with PS less than 5 nm, 5–100 nm, and 100–10,000 nm, respectively. Due to the flexibility of porous size, these kinds of separators are suitable for RFBs [173,174]. The permeability of the PMs is controlled by tuning the PS, a strategy that is beneficial. A small PS can effectively enhance ion selectivity by minimizing crossover, but it badly affects the VE due to increased ohmic resistance. Researchers optimized the PS of 5 nm to provide a trade-off between permeability and resistance [175]. This can be achieved by adding additives, such as polymers, to both the surface and the interior of the porous membrane. Furthermore, functional groups can also be added to the membrane to improve the ion selectivity. PMs performance can also be adjusted by adding additives, mostly made from polymers such as polyethylene (PE), polypropylene (PP), and polyvinylidene fluoride (PVDF) to their surface or interior. Preparation methods, including the integrating of organic/inorganic nanomaterials [43], grafting and copolymerization modification [176], introducing functional surface layers [177], and polymer blending [178], have been developed to enhance the functionality of PMs.

Introduction to MOF/COF porous separators /membranes

Recently, porous materials have gained tremendous attention from researcher due to their outstanding performance in various practical

fields. Chemists investigated multiple methods, but the synthesis of porous frameworks with discrete pores became challenging until the concept of reticular chemistry was introduced. This concept applies to topological engineering by linking molecules or clusters (organic or inorganic) building blocks into crystalline structures (open frameworks) via strong bonds [179–181]. Later, they proposed the concept of a metal–organic framework (MOF), a type of porous material. To date, approximately 60,000 MOF-based structures, formed by combining different metal clusters and organic linkers, have been reported [182,183]. The MOF-based separator offers several advantages over other commercially available microporous separators, such as activated carbon or zeolite, including a high specific surface area (500–7000 m^2/g) and good thermal resistance and stability [184]. Similar to COF-based membranes, the functionality of MOFs can be delicately tailored by optimizing pore size through the use of favorable metal ions or organic ligands [185,186]. In addition to excellent chemical stability in acidic and basic media, exceptional functionalizability provided by controlled pores, and high surface area of MOFs, the uniform and intrinsic pore structures of MOFs [187–198] are also a reason why MOFs can be widely used in membrane preparation. Functional groups (e.g., $-SO_3H$, $-NH_2$) can be introduced into MOF frameworks according to requirement, which can facilitate proton conduction via hydrogen bonding or proton hopping mechanisms [190]. Additionally, MOFs can also significantly reduce the penetration risk of vanadium ions or other redox-active species through the membrane, ultimately minimizing the trade-off effect in RFBs [191].

MOFs are made of metal clusters that coordinate with organic ligands [125], whereas COFs are composed of light elements or symmetric organic units connected by strong covalent bonds [192]. COF materials (with PS range of 0.5–5 nm [193]) have demonstrated innovative and potential roles not only as separator membranes [194] but also in various fields such as catalysis [195], optoelectronics/ semiconductors [196,197], sensor technology [198], and energy conversion [199], due to their unique properties that align well with current requirements in membrane engineering. Until now, it has already been used in various forms, including supported COF membranes grown on other materials [200], composite COF Membranes embedded with other materials [201], and self-standing COF membranes in membrane technology [202].

MOF/ COF-based membranes can be distinguished from other types of membranes by their unique structure, as they are designed at the molecular level and consist of flexible, highly porous crystalline materials [203]. Both COFs and MOFs have highly ordered porous framework networks, which are a key requirement for membrane structure [126,203]. Their customizable frameworks present them as more adaptable membranes with greater chemical and mechanical stability, precise ion sieving, and the ability to control the penetration of active species due to modifiable pore sizes. However, other membranes lack an ordered pore structure, which limits their selectivity and permeability because of the trade-off effect [204]. Additionally, their manufacturing process is complex, small-scale, and expensive, which limits their industrial application [205]. It also highlights the need for a membrane that can be easily fabricated and conveniently produced at a large scale while achieving well-ordered, high, and permanent homo-porosity, affordability, functional modifiability, excellent thermal stability, and chemical stability [206]. These advanced porous structures are already grafted with IEM-based membranes to improve ion selectivity through the incorporation of functional groups [207]. Therefore, MOF/COF membranes are regarded as the most advanced functional membranes (AFMs) due to their unique structural flexibility, large surface area, and high porosity in the field of RFBs [45,46].

4. Recent research about MOF-based membranes

One of the most widely used membranes in recent years has been perfluorinated sulfonic acid membranes (PFSA, e.g., Nafion) due to their chemical stability. However, they are considered unfavorable due to high costs and active species crossover [48]. Researchers introduced techniques for membrane surface modification, e.g., sulfonation, cross-linking, and polyelectrolyte coatings, inorganic fillers (like silica, TiO_2, and ZrO_2), to mitigate the crossover of active species. Researchers also propose several non-perfluorinated exchange membranes, such as polybenzimidazole (PBI) [208–211], SPEEK [147,212,213], sulfonated polyimide (SPI) [214], and sulfonated poly (arylene thioether ketone) [215], to reduce costs and achieve high energy efficiencies. Nevertheless, the crossover of active species or ion selectivity remains a significant challenge. Reported MOF-based composite separators /membranes are described below.

4.1. PBI/MOF-based membranes

PBI is a widely used membrane, but it requires improvement in terms of proton transportation and selectivity. To enhance ion selectivity, Liu, S., et al. [191] proposed a novel membrane for VRFBs by integrating a highly porous MOF with sulfonated polybenzimidazole (sPBI). The PBI membrane grafted with UiO-66 (a MOF with 0.6 nm PS); by optimizing the degree of sulfonation (DS) in PBI and modifying MOFs such as UiO-66-X (where X = NH_2 or OH), they improved ion selectivity, as the prepared MOF's pore size lies between protons (0.24 nm) and vanadium ions (V^{n+}, >0.6 nm) facilitates proton migration while blocking V^{n+}. DS indicates the percentage of $-SO_3H$ groups in the polymer matrix; membranes with 50 % DS show optimal performance. The 50-sPBI-UiO-66-OH exhibits stability over 100 cycles and a self-discharge time of 200 h, with CE 98.9 %, VE 92.45 %, EE 91.4 % at 50 mA/cm^2, and proton selectivity of 12.30 × 10^4 S min/cm^3, significantly surpassing standard membranes under the same conditions. Luan, C., et al. [216] implemented a prospective strategy by introducing a MOF (UIO-66-NH_2) based linker to facilitate proton conduction. A post-synthetic modification of Zr-MOFs (PSM) in the PBI matrix enhances proton transport sites and optimizes PBI/PSM hybrid membranes (0–2.5 wt%). The ion selectivity of the (PBI/PSM-1.5) membrane is fourfold that of pure PBI, attributed to 1) Donnan exclusion, 2) size sieving through 4 Å MOF pores, and 3) acid-base pairs between $–SO_3H$ of PSM and $–C_3H_3N_2$ of PBI. Membrane performance was evaluated through charge–discharge experiments for 600 cycles at various current densities (100–500 mA cm^{-2}), achieving 75.4 % EE at a high current density of 500 mA cm^{-2}. Liang, D., et al. [217] aim to improve the performance of sulfonated polybenzimidazole (sPBI) membranes by grafting them with conventional MOF (UiO-66), successfully overcoming the trade-off between proton exchange and vanadium ion crossover. For optimal performance, different DS (10 %, 20 %, 30 %, 50 %) were synthesized for PBI and 50 % sPBI with UiO-66 wt fractions (2 %, 5 %, 8 %, 10 %) via casting and activated with H_2SO_4. Membranes showed excellent thermal (>230 °C) and chemical stability after 2 weeks in VO^{2+} solution. The 50-sPBI-UiO-5 increased proton conductivity to 17.8 mS/cm while minimizing vanadium crossover at 2.9 × 10^{-9} cm^2/min and achieved IEC value of 0.24 mmol g^{-1}; electrochemical behavior showed EE, VE, and CE at 82.84 %, 85.32 %, and 97.09 %, respectively, at 120 mA cm^{-2}. After 200 cycles, the optimized membrane retained CE (93.83 %), VE (83.68 %), and EE (78.52 %), demonstrating superior performance. It maintained excellent dimensional stability (70.5Mpa tensile strength) without structural damage after 200 cycles and a high-capacitance retention rate of 39.67 % over 50 cycles.

4.2. SPEEK/MOF-based membranes

As existing perfluorinated membranes face several drawbacks and alternative non-fluorinated options like SPEEK still struggle with certain performance parameters, these challenges must be addressed. Zhai, S., et al. [218] incorporated water-insoluble phosphotungstic acid-MOF (HPW-MOF, nanohybrids HMN) into the SPEEK matrix and successfully improved proton conductivity while restricting V^{n+} permeability.

They introduce a methodology to create chemical bonds between HPW and MOF (MIL-101-NH_2) using sintering at 275 °C, resulting in stable nanohybrids (HMN). This improved the membrane's mechanical stability against the leaching of HPW, preventing performance decline. HPW helps overcome the trade-off between proton transport and vanadium ion crossover by occupying MIL-101-NH_2 pores. They optimized filler content in SPEEK/HMN-X (X = 1.5 %, 3 %, 4.5 %, 6 %, 7.5 %), finding SPEEK/HMN-6 as the best-performing membrane with proton conductivity of 0.070 S/cm (63 % higher than pristine SPEEK), vanadium permeability of 1.4 × 10^{-7} cm^2/min (80 % lower than pristine SPEEK), and 7 times higher ion selectivity of 4.8 × 10^5 S min/cm^3. Integrated with the optimized membrane, the VRFB achieved 82.1 % EE at 120 mA/cm^2, and the self-discharge time reached 420 h, indicating a better vanadium ion barrier. After 200 cycles, EE retention was 78.4 %, showing improved cycling stability. Lu, Y., et al. [219] introduced hybrid membrane synthesis using polydopamine (PDA) modified MOF-808 as a filler within a SPEEK matrix. PDA coating on MOF-808 has dual functionality 1) facilitates Donnan exclusion (behaves as a diffusion barrier against vanadium crossover, and 2) promotes acid-base pairs formation (between –SO_3H of SPEEK and –NH_2 of PDA) to enhance proton conductivity. To break the tradeoff between optimized proton conduction and blocking of V^{n+}, they coated PDA for different durations (5 min, 10 min, 30 min, and 6 h). The S/PDA@808–6 h membrane achieved 97.8 % CE at 20 mA cm^{-2} and had the lowest vanadium crossover at 8.06 × 10^{-8} cm^2/min, indicating good vanadium ion resistance but limiting proton conductivity. The 10-minute PDA-modified membrane (S/PDA@808–10 min) was optimal, showing proton conductivity of 0.0525 S/cm due to strong acid-base interactions; it outperformed reference membranes with 85.3 % VE and 83.9 % EE at 120 mA cm^{-2} and demonstrated durability over 1600 cycles, highlighting the potential of surface-modified MOF fillers in membrane technology. Xin, L., et al. [220] introduced Zr-MOFs (MOF-801 and MOF-808) as fillers in SPEEK membranes to enhance the ion sieving effect and proton transport in VRFBs. MOF-801 has a smaller triangular porous gateway of 3.5 Å, which enhances the ion sieving effect and leads to higher CE, while MOF-808 can increase VE due to more interconnected proton transport sites. S/MOF-801exhibited CE of 98.5–99.2 %, and S/MOF-808 exhibited VE of 93.7–84.1 % at different current densities (40–120 mA cm^{-2}), and both MOFs showed good chemical strength in acidic medium. To couple the benefits of both MOFs, they also prepare a binary MOF-801/MOF-808 composite membrane with a tailorable porous structure. Desired performance can be achieved through a balanced trade-off between ionic selectivity and proton conductivity, as a result, improving EE in RFBs. Cao, H., et al. [221] prepared a polycrystalline ion-selective membrane made of MOF-801 on an α-Al_2O_3 substrate, which was then spin-coated with a sub-10 nm polymeric layer of SPEEK to seal defects for VRFB systems. They reported proton conductivity of up to 0.028 S/cm, with ion selectivity 20 times higher than conventional Nafion-117. It achieved 96.1 % CE and 83.2 % EE at 20 mA/cm^2, demonstrating its long-term cycling stability under low current densities. Zhai, S., et al. [222] introduced S-UiO into the SPEEK membrane, prepared by modifying MOF (UiO-66-NH_2) pores with polystyrene sulfonic acid (PSSA) through in situ polymerization. SPEEK/S-UiO-X membranes were prepared by integrating S-UiO into the SPEEK matrix at various wt% (5 %, 10 %, 15 % and 20 %). The SPEEK/S-UiO-15 achieved optimal performance by providing 63 % higher proton conductivity, 83 % lower vanadium ion permeability, and 872 % higher ion selectivity than the pristine SPEEK membrane. The VFB test cell assembled with optimal membrane exhibited 83.9 % EE at 120 mA/cm^2, and the self-discharge time was twice compared to the pristine SPEEK. Moreover, it has expanded hydrophilic domains and only 4.2 % weight loss after being placed in a 3 M test solution (H_2SO_4 + 1.5 M VO^{2+}) for 30 days, indicating its better chemical stability. However, they provide a prospective strategy to enhance PEMs for VRFBs. Xiao, L., et al. [223] proposed the incorporation of carbonized MOF (ZIF-8) in the SPEEK matrix by the solution-casting method. Unlike stable MOFs (e.g., UiO-66 or MIL-101), ZIF-8 has stability issues, and carbonization is a prospective strategy to make it adoptable in harsh environments. The resulting material was effectively integrated with proton-conductive membranes with 1–4 wt% to improve its overall performance. The optimized SPEEK/CZIF-8–3 % membrane outperformed pristine membranes regarding ion sieving, mechanical strength, and proton conductivity. CZIF-8 is hydrophilic, so its WU increased up to 44 % for optimal membrane, with ion selectivity about 2.6-fold higher than the pristine membrane. Meanwhile, IEC reached 1.8 mmol g^{-1} with proton conductivity of 0.078 S/cm and vanadium ion permeability significantly reduced up to 4.23 × 10^{-7} cm^2/min. In the electrochemical test, the VRFB cell achieved CE 99.1 % and EE 82.7 % at 100 mA cm^{-2} and exhibited excellent cyclic stability over 1000 cycles, with minimal capacity degradation. They introduced carbonization of unstable MOF as an effective technique to enhance overall performance, making it a promising candidate in membrane science.

4.3. Nafion/MOF-based membranes

Traditional inorganic fillers were also grafted into Nafion to enhance membrane performance, significantly reducing sulfonic acid density and requiring further surface modification. However, UiO-66-SO_3H inherently contains this functional group to facilitate proton conduction and act as a partial barrier against vanadium ion crossover. Zhang, D., et al. [224] embedded it in a Nafion matrix to fabricate a hybrid membrane (Nafion/S-U66-X, X = 1–5 wt%) using the solution casting method and evaluated its performance in a VRFB cell. Nf/S-U66-3 exhibited the best performance by achieving proton conductivity of 44.04 mS cm^{-1}.Vanadium ion inhibition increased 3-fold, and ion selectivity was enhanced 5-fold compared to the pristine Nafion membrane. The optimized membrane showed 52 MPa tensile strength in reference to mechanical stability. In the electrochemical efficiency metrics, VE and EE reached 91.5–78.4 % and 86.0–76.1 %, respectively, at 80–220 mA cm^{-2}. The self-discharge time for the optimized membrane increased to 86.09 h, and it also showed long-term stable efficiency over 1000 cycles with a minimal capacity decay rate. After incorporating unmodified MOFs into Nafion, the membrane experiences significant proton impedance due to decreased sulfonated group densities. To overcome this issue, Yang, X. B., et al. [225] developed a Nafion composite membrane (UiO-66-NH_2@PWA) combining phosphotungstic acid (PWA) and UiO-66-NH_2 (a Zr-based MOF) using the solution casting method. The proposed MOF structure introduced twistiness, serving as a barrier for vanadium ions and facilitating proton transport. PWA enhanced proton conduction, compensating for any conductivity loss from MOF incorporation. Nafion-(UiO-66-NH2@PWA) at 3- wt% shows ion selectivity of 2.66 × 10^5 S min/cm^3, nearly eight times higher than Nafion. It maintains stability over 100 cycles, with a self-discharge time of 56 h (39 h for Nafion), sustained CE of 93.28 % and EE of 81.17 % at 100 mA/cm^2, reduces vanadium permeability to 3.46 × 10^{-7} cm^2/min, and improves proton conductivity to 0.092 S/cm, outperforming commonly available membranes under the same conditions. Traditional methods for synthesizing MOFs, such as hydrothermal synthesis, take a long time and yield inconsistent MOF properties. Gao, Q., et al. [226] proposed a feasible microwave-assisted synthesis method for a MOF (UIO-66-NH_2) and incorporated it with the Nafion matrix to develop a composite membrane (MU-NH_2/Nf-X, where X = 1, 2, 3, 6, 9). MU-NH_2/Nf-3 (3 wt % UIO-66-NH_2) showed the optimal proton conductivity of 122.18 mS/cm, while vanadium ion permeability was 0.78 × 10^{-7} cm^2/min. The optimized membrane achieved CE of 97.9 % and EE of 83.8 % at 100 mA cm^{-2} and maintained consistent performance over 200 cycles with lower capacity decay than standard membranes. This synthesis technique enables faster and higher-quality MOF preparation than traditional methods. Choi, H.J., et al. [227] incorporated Al-based MOFs (CAU-10-X, where X = –OH, –CH_3, –OS1, –OS2) in conventional Nafion-based membranes via the casting method to enhance the membrane performance. These MOFs were initially dispersed in a Nafion solution,

then cast and polymerized into thin membranes approximately 50 μm thick. To evaluate the prepared membrane, charge–discharge experiments were conducted for 100 cycles at various current densities in a VRFB signal cell, N/CAU-10-OS1, which contains hydrophilic functional groups such as –OH and –SO_3H. A 0.6 wt% concentration exhibited optimal efficiencies, achieving 80.34 % capacity retention even after 100 cycles at 160 mA cm^{-2}. This formulation not only improved ion selectivity up to 11.95 × 10^4 S min/cm^3 but also significantly reduced vanadium ion crossover to 4.36 × 10^7 cm^2/min, providing an IEC of 1.46 mmol g^{-1}. It demonstrated 77.56 % EE, outperforming pristine Nafion. Moreover, it was cost-effective and half the thickness of conventional Nafion 115. This composite membrane shows promise due to its enhanced efficiency, durability, and potential cost benefits for next-generation VRFB applications.

4.4. QPM/MOF-based membrane

Sharma, P., et al. [228] proposed a novel hybrid membrane (IMOF@QPM) created by incorporating a cationic MOF (IMOF) into a quaternized poly(2,6-dimethylphenylene oxide) (QPM) base polymer matrix using the solution casting method to enhance the overall performance of VRFBs. IMOF@QPM enhanced ionic selectivity to 5.2 × 10^5 S min/cm^2 while restricting vanadium crossover to 2.32 × 10^{-7} cm^2/min and maintained ionic conductivity at about 12.00 × 10^{-2} S/cm at 25 °C and 4.86 × 10^{-1} S/cm at 80 °C. With this membrane, a single-cell VRFB achieved a CE, VE, and EE of 98.0 %, 91.0 %, and 85.3 %, respectively, at 100 mA cm^{-2}. It also showed stability even after 800 cycles, with a capacitance retention rate of 96.0 % at 100 mA cm^{-2}. The novel IMOF enhances ion selectivity, inhibits vanadium permeability, and provides long-lasting durability, utilizing QPM instead of expensive PFSA (e.g., Nafion), making this hybrid membrane more cost-effective.

4.5. Celgard/MOF-based membranes

As the lack of effective separators with advanced performance limits the development of nonaqueous Li/ferrocene RFBs, Peng, S., et al. [229] introduced a novel gradient-distributed MOF-based porous membrane by incorporating the CuBTC (HKUST-1) MOF into a porous polymeric membrane (Celgard) through an in situ growth method. This approach reduces the effective pore size while maintaining high ionic conductivity. The modified membrane improves ion selectivity by allowing Li^+ ions (0.15 nm) to pass while preventing larger ferrocene molecules (0.7 nm) from doing so. RFBs equipped with this membrane demonstrate a high discharge capacity, with a reduced capacity decay rate of 0.09 % per cycle over 300 cycles, compared to the pristine membrane's 0.24 % per cycle. Additionally, the battery's CE and EE increased from 88.0 % to 97.4 % and from 74 % to 78.6 %, respectively, following MOF modification in Celgard. The open-circuit voltage also remains stable over extended periods. Yuan J., et al. [230] proposed another approach to address the shortage of high-performance membranes in Non-aqueous redox flow batteries (NARFBs) and a strategy to modify commercially available Celgard membranes. They synthesized 2D Ni-MOF nanosheets dispersed in DMF and deposited on a porous Celgard membrane via vacuum filtration, introducing a practical approach. The 2D NS-MOF@Celgard (500 nm layer) achieved optimal battery performance with 91.0 %, 93.7 %, and 85.1 % for CE, VE, and EE, respectively, at 4 mA cm^{-2}, showing long-term stability over 100 cycles. Unlike conventional membranes, the 2D MOF nanosheet-modified separator effectively addresses the trade-off between active species crossover and supporting electrolyte ions in NARFBs, which face limited energy storage applications due to a lack of efficient membranes.

4.6. PTFE/MOF-based membrane (MMM separator)

Yuan, J., et al. [231] Synthesized a flexible, porous MOF-5 membrane blended with polytetrafluoroethylene (PTFE) using a unique "dough rolling method" to enhance performance. Prepared uniform membrane (MMM separator) inhibits large $Fc1N112^+$ species crossover while allowing smaller Li^+ ion crossover, improving selectivity. This membrane achieves a CE of 99.7 % and EE of 80.9 %, maintaining a 99.96 % capacitance retention rate after 200 cycles at 4 mA cm^{-2}. This strategy enhances chemical and mechanical strength, and its unique synthesis methodology makes it cost-effective through recyclability and scalability.

All reported MOF membranes were tested at various current densities, achieving different EE%, as shown in Fig. 7(a). EE% depends on membrane ion transport characteristics. High proton conductivity reduces internal resistance, improving VE, while high ion selectivity minimizes species crossover, enhancing CE. Balancing these properties is crucial for maximizing EE%. The ion transport characteristics are shown in Fig. 7(b). Comparatively, the Nafion grafted membrane Nafion/MU-NH_2 achieved a strong trade-off between proton conductivity and ion selectivity, resulting in approximately 84 % EE at 100 mA cm-2 with consistent performance over 200 cycles and lower capacity fade. According to Fig. 7 and the literature on MOF-integrated composite membranes, it is demonstrated that performance metrics are improved compared to conventional membranes. However, in most of the reported membranes, these improvements are still insufficient for effective performance, particularly in terms of proton conductivity and ion selectivity, due to a lack of optimized porosity. The strategies or modifications mentioned, which involve optimizing the sulfonation degree (SD) in MOF composite membranes, enhance transport characteristics. Introducing –SO_3H groups creates continuous proton-conducting pathways for proton hopping. As a bulky group, it promotes crosslinking when grafted inside pores, tightening the structure and reducing free volume by creating an ion cloud that narrows the effective pore size. Nevertheless, MOF-based membrane engineering remains in a preliminary stage for application in RFBs.

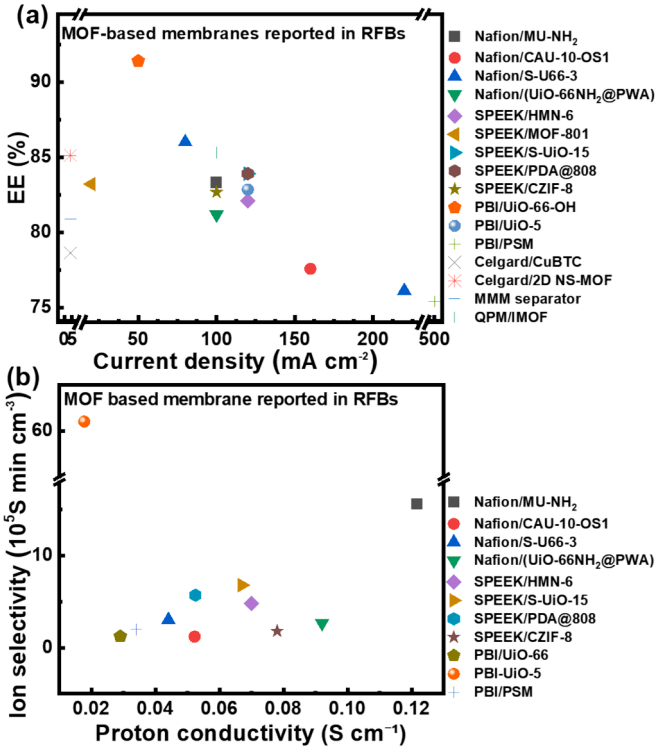

Fig. 7. Performance comparison of the MOF-based membranes reported in recent years, (a) EE%, (b) proton conductivity vs ion selectivity.

5. Recent research about COF-based membranes

Various groups have also attempted to incorporate multiple COFs prepared by novel strategies into existing membranes to create more effective separators and assemble them in RFBs to get improved performance and stability. Reported COF-based composite separators /membranes are described below.

5.1. PBI/COF-based membranes

PBI is a widely used polymer in membrane technology due to its exceptional thermal, chemical, and mechanical durability [208,232]. In 2015, it was reported that VRFBs without any backbone of ion exchange functional groups can retain their excellent chemical stability with negligible vanadium crossover. However, forming a desired proton exchange network in the PBI membrane is always challenging due to its structural constraints, which are crucial for proton conductivity [233]. Its dense alignment of molecular chains reduces proton conductivity and hinders its effectiveness as a permselective membrane [234]. Researchers incorporate inorganic fillers into the PBI matrix to enhance selectivity; however, this can compromise the membrane's durability due to interfacial defects [235–240]. To address these drawbacks, grafting with customizable architecture (COF) in the PBI matrix significantly enhances selectivity. Di, M., et al. [241] proposed an advancement in the PBI matrix, which involves embedding a Schiff base network-type COF (SNW-1) with a pore size of 0.48 nm using a solution casting method for VRFBs. This configuration only permits the transport of small-sized protons (<0.24 nm) while blocking the larger vanadium ions (>0.6 nm) due to their size. They claimed it is the first COF-based proton permselective membrane (PBI/SNW-x% composite membranes, where x% is the COF mass ratio), achieving high efficiencies in VRFB systems. They enhanced ion selectivity, eliminated vanadium crossover, and reduced area resistance, resulting in a high CE of 98.7–99.6 % and EE of 93.5–76.4 % across a range of current densities 40–180 mA cm^{-2}. The WU slightly increased due to the hydrophilic micropores of SNW-1; however, the SR remained below 5 % for all PBI/SNW membranes, ensuring good dimensional stability. The PBI/SNW-25 % membrane demonstrated optimal chemical stability and maintained its performance over 500 cycles (>1300 h) without structural degradation. This study presents a novel COF-based strategy to address the trade-off between proton conductivity and selectivity, offering a promising alternative to commercial Nafion membranes for RFBs. As area resistance limits proton conductivity in blended membranes, Di, M., et al. [242] modified the preparation method by integrating precipitation–evaporation in the casting method. The flexible composite membranes consist of a hollow spherical COF (HTpBD) selective layer supported by a porous PBI substrate. This involves synthesizing naturally settled Fe_3O_4@TpBD microspheres to create the selective layer, followed by the etching of Fe_3O_4 to form hollow COF pores that optimize proton transport. The optimized DPBI/HTpBD-9 membrane exhibited 99.5 % CE, 81.1 % VE, and 91.2 % EE at 180 mA cm^{-2}. It demonstrated high cyclic stability for 500 cycles, with CE decreasing only 0.9 % at 55 °C, showcasing excellent thermal stability. This proposed design maintained strong mechanical strength, flexibility, and durability. Wang, J., et al. [243] synthesized two high crystallinity COFs (TpPa, STpPa) with stable keto-structure, incorporated into the PBI matrix using solution-casting at room temperature with doping ratios of 0 %, 1 %, 3 %, and 5 %. TpPa refers to β-Ketoenamine-linked COF prepared with PS 1.8 nm, whereas STpPa is sulfonated TpPa COF with smaller PS 1.2 nm, which can effectively improve proton conductivity and control vanadium crossover. The P/STpPa-3 % membrane competes with both pristine PBI and commercially available Nafion 212, achieving higher proton conductivity up to 69.2 mS/cm along with lower vanadium permeability 16.43×10^{-9} cm^2/min and higher EE (91.38 %–74.38 %) at different current densities (40–240 mA cm^{-2}). Additionally, it demonstrated excellent cycling stability over 800 cycles at 160 mA cm^{-2} with over 80 % efficiency retention. Conventional COF-based membranes for RFBs suffer from the intrinsic rigidity or brittleness of COF material, as they are blended as nanoparticles with existing polyelectrolytes (e.g., Nafion) to modify them into the membrane. Consequently, discontinuity in ion transport and poor selectivity occur due to the agglomeration of these particles [241]. It is essential to develop more efficient methods to enhance the functionality of COF in membrane technology. Xie, G. et al. [244] introduced a free-standing TFP-TAPA COF nanofiber membrane fabricated using an in-situ growth-template etching method and densified it with PBI. Due to the Donnan exclusion effect and the membrane structure feature (6 Å pore size), it achieves ion selectivity three times that of Nafion. Performance evaluation indicates that this membrane attained 80.5 % EE at 200 mA/cm^2, significantly higher than other embedded COF membranes under the same conditions. It also exhibited an IEC of 1.58 mmol g^{-1} with a low area resistance of approximately 0.09 Ω cm^2, greatly reduces vanadium permeability, and maintains stable cycling over 300 charge–discharge cycles with minimal capacity degradation. The study emphasizes how continuous nanofiber structures mitigate the limitations of nanoparticle-based COF membranes, providing a promising and scalable solution for next-generation VRFBs.

5.2. SPEEK/COF-based membranes

Proton conductivity can be improved by optimizing the degree of sulfonation; however, a higher DS typically impacts dimensional and mechanical stability while increasing active species crossover [213,245]. Consequently, this limits its practical applications because of the decline in electrochemical performance. Nevertheless, integrating nanofillers into the SPEEK matrix membrane is a viable strategy to address these issues [246]. SPEEK is commonly used as a proton-conductive material because of its flexible membrane design, mechanical strength, and cost-effectiveness [73,120,154,247]. Li, J., et al. [248] Introduced a sulfonated Schiff base network-type COF nanofiller (SSNW-1 COFs) with varying SSNW-1 content (1–5 wt%) in the SPEEK matrix for VRFB. The fillers are functionalized with ($–SO_3^-$) groups to enhance compatibility with SPEEK. The SPEEK/SSNW-3 % membrane demonstrated optimal performance by minimizing vanadium ion crossover to 4.02×10^{-9} cm^2/s and achieving an IEC of 1.91 mmol g^{-1} with a higher proton conductivity (36.8 mS/cm) than the pristine membrane. It delivers strong electrochemical performance with 85.7 %, 99.8 %, and 85.9 % for EE, CE, and VE, respectively, at 80 mA/cm^2 and exhibits cyclic stability over 200 cycles with negligible degradation. Thus, they successfully enhanced the membrane's overall performance by incorporating COF nanofiller into the SPEEK membrane while maintaining its structural stability. Since SNW-1 is composed of agglomerated particles, this agglomeration may restrict its ability to block vanadium ions effectively. Growing this agglomerated structure into a more continuous and well-connected 2D plane may help get a higher effective blocking area for V^{n+} and improve its performance as a vanadium barrier.

COFs have tunable pore structures suitable for proton transport and selectivity, but poor crystallinity and mechanical instability limit applications [249]. Wu, Yulin, et al. [250] presented self-standing COF membranes made via a novel crystallization strategy using SPEEK as a scaffold; its sulfonic acid groups interact with the COF precursor, guiding the growth of TpPa–SO_3H membranes and improving crystalline order. The membranes exhibited interconnected nanochannels, increased porosity, and a larger surface area. Mechanical tests confirmed improved flexibility, elasticity, and excellent thermal and acid stability. The optimized 1 % SPEEK membrane showed superior proton conductivity (0.075 S/cm), low area resistance, and excellent selectivity for proton transport over redox-active species due to electrostatic repulsion and well-defined pore size distribution. It achieves a CE > 97 % and EE of 81 % at a low current density of 40 mA/cm2. Long-term cycling (300 cycles) demonstrates the membrane's durability and structural integrity. This study offers a scalable strategy for designing high-performance COF

membranes with broader applications in electrochemical energy systems.

Xu, W., et al. [251] first synthesized a COF-based sulfonated piperazine covalent triazine frameworks (s-pCTFs) as a functional filler in the membrane. This provides sub-nanometer channels (~1.5 nm) using an efficient ultrasonic method for the selective ion transport. It introduces a membrane based on an exterior–interior ion transport mechanism, utilizing exterior (−SO_3H) groups to enhance proton attractivity. The interior sub-2-nm N-rich triazine channels facilitate H^+ transport and inhibit V^{n+} through the Donnan exclusion effect. Hybrid membranes with 3 wt% (S/s-pCTF-3) exhibited an IEC of 2.75 mmol g^{-1}, proton conductivity up to 30.9 mS cm^{-1}, and high EE of 92.41 % at 40 mA cm^{-2} and 78.53 % at 200 mA cm^{-2}. They outperform common membranes, maintaining EE around 87.2 to 85 % over 900 cycles at 120 mA cm^{-2} and extending self-discharge voltage holding time to 134.2 hr. This method effectively reduces the hydrolytic/oxidative instability observed in other COFs.

SCOF membrane with the combination of optimal high DS, reduced PS, and its compatibility with polymer matrix after grafting in SPEEK matrix, improved its overall performance, especially ion selectivity. To create an optimized pore structure that facilitates selective proton transportation, Afzal et al. [252] proposed a SCOF/SPEEK hybrid membrane by grafting SCOF(NUS-9) into the SPEEK matrix using the solution casting method with different SCOF loadings (62.5–78.5 wt%). The SCOF/SPEEK-75 membrane exhibited an IEC of 3.23 mmol g^{-1}, resulting in superior proton conductivity of 0.065 S/cm, the highest ionic selectivity of 5.96 × 10^5 S min/cm^3, and low vanadium ion permeability of 1.52 × 10^{-7} cm^2/min. It also reached 98.6 % CE, 91.6 % EE at 100 mA/cm^2, and a Self-discharge time of 130.6 hr, significantly longer than Nafion (21.4 hr) and SPEEK (32.3 hr). Xu, W., et al. [253] developed a zwitterionic covalent organic framework (Cys-COF) into a SPEEK matrix, using a Thiol-ene click reaction and forming a hybrid membrane. The zwitterionic cysteine groups narrowed the COF channel size (~1.1 nm) and introduced the Donnan repulsion effect. The optimal hybrid membrane (S/Cys-COF-2) showed an IEC of 1.93 mmol g^{-1}, resulting in an ideal balance between proton conductivity and vanadium resistance. The S/Cys-COF-2 membrane offers a self-discharge time of 67.5 h, extended stability over 550 h, and completed 1100 cycles with prolonged CE (95.01 %–98.84 %), VE (95.15 %–77.84 %), and EE (90.41 %–76.94 %) at 40–200 mA/cm^2. The proton selectivity of 4.11 × 10^5 S min/cm^3 significantly outperformed pristine SPEEK membranes under the same conditions. To overcome the tradeoff between proton transfer and V^{n+} permeability in pristine SPEEK, Liu, H., et al., [254] proposed a new strategy to manipulate it as a proton exchange membrane (PEM) by incorporating self-exfoliated guanidinium-based ionic-covalent organic nanosheets (TpTGCl) into it. TpTGCl nanosheets were dispersed in DMF, blended with SPEEK at 1–4 wt%, cast into a mold, dried at 80 °C under vacuum, and immersed in 1 M H_2SO_4 for 1 day. This process ensured uniform dispersion of TpTGCl for high ionic selectivity as PEM. The optimized SP/TpTG-3 membrane exhibited an IEC of 1.85 mmol g^{-1}, achieved proton conductivity up to 133 mS cm^{-1}, and vanadium permeability of 12.9 × $10^{-7}$$cm^2$ min^{-1}. It also exhibited excellent battery efficiencies across various current densities. CE increased from 93.6 % to 98.3 %, VE decreased from 93.1 % to 78.8 %, and EE decreased from 87.05 % to 77.4 % at 60–180 mA cm^{-2}. Charge-discharge cycles showed stable capacity retention over 300 cycles, highlighting the importance of ionic-covalent organic nanosheets (iCONs) as an advanced PEM. This work improved proton conductivity, but vanadium inhibition was not sufficiently achieved. Therefore, a new approach of grafting two-dimensional functionalized graphene oxide (GO) along COF in the SPEEK matrix was introduced [255]. The functionalized GO has already been integrated with SPEEK membranes to improve their exchange properties [150,256–259]. Its dense and non-porous 2D structure might reduce vanadium crossover owing to complex diffusion channels, and simultaneously, the porous COF can efficiently exchange protons. Combining the advantages of both could yield a high-performance membrane. Zhang, Y., et al., [255] fabricated composite membranes (S/GO-TpTG-x, x refers to GO-TpTG content in SPEEK), containing a COF with cationic guanidine groups (TpTG) crosslinked to GO by the reaction between –NH_2 and –COOH groups. The best S/GO-TpTG-3 membrane exhibited an IEC of 1.92 mmol g^{-1}, resulting in proton conductivity of 82.7 mS cm^{-1}, vanadium ion crossover was minimized up to 10^{-8} cm^2 min^{-1}, with high H^+/ V^{n+} selectivity of 77.9 × 10^3 S min cm^{-3}. The VRFB test cell assembled with S/GO-TpTG-3 membrane achieved 81.0 % EE at a high current density of 200 mA cm^{-2}, it also showed superior CE, VE, and self-discharge time (209.8 hr) compared to the SPEEK and Nafion membranes. The composite membranes showed improved mechanical strength and thermal robustness due to better compatibility between GO-TpTG and the SPEEK matrix. This work highlights the potential of COF-GO hybridization as an innovative strategy for advancement in RFB membranes.

5.3. PFSA/COF-based membranes

Meng, X., et al. [260] utilized the concept reported in [254] and fabricated a Schiff base network-type COF (SNW) by using graphene oxide (GO) nanosheets as a reaction template and incorporating it in a series of different PFSA (PFSA-GO/SNW-x) membranes through in-situ growth. Pure PFSA available membranes also face rapid capacity fade and self-discharge issues due to huge active species crossover [261]. However, researchers tried to fix these problems by extending membrane thickness, but it increased internal resistance and soared manufacturing expense [262]. This strategy significantly minimized these drawbacks. After utilizing GO, agglomeration issues were resolved by creating a continuous 2D COF structure with uniform pores (~0.48 nm), which significantly reduced vanadium ion crossover up to 1.32 × 10^{-7} cm^2/min in PFSA-GO/SNW-10 with the highest selectivity 36.68 × 10^3 S min/cm^3. The obtained membrane (PFSA-GO/SNW-1) maintained high proton conductivity up to 94.0 mS/cm, higher than pristine PFSA. VRFB using optimized (PFSA-GO/SNW-7) membrane showed excellent electrochemical performance, CE around 97.47–98.18 %, and EE around 93.04–85.71 % at 40–120 mA /cm^2. This membrane also exhibited stable performance after 800 charge/discharge cycles at 120 mA /cm^2 without any noticeable capacity degradation. These findings exhibited that this technique to fabricate multi-functionalized surfaces has significant potential for next-generation membrane technology, especially in RFBs.

5.4. Nafion/COF-based membrane

Sulfonated covalent organic frameworks (SCOFs) effectively facilitate fast proton hopping and exhibit low swelling ratios in RFBs [263,264]. However, their wide implementation is restricted by a few drawbacks, such as the struggle to efficiently transport H^+ from V^{n+} due to large pore diameters (>15 Å), and their poor stability in harsh acidic and oxidative media poses challenges for their durability in RFBs [265,266]. Pang, B., et al. [267] Reported continuous TpPa-SO_3H SCOF membranes grafted with Nafion (SCOF/Nf-x, x denotes the weight ratio) aim to overcome these challenges. They created a wedge-tenon reinforcement structure which, through hydrogen bonds and ionic interactions, reduced the PS to about 5–10 Å, facilitating proton hopping by crystalline highway and contributing to remarkably high proton conductivity of 143.9 mS/cm with an IEC of 2.14 mmol g^{-1} at 25 °C, with a low swelling ratio of 3.1 %. SCOF/Nf-0.60 exhibits low VO^{2+} permeability of 1.72 × 10^8 cm^2/s and ion selectivity of 9.25 × 10^9 mS s/cm^3, outperforming Nafion and self-supporting SCOF membrane by 5.3- and 1.1 times, respectively. It also achieved a high EE of 85.5 % at 100 mA cm^{-2} with stable performance over 500 cycles, showing only a 0.13 % per cycle capacity decay rate afterwards.

All reported COF membranes were also tested at various current densities, achieving different EE%, as shown in Fig. 8(a). EE% depends on membrane ion transport characteristics, as shown in Fig. 7(b). The

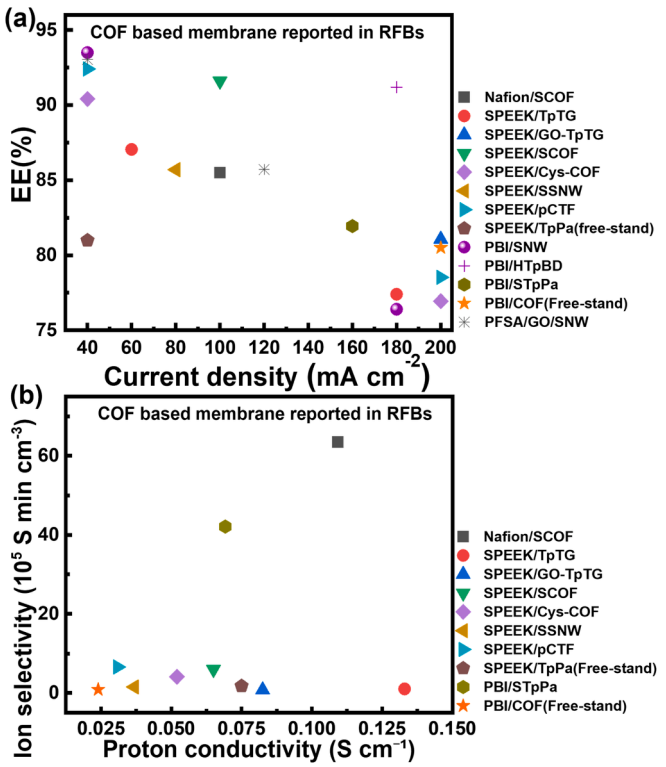

Fig. 8. Performance comparison of the COF-based membranes reported in recent years, (a) EE%, (b) proton conductivity vs ion selectivity.

Nafion grafted membrane Nafion/SCOF achieved a good trade-off between proton conductivity and ion selectivity, resulting in approximately 85.5 % EE at 100 mA cm^{-2} with consistent performance over 500 cycles, showing only a 0.13 % per cycle capacity decay rate afterwards. As they introduced a wedge-tenon structure that reduced the PS to about 5–10 Å through hydrogen bonds and ionic interactions. This innovative approach effectively enables proton hopping and improves proton conductivity, ultimately enhancing overall battery performance. According to Fig. 8 and the literature on COF-integrated composite membranes and freestanding COFs, it is evident that performance metrics have improved but still require further enhancement for optimal performance. Researchers introduced novel stable crystalline COFs, including the piperazine covalent triazine framework (pCTF), the zwitterionic covalent organic framework (Cys-COF), and the Schiff base network-type COF (SNW-1). They also employed new strategies to graft COFs with ionic covalent nanosheets (iCONs) and graphene oxide (GO) to address existing limitations in COF-based membranes and enhance performance metrics; however, all of these approaches require further improvement.

Although all the strategies described in the last two sections enhance MOF/COF membrane functionality, some limitations and factors still need to be addressed for their large-scale implementation in the real world. The performance evaluation and the names of fabrication methods for all the mentioned MOF/COF-based membranes used in different RFBs are summarized in Table 3, compared to the widely used Nafion 117 membrane. Various straightforward methods that recent groups have utilized to prepare MOF/COF membranes in RFBs are also illustrated in Fig. 9. One of the main advantages of MOF/COF membranes is the availability of feasible and diverse preparation methods; these groups employed conventional and simple methodologies to synthesize membranes. A recent study [268] on addressing the morphological and structural issues and enhancing the mechanical strength of membranes through control of membrane preparation parameters has been reported.

MOF/COF membranes show varying energy efficiencies (EE) at different current densities, as illustrated in Fig. 10(a). This impacts how quickly a battery can charge and discharge, affecting performance, efficiency, and capacity retention over time. Batteries with high EE at elevated current densities are ideal for applications like electric vehicles (EVs) and uninterruptible power supplies (UPS), requiring fast and reliable power. In contrast, lower current densities are better suited for grid storage and lab testing to improve stability and longevity. Ion selectivity and proton conduction are also primarily necessary for evaluating membrane function; these parameters are also summarized compared to the widely commercialized Nafion117 membrane for RFBs in Fig. 10(b). Most of the modified MOF/COF membranes showed better results and outperformed Nafion117 regarding proton conductivity, ion selectivity, and Energy efficiencies. The Nafion-MOF modified membrane (Nafion/MU-NH_2) and the Nafion-COF modified membrane (Nafion/SCOF) have shown noticeable ion transport properties, clearly highlighting the importance of these innovative frameworks in this field. Moreover, other modified membranes like PBI/STpPa and PBI-UiO-5 are also displaying enhanced ion selectivity or proton conductivity. Researchers are excitedly optimistic that they can achieve an overall improved performance by exploring their fundamental structure–property–performance relationships. This approach will create a balanced integration of these essential parameters, ultimately resulting in developing next-generation membranes designed to improve the efficiency and durability of RFBs.

6. MOF/COF-based membrane challenges and strategies for improvement

MOF/COF membranes have gained popularity as promising candidates for RFBs due to their flexibility, tunable porosity, high chemical stability, and selective ion transport properties, becoming next-generation separators over the past five years. Although the fabrication methods and application of MOF/COF membranes have made great progress, several bottlenecks still hinder their widespread implementation in this field. For optimal operation, several parameters must be considered when fabricating porous structure-based membranes, all of which are interconnected and require a balanced trade-off among them. Addressing these challenges through innovative strategies is crucial for advancing RFBs. These challenges include:

I. Limited chemical stability under harsh conditions: MOF/ COF materials often suffer from hydrolytic and oxidative degradation, due to prolonged exposure to harsh industrial conditions, including temperature variations, pH (mostly acidic < 3), and corrosive solvents (typically 1–3 M H_2SO_4), which leads to frameworks collapse and loss of functionality of membrane, retention stability against these conditions is essential for their durability and practical application. To enhance the stability of the COF membrane, it is necessary to focus on designing and modifying the membrane through new strategies such as using stable MOF/COF materials that can help to retain their structures, for example, Zr-based MOFs (UiO-66) induced resistance against degradation in acidic medium has been already embedded into membranes [191] and researchers also introduced β-ketoenamine linker COF membrane with improved chemical stability [243]. other linkers such as imide, hydrazones, acridines, or triazine-based linkages also have strong bonding compared to imine bonds to exhibit superior hydrolytic stability in both acidic and alkaline environments. Xiao, L., et al. [223] found that carbonizing MOF before integrating it into exciting membranes is a promising strategy to make it adaptable in harsh environments. Perfluorinated sulfonic acid membranes (PFSA, e.g., Nafion) are widely used due to their good chemical stability, but they have poor ion selectivity [48]. This issue can be resolved by using MOF/COF structures, resulting in optimized membranes even in

Table 3
Recent COF- and MOF-based membranes and their performance in RFBs.

Year	Membrane Name	Preparation method	WU/ SR (%)	Proton Conductivity (S cm^{-1})	Ion Permeability (cm^2 min^{-1})	Ion Selectivity (S min cm^{-3})	Current Density (mA cm^{-2})	EE/CE/VE (%)	Reference
–	**Nafion117**	–	17.7/ 28.5	0.07	5.15×10^{-7}	1.36×10^{5}	100	77/93.16/81.82	[217]
					MOF				
2017	50-sPBI-UiO-66-OH	solution casting	–	0.029	2.37×10^{-7}	12.30 x 10^{4}	50	91.4/98.9/92.45	[191]
2018	CuBTC/Celgard	in situ growth	–	–	–	–	4	78.6/97.4/-	[229]
2019	N-(UiO-66NH_2 @PWA)-3 wt%	solution casting	<26/ <23	0.092	3.46×10^{-7}	2.66×10^{5}	100	81.17/93.28/-	[225]
2020	2D NS-MOF@Celgard	vacuum filtration	–	–	–	–	4	85.1/91.0/93.7	[230]
2021	IMOF@QPM	solution casting	22.3/ 11.7	0.12	2.32×10^{-7}	5.2×10^{5}	100	85.3/98.0/91.0	[228]
2021	Nf/S-U66-3	solution casting	20.6/ 7.98	0.04404	3-fold less than Nafion	30.11×10^{4}	80,220	86.0/-/91.576.1/-/ 78.4	[224]
2022	N/CAU-10-OS1	solution casting	10/6.12	0.05221	4.36×10^{-7}	11.95×10^{4}	160	77.56/-/-	[227]
2022	50-sPBI-UiO-5	solution casting	10.6/ 6.5	0.0178	2.9×10^{-9}	6.1×10^{6}	120	82.84/97.09/85.32	[217]
2022	SPEEK/HMN-6	solution casting	<32/ <15	0.070	1.4×10^{-7}	4.8×10^{5}	120	82.1/99.0/81.5	[218]
2022	MMM separator	dough rolling	–	–	–	–	4	80.9/99.7/-	[231]
2022	s-MOF-801	secondary hydrothermal growth	–	0.028	–	20-fold of Nafion	20	83.2/96.1/-	[221]
2022	SPEEK/S-UiO-15	in situ growth	<40/ <24	0.067	1×10^{-7}	6.8×10^{5}	120	83.9/-/-	[222]
2023	S/PDA@808–10 min	solution casting	<47/ <11	0.0525	9.2×10^{-8}	5.7×10^{5}	120	83.9/-/85.3	[219]
2023	PBI/PSM-1.5	solution casting	<21/ <12	0.034	1.8×10^{-7}	20×10^{4}	500	75.4/99.5/ 76.0	[216]
2023	SPEEK/CZIF-8–3 %	solution casting	<45/ <17	0.078	4.23×10^{-7}	1.8×10^{5}	100	82.66/99.1/-	[223]
2024	MU-NH_2/Nf-3	microwave-assisted	20/3	0.12168	0.78×10^{-7}	15.60×10^{5}	100	83.8/97.9/85.5	[226]
	COF								
2020	PBI/SNW-25 %	solution casting	<17/ <5	–	47.4×10^{-7}	–	40,180	93.5/98.7/-,76.4/ 99.6/-	[241]
2022	DPBI/HTpBD-9	solution casting	–/-	–	7.2×10^{-10}	–	180	91.2/99.5/81.1	[242]
2022	SPEEK/SSNW-3 %	nucleophilic ring-opening reaction	23/12.5	0.0368	24.1×10^{-8}	1.53×10^{5}	80	85.7/99.8/85.9	[248]
2023	TpPa-SO_3H/SPEEK-1 %	in situ growth	<32/ <3	0.075	4.23×10^{-7}	1.77×10^{5}	40	81.0/87.8/83.0	[250]
2023	S/s-pCTF-3	ultrasonic method	<25/ <13	0.0309	4.7×10^{-8}	65.65×10^{4}	40,200	92.41/97.5/ 95.0,78.53/99.03/ 79.50	[251]
2024	P/STpPa-3 %	solution casting	–/<6	0.0692	16.43×10^{-9}	4.21×10^{6}	160	81.94/99.03/82.74	[243]
2024	S/Cys-COF-2	Thiol-ene reaction	<24/ <9.5	0.052	1.265×10^{-7}	4.11×10^{5}	40,200	90.41/95.01/ 95.15,76.94/98.84/ 77.84	[253]
2024	COF(Free-stand) fiber ICM 15 %	in-situ growth	16/<2	0.025	2.88×10^{-7}	8.5×10^{4}	200	80.5/-/-	[244]
2024	SCOF/Nf-0.60	vacuum-assisted filtration	51.6/ 4.5	0.1092	10.3×10^{-6}	6.35×10^{6}	100	85.5/-/-	[267]
2024	PFSA-GO/SNW-7	in-situ growth	15.8/ 11.2	0.005	2.09×10^{-7}	2.424×10^{4}	40,120	93.04/97.47/- ,85.71/98.18/-	[260]
2025	SP/TpTG-3	solution casting	<41/ <8.5	0.133	12.9×10^{-7}	1.03×10^{4}	60,180	87.05/93.6/ 93.1,77.4/98.3/78.8	[254]
2025	S/GO-TpTG-3	solution casting	<32/ <10	0.0825	1.06×10^{-8}	7.79×10^{4}	200	81.0/97.8/83.0	[255]
2025	SCOF/SPEEK-75	solution casting	57.23/ 8.41	0.065	1.52×10^{-7}	5.96×10^{5}	100	91.6/98.6/-	[252]

harsh environments. Some novel high-crystallinity COFs, such as TpPa and STpPa, with stable keto structures, have already demonstrated good structural retention without degradation in harsh acidic conditions due to their β-ketoenamine-linked structure, which requires a proper reaction time for the formation of a chemically stable framework [243]. However, a proper reaction period, which is reported to be 3–5 days, and dialysis (removal of extra unreactive precursors) duration (5–7 days), with optimized parameters such as reaction temperature, and suitable (COF precursors (monomers) and solvent), is crucial for stable framework formation [244].

II. Mechanical strength: High water uptake can facilitate proton conductivity but causes excessive swelling, which not only increases active species crossover but also leads to membrane deformation or failure. Improving the mechanical strength of MOF/COF-based membranes is essential to achieving optimal performance of RFBs. Researchers need to focus on strategies such as strengthening interlayer interactions, optimizing structural design, and developing composite materials to enhance the

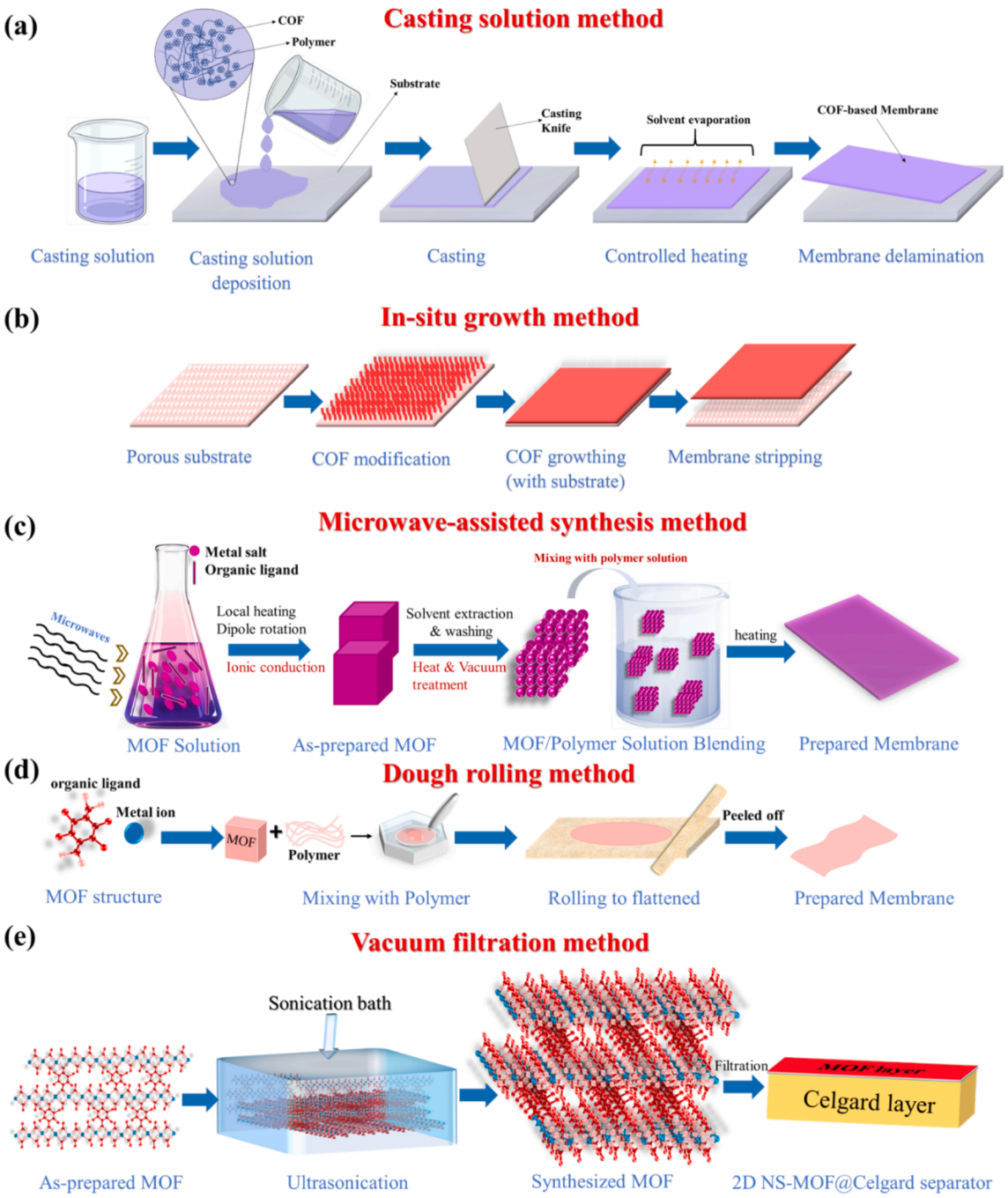

Fig. 9. Illustration of different methods recent groups utilized to prepare MOF/COF membranes in RFBs.

mechanical integrity of membranes. Some hybrid COF/MOF membranes have already been proposed that are embedded in stable polymer matrices such as Nafion, SPEEK, or PBI, to retain their porous structure and mechanical strength [217,220,224]. Proton conductivity can be enhanced by controlling hydrophilic functionalization, such as ($-SO_3H$, –COOH, and $–NH_2$), without compromising mechanical stability. Excessive water absorption can also be prevented by incorporating hydrophobic channels into membranes. These approaches have the potential to significantly improve the mechanical strength of MOF/COF membranes and expand their durability capabilities.

III. Facile fabrication and processability: COFs/MOFs are composed of microcrystals or powder-based precursors and require integration into continuous membranes, typically under mild conditions. Many do not dissolve in common solvents, making the application of conventional methods such as standard solution casting or coating techniques challenging. Traditional membrane fabrication methods, such as spin coating and pressure-assisted or vacuum-assisted filtration, face hurdles due to the coating layer's poor mechanical strength, which makes it prone to falling off. The in-situ growth method also has limited application because of poor adhesion, non-uniform coating, and restricted polymer compatibility, which are affected by particle aggregation and pore-blocking issues. After addressing these issues, researchers proposed some novel strategies for effective processability, such as the casting-precipitation-evaporation method [242], Schiff base network-type COF (SNW) by using graphene oxide (GO) nanosheets as a structural template [241], and dough rolling

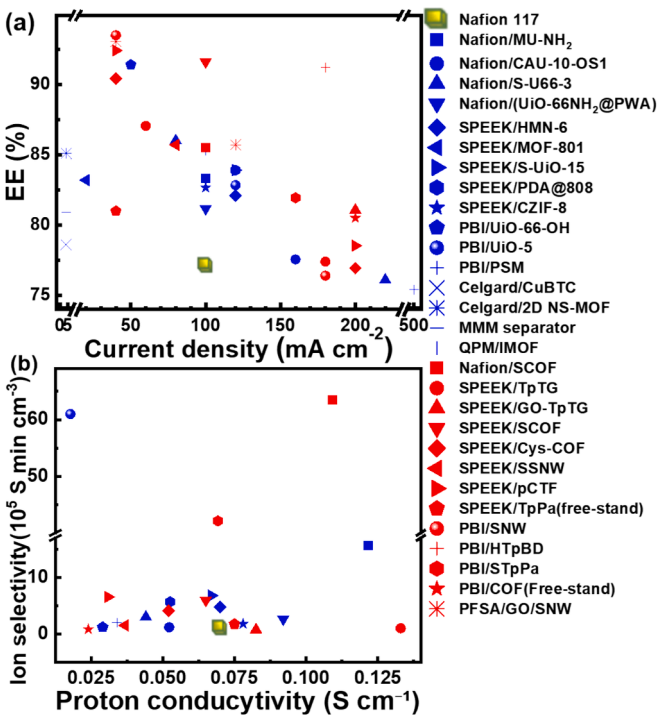

Fig. 10. Performance comparison of the MOF/COF membranes reported in recent years with widely used Nafion 117 in RFBs, (a) EE%, (b) proton conductivity vs ion selectivity, (blue color represents MOF, while red color represents COF-based membranes).

method [231], but all in infant stages and need further improvement for uniform and crack-free membrane production at large-scale.

IV. Desired pore dimensions: The main advantage of integrating MOF/COF material as a separator in RFBs is its tunable porosity. However, most reported porous membranes with pore sizes > 7 nm are unsuitable for separation, as the hydrated proton size is $<$ 3 nm and vanadium ions range from 0.45 to 0.55 nm [267]. Rational design with controlled sub-nanometer scale channels (accurate porous size < 7 nm) to strictly sieve hydrated protons from active species (vanadium ions) presents many challenges [221]. Researchers focused on reducing the pore size to enhance proton transportation while inhibiting active species crossover. Several studies have proposed bilayer or multilayer gradient pore structures in membranes to achieve this reduction. However, the uniformity of these structures remains a major challenge due to the disordered interleaved stacking of framework layers, which leads to inconsistent ionic transport properties. Modifying functional side chains can induce ordered stacking, but achieving precise pore tuning without compromising mechanical stability remains difficult. One group proposed a piperazine covalent triazine framework (pCTF) material with sub-2-nm channels using a facile ultrasonic method [251]. Xu, W., et al. developed a zwitterionic covalent organic framework (Cys-COF) to narrow down the COF channel size (~1.1 nm) [253]. Another group introduced water-insoluble nanohybrids (HPW) in MOF pores to block vanadium crossover [218]. However, there is still a lack of precise sub-nanometer pore engineering to enhance ion selectivity by reducing pore size. Wang, J., et al. introduced the $-SO_3H$ group in COF precursors as a pre-functionalization treatment in STpPa, which not only facilitates proton hopping but also decreases PS from 1.8 nm to 0.86 nm [243]. This indicates the importance of degree sulfonation for optimized PS, and the introduction of bulky functional groups or hydrogen-bonding interactions can effectively decrease PS. Porous crystalline materials connected by stable covalent bonds have already been reported with PS of (SNW-1 0.48 nm, SSNW-1 0.43 nm, TFP-TAPA 0.6 nm). However, in TFP-TAPA, COFs with PS 0.6 nm (AB stacking) are achieved along 1 nm (AA stacking), indicating that the confined or template-guided synthesis is essential to promote offset stacking [244]. Polar solvents help in weakening π–π interactions and promote AB stacking with reduced PS, indicating that the choice of solvent can significantly influence PS control. Therefore, the selection of the precursors, solvents, and optimized reaction conditions (e.g., temperature, reaction time, degree of sulfonation) is significant in optimized porosity.

V. Upscaling of COF/MOF membranes: Scaling up the production of MOF/COF membranes from the laboratory to the industrial level presents significant hurdles due to the precise synthesis conditions required, including temperature, pressure, and stoichiometry. Traditional methods, such as interfacial polymerization and in situ growth, are difficult to scale, while continuous production remains a challenge. To address these issues, various scalable fabrication techniques have been explored. The hot pressing (HoP) method is a novel and feasible strategy that applies high temperature and pressure simultaneously for the fabrication of MOF membranes on a large scale [269]. Upscaling COF membranes through solution casting and vapor-assisted methods can be achieved with better control over crystallinity and orientation. Other advanced approaches, such as microwave synthesis, microfluidic synthesis, and mechanochemical methods, are limited to specific COF structure formations. Integrating these fabrication techniques into continuous industrial processes is essential for overcoming scalability challenges. As research progresses, further advancements in cost-effective, rapid manufacturing are necessary to accelerate the industrial adoption of MOF/COF membranes.

This section is summarized in Table 4 for easy access. Despite these significant challenges, the unique features of COF/MOF membranes and ongoing research into innovative strategies show promising potential. Researchers are focusing on utilizing MOF/COF-based separators/membranes, aiming to address and resolve existing issues and limitations in the MOF/COF-based separator technology for RFBs, as most of the research discussed in this review has been conducted in the last three years. This progress could ultimately lead to stable, high-performance membranes that meet industrial demands for selective separations in RFBs, paving the way for the next generation of sustainable technologies.

7. Conclusion

RFBs stand out as highly promising candidates for large-scale energy storage systems to replace fossil fuel sources. However, unlocking their real-world potential requires detailed research on their design aspects and pivotal components; the role and importance of separators cannot be neglected. Researchers have extensively explored various types of membranes, ranging from conventional ion exchange membranes (IEMs), which include cation exchange membranes (CEMs), anion exchange membranes (AEMs), and amphoteric ion exchange membranes (AIEMs), to non-ionic porous membranes. Each type has its advantages and drawbacks, which are briefly summarized along with performance evaluation in a dedicated section. Additionally, some approaches to evaluating the performance of membranes in RFBs have been reported.

Herein, a comprehensive review of MOF- and COF-based separators/membranes is presented. MOF/COF materials are preferred for RFB separators, especially for achieving a balanced trade-off between proton conductivity and active species permeability. This paper provides an overview of the functionalities of recently reported MOF/COF membranes, research trends, and challenges in existing membrane

Table 4
MOF/COF-based membrane challenges and strategies for improvement in RFBs.

Challenges	Specific Issues	Improvement Strategies	Reference
Insufficient chemical stability	MOF/COF materials degrade in acidic environments.	Enhancing intrinsic stability Choosing robust linkages Crosslinking strategies Oxidation-Resistant coatings	[187,239]
Poor mechanical strength	High water uptake along with excessive swelling leads to deformation.	Enhancing intrinsic framework strength Embedding in high-strength polymers Optimizing membrane thickness & water management Optimized controlled crosslinking Incorporate hydrophilic-hydrophobic hybrid fillers	[213,216,220]
Non-processability	Limitations for MOF/COF precursors integration into continuous membranes.	Novel fabrication strategies (e.g., casting-precipitation-evaporation) Using the structural template (e.g., graphene oxide nanosheet) Improve the existing fabrication method	[227,237,238,260]
Pore dimensions	Difficulty in controlling the desired pore size	Bilayer or multilayer stacking Addition of Water-insoluble nanohybrids in pores Incorporation of porous organic materials	[214,248,254]
Scalability	Challenges in upscaling from the laboratory to the industrial level	Novel and feasible strategies (e.g., hot pressing method) Large-scale production via traditional methods by improving crystallinity and orientation of the material	[226,269]

engineering. It also includes tables for easy access to studied data regarding various optimized MOF/COF membranes, synthesis methods, and their associated performance for comparative analysis or evaluation to fine-tune future research directions. These membranes offer greater functionality than conventional membranes due to their modifiability in pore channels, ion selectivity, and design flexibility. Additionally, these advanced porous structures are grafted with IEM-based membranes to enhance ion selectivity through the incorporation of functional groups, and the cost has considerably decreased over time due to developments and modification methods. Nonetheless, challenges persist regarding chemical and mechanical stability, processability, and scalability. Some potential strategies to overcome these issues are also proposed. In essence, it highlights the ongoing quest to advance RFB technology through MOF/COF innovations and underscores the significance of understanding the evolving landscape of membrane materials and their impact on RFB efficiency. By addressing these advanced functional membranes, future membrane science can be designed to deliver superior performance, ultimately unlocking the full commercial potential of RFBs and advancing the global shift toward sustainable energy storage.

CRediT authorship contribution statement

Iqra Shaheen: Writing – original draft, Methodology, Investigation, Data curation, Conceptualization. **Wei-Hao Chiu:** Writing – review & editing, Supervision, Methodology, Conceptualization. **Shih-Hsuan Chen:** Writing – review & editing, Data curation, Conceptualization. **Kun-Mu Lee:** Writing – review & editing, Supervision, Resources, Funding acquisition, Conceptualization.

Declaration of competing interest

The authors declare that they have no known competing financial interests or personal relationships that could have appeared to influence the work reported in this paper.

Acknowledgments

The authors thank the support from National Science and Technology Council, Taiwan (Grant Number: 111-2223-E-182-001-MY4, 112-2221-E-182-020-MY2), Chang Gung University, Taoyuan, Taiwan (URRPD2Q0041) and Chang Gung Memorial Hospital, Linkou, Taiwan (CMRPD2N0072).

Data availability

No data was used for the research described in the article.

References

[1] R. López-Vizcaíno, E. Mena, M. Millán, M.A. Rodrigo, J. Lobato, Performance of a vanadium redox flow battery for the storage of electricity produced in photovoltaic solar panels, Renew. Energy 114 (2017) 1123–1133, https://doi.org/10.1016/j.renene.2017.07.118.
[2] P. Alotto, M. Guarnieri, F. Moro, Redox flow batteries for the storage of renewable energy: a review, Renew. Sustain. Energy Rev. 29 (2014) 325–335, https://doi.org/10.1016/j.rser.2013.08.001.
[3] S. Solomon, G.-K. Plattner, R. Knutti, P. Friedlingstein, Irreversible climate change due to carbon dioxide emissions, Proc. Natl. Acad. Sci. U.S.A. 106(6) (2009) 1704–1709, https://doi.org/10.1073/pnas.0812721106.
[4] M. Suryabhan, Environmental degradation and renewable energy, Int. Adv. Res. Sci. Commun. Technol. (2024) 160–165, https://doi.org/10.48175/IJARSCT-19529.
[5] V.G. Nguyen, R. Sirohi, M.H. Tran, T.H. Truong, M.T. Duong, M.T. Pham, D.N. Cao, Renewable energy role in low-carbon economy and net-zero goal: Perspectives and prospects, Energy Environ. 0(0) 0958305X241253772. doi: 10.1177/0958305x241253772.
[6] D. Bhatnagar, H.S. Rabinowitz, D.S. Boff, G. Pennell, C.A. Holland, M.R. Weimar, B. Huang, D. Wu, A.H. Bonneville, Nontechnical barriers to geothermal development, Pacific Northwest National Lab, (PNNL), Richland, WA (united States) (2022), https://doi.org/10.2172/1879758.
[7] R. Meirbekova, D. Bonciani, D.I. Olafsson, A. Korucan, P. Derin-Güre, V. Harcouët-Menou, W. Bero, Opportunities and challenges of geothermal energy: a comparative analysis of three european cases—Belgium, Iceland, and Italy, Energies 17 (16) (2024) 4134, https://doi.org/10.3390/en17164134.
[8] S. Aadya, Current trends and future directions in renewable energy systems, Int. J. Res. Publ. Semin. 15 (2) (2024) 186–198, https://doi.org/10.36676/jrps.v15.i2.1408.
[9] Z. Meng, Q. He, X. Shi, D. Cao, D. Du, Research on energy utilization of wind-hydrogen coupled energy storage power generation system, Sep. Purif. Technol. 313 (2023) 123439, https://doi.org/10.1016/j.seppur.2023.123439.
[10] C. Bussar, M. Moos, R. Alvarez, P. Wolf, T. Thien, H. Chen, Z. Cai, M. Leuthold, D. U. Sauer, A. Moser, Optimal allocation and capacity of energy storage systems in a future european power system with 100% renewable energy generation, Energy Procedia 46 (2014) 40–47, https://doi.org/10.1016/j.egypro.2014.01.156.
[11] I. Papic, Simulation model for discharging a lead-acid battery energy storage system for load leveling, IEEE Trans. Energy Convers. 21 (2) (2006) 608–615, https://doi.org/10.1109/TEC.2005.853746.
[12] A.Z. Weber, M.M. Mench, J.P. Meyers, P.N. Ross, J.T. Gostick, Q. Liu, Redox flow batteries: a review, J. Appl. Electrochem. 41 (10) (2011) 1137–1164, https://doi.org/10.1007/s10800-011-0348-2.
[13] L. Fan, Z. Tu, S.H. Chan, Recent development of hydrogen and fuel cell technologies: a review, Energy Rep. 7 (2021) 8421–8446, https://doi.org/10.1016/j.egyr.2021.08.003.
[14] T. Chen, Y. Jin, H. Lv, A. Yang, M. Liu, B. Chen, Y. Xie, Q. Chen, Applications of lithium-ion batteries in grid-scale energy storage systems, Trans. Tianjin Univ. 26 (3) (2020) 208–217, https://doi.org/10.1007/s12209-020-00236-w.
[15] J.-Y. Hwang, S.-T. Myung, Y.-K. Sun, Sodium-ion batteries: present and future, Chem. Soc. Rev. 46 (12) (2017) 3529–3614, https://doi.org/10.1039/C6CS00776G.
[16] D.E.O. Juanico, Revitalizing lead-acid battery technology: a comprehensive review on material and operation-based interventions with a novel sound-assisted charging method, Front. Batter. Electrochem. 2 (2024), https://doi.org/10.3389/fbael.2023.1268412.
[17] T.M. Lim, M. Ulaganathan, Q. Yan, Chapter 14 - advances in membrane and stack design of redox flow batteries (RFBs) for medium- and large-scale energy storage, in: C. Menictas, M. Skyllas-Kazacos, T.M. Lim (Eds.), Advances in Batteries for

Medium and Large-Scale Energy Storage, Woodhead Publishing, 2015, pp. 477–507, https://doi.org/10.1016/B978-1-78242-013-2.00014-5.
[18] L. Pan, H. Rao, J. Ren, S. Wan, Z. Guo, Z. Wang, M. Han, X. Fan, J. Sun, Y. Li, Innovations in stack design and optimization strategies for redox flow batteries in large-scale energy storage, Innov. Energy 1(3) (2024) 100040-1-100040-18. doi: 10.59717/j.xinn-energy.2024.100040.
[19] L.F. Arenas, F.C. Walsh, Redox Flow Batteries for Energy Storage, in: L.F. Cabeza (Ed.), Encyclopedia of Energy Storage, Elsevier, Oxford, 2022, pp. 394-406. doi: 10.1016/B978-0-12-819723-3.00049-4.
[20] J.D. Milshtein, Electrochemical engineering of low-cost and high-power redox flow batteries, Massachusetts Institute of Technology (2017). http://dspace.mit.edu/handle/1721.1/7582.
[21] A.G. Olabi, M.A. Allam, M.A. Abdelkareem, T. Deepa, A.H. Alami, Q. Abbas, A. Alkhalidi, E.T. Sayed, Redox flow batteries: recent development in main components, emerging technologies, diagnostic techniques, large-scale applications, and challenges and barriers, Batteries 9 (8) (2023) 409, https://doi.org/10.3390/batteries9080409.
[22] M. Shoaib, P. Vallayil, N. Jaiswal, P. Iyapazham Vaigunda Suba, S. Sankararaman, K. Ramanujam, V. Thangadurai, Advances in redox flow batteries–a comprehensive review on inorganic and organic electrolytes and engineering perspectives, Adv. Energy Mater. 14 (32) (2024) 2400721, https://doi.org/10.1002/aenm.202400721.
[23] M. Pahlevaninezhad, A.K. Singh, T. Storwick, E. Esther Miller, A. Yang, M. Pahlevani, M. Pope, E.P.L. Roberts, An advanced composite membrane for the all-vanadium redox flow battery, ECS Meeting Abstracts MA2022-01(3) (2022) 466, https://doi.org/10.1149/MA2022-013466mtgabs.
[24] M.M. Ikhsan, S. Abbas, S.-Y. Choi, X.H. Do, H.Y. Ha, A. Bentien, K. Azizi, H. A. Hjuler, D. Henkensmeier, Electrode laminated with ion-selective blocking layer for use in vanadium redox flow batteries, Mater. Today Chem. 34 (2023) 101830, https://doi.org/10.1016/j.mtchem.2023.101830.
[25] H. Lim, A. Lackner, R. Knechtli, Zinc-bromine secondary battery, J. Electrochem. Soc. 124 (8) (1977) 1154, https://doi.org/10.1149/1.2133517.
[26] X. Xia, H.-T. Liu, Y. Liu, Studies of the feasibility of a Ce4+/Ce3+ V 2+/V 3+ redox cell, J. Electrochem. Soc. 149 (4) (2002) A426, https://doi.org/10.1149/1.1456534.
[27] B. Li, Z. Nie, M. Vijayakumar, G. Li, J. Liu, V. Sprenkle, W. Wang, Ambipolar zinc-polyiodide electrolyte for a high-energy density aqueous redox flow battery, Nat. Commun. 6 (1) (2015) 6303, https://doi.org/10.1038/ncomms7303.
[28] M. Rychcik, M. Skyllas-Kazacos, Characteristics of a new all-vanadium redox flow battery, J. Power Sources 22 (1) (1988) 59–67, https://doi.org/10.1016/0378-7753(88)80005-3.
[29] Z. Yang, L. Tong, D.P. Tabor, E.S. Beh, M.A. Goulet, D. De Porcellinis, A. Aspuru-Guzik, R.G. Gordon, M.J. Aziz, Alkaline benzoquinone aqueous flow battery for large-scale storage of electrical energy, Adv. Energy Mater. 8 (8) (2018) 1702056, https://doi.org/10.1002/aenm.201702056.
[30] W. Liu, Y. Liu, H. Zhang, C. Xie, L. Shi, Y.-G. Zhou, X. Li, A highly stable neutral viologen/bromine aqueous flow battery with high energy and power density, Chem. Commun. 55 (33) (2019) 4801–4804, https://doi.org/10.1039/C9CC00840C.
[31] Z. Li, Y.-C. Lu, Polysulfide-based redox flow batteries with long life and low levelized cost enabled by charge-reinforced ion-selective membranes, Nat. Energy 6 (5) (2021) 517–528.
[32] Z. Li, G. Weng, Q. Zou, G. Cong, Y.-C. Lu, A high-energy and low-cost polysulfide/iodide redox flow battery, Nano Energy 30 (2016) 283–292, https://doi.org/10.1038/s41560-021-00804-x.
[33] M. Skyllas-Kazacos, F. Grossmith, Efficient vanadium redox flow cell, J. Electrochem. Soc. 134 (12) (1987) 2950, https://doi.org/10.1149/1.2100321.
[34] X. Wang, J. Deng, Y. Zhu, C. Chaemchamrat, O. Fontaine, Principle, advantages and challenges of vanadium redox flow batteries, Sci. Technol. Adv. Mater. 6 (2024), https://doi.org/10.37155/2717-526X-0602-1.
[35] D. Zhang, X. Zhang, C. Luan, B. Tang, Z. Zhang, N. Pu, K. Zhang, J. Liu, C. Yan, Zwitterionic interface engineering enables ultrathin composite membrane for high-rate vanadium flow battery, Energy Storage Mater. 49 (2022) 471–480, https://doi.org/10.1016/j.ensm.2022.04.033.
[36] D. Cheng, Y. Li, J. Zhang, M. Tian, B. Wang, Z. He, L. Dai, L. Wang, Recent advances in electrospun carbon fiber electrode for vanadium redox flow battery: properties, structures, and perspectives, Carbon 170 (2020) 527–542, https://doi.org/10.1016/j.carbon.2020.08.058.
[37] B. Schwenzer, J. Zhang, S. Kim, L. Li, J. Liu, Z. Yang, Membrane development for vanadium redox flow batteries, ChemSusChem 4 (10) (2011) 1388–1406, https://doi.org/10.1002/cssc.201100068.
[38] D.N. Buckley, A. Bourke, D. Oboroceanu, C. Lenihan, M. Al Hajji Safi, N. Quill, M. A. Miller, R.F. Savinell, J.S. Wainright, V. Sasikumar, S P, M. Rybalchenko, P. Amini, R.P. Lynch, (Invited) some aspects of electrode kinetics and electrolyte stability in vanadium flow batteries, ECS Trans. 109 (10) (2022) 3, https://doi.org/10.1149/10910.0003ecst.
[39] L. Cao, A. Kronander, A. Tang, D.-W. Wang, M. Skyllas-Kazacos, Membrane permeability rates of vanadium ions and their effects on temperature variation in vanadium redox batteries, Energies 9 (12) (2016) 1058, https://doi.org/10.3390/en9121058.
[40] J.C. Duburg, K. Azizi, S. Primdahl, H.A. Hjuler, E. Zanzola, T.J. Schmidt, L. Gubler, Composite polybenzimidazole membrane with high capacity retention for vanadium redox flow batteries, Molecules 26 (6) (2021) 1679, https://doi.org/10.3390/molecules26061679.
[41] G. Wang, J. Kang, S. Yang, M. Lu, H. Wei, Influence of structure construction on water uptake, swelling, and oxidation stability of proton exchange membranes, Int. J. Hydrog. Energy 50 (2024) 279–311, https://doi.org/10.1016/j.ijhydene.2023.08.129.
[42] Y. Zhang, D. Zhang, C. Luan, Y. Zhang, W. Yu, J. Liu, C. Yan, An economical composite membrane with high ion selectivity for vanadium flow batteries, Membranes 13 (3) (2023) 272, https://doi.org/10.3390/membranes13030272.
[43] L. Ling, M. Xiao, D. Han, S. Ren, S. Wang, Y. Meng, Porous composite membrane of PVDF/Sulfonic silica with high ion selectivity for vanadium redox flow battery, J. Membr. Sci. 585 (2019) 230–237, https://doi.org/10.1016/j.memsci.2018.11.082.
[44] O. Shekhah, J. Liu, R. Fischer, C. Wöll, MOF thin films: existing and future applications, Chem. Soc. Rev. 40 (2) (2011) 1081–1106, https://doi.org/10.1039/C0CS00147C.
[45] X. Liu, J. Wang, Y. Shang, C.T. Yavuz, N.M. Khashab, Ionic covalent organic framework-based membranes for selective and highly permeable molecular sieving, J. Am. Chem. Soc. 146 (4) (2024) 2313–2318, https://doi.org/10.1021/jacs.3c11542.
[46] M. Deghankar, R. HMTShirazi, T. Mohammadi, Preparation Techniques and Characterizations of Metal Organic Framework-Based Membranes (2024), https://doi.org/10.1016/b978-0-323-95486-0.00009-0.
[47] M.T. Tsehaye, R.A. Tufa, R. Berhane, F. Deboli, K.A. Gebru, S. Velizarov, Modified membranes for redox flow batteries—a review, Membranes 13 (9) (2023) 777, https://doi.org/10.3390/membranes13090777.
[48] J. Xi, Z. Wu, X. Qiu, L. Chen, Nafion/SiO2 hybrid membrane for vanadium redox flow battery, J. Power Sources 166 (2) (2007) 531–536, https://doi.org/10.1016/j.jpowsour.2007.01.069.
[49] M. Skyllas-Kazacos, M. Chakrabarti, S. Hajimolana, F. Mjalli, M. Saleem, Progress in flow battery research and development, J. Electrochem. Soc. 158 (8) (2011) R55, https://doi.org/10.1149/1.3599565.
[50] S. Kim, E. Thomsen, G. Xia, Z. Nie, J. Bao, K. Recknagle, W. Wang, V. Viswanathan, Q. Luo, X. Wei, 1 kW/1 kWh advanced vanadium redox flow battery utilizing mixed acid electrolytes, J. Power Sources 237 (2013) 300–309, https://doi.org/10.1016/j.jpowsour.2013.02.045.
[51] J.L. Tami, M.M.R. Mazumder, G.E. Cook, S.D. Minteer, A.J. McNeil, Protocol for evaluating anion exchange membranes for nonaqueous redox flow batteries, ACS Appl. Mater. Interfaces 16 (40) (2024) 53643–53651, https://doi.org/10.1021/acsami.4c07026.
[52] Q. Duan, S. Ge, C.-Y. Wang, Water uptake, ionic conductivity and swelling properties of anion-exchange membrane, J. Power Sources 243 (2013) 773–778, https://doi.org/10.1016/j.jpowsour.2013.06.095.
[53] S. Mehanathan, H. Mohamed, J. Jaafar, H. Ilbeygi, Composite proton electrolyte membranes C poly ether-ether ketone (SPEEK) at various amount of mesoporous phosphotungstic acid (mPTA) for hydrogen fuel cell application, J. Appl. Membr. Sci. 24 (3) (2020), https://doi.org/10.11113/amst.v24n3.185.
[54] P.P. Sharma, Y. Jeon, D. Kim, Alkaline stable anion exchange membranes based on cross-linked poly(arylene ether sulfone) bearing dual quaternary piperidines for enhanced anion conductivity at low water uptake, Molecules 27 (2) (2022) 364, https://doi.org/10.3390/molecules27020364.
[55] Y. Zhao, P. Xiang, Y. Wang, X. Sun, D. Cao, H. Zhu, A high ion-conductive and stable porous membrane for neutral aqueous Zn-based flow batteries, J. Membr. Sci. 640 (2021) 119804, https://doi.org/10.1016/j.memsci.2021.119804.
[56] B. Zhang, Z. Yang, Q. Liu, Y. Liu, Y. Fu, X. Zhang, S. Jiang, X. Zhang, E. Zhang, K. Wang, Swelling-induced cross-linked pyridine-containing membranes with high stability and conductivity for vanadium redox flow batteries, ACS Sustain. Chem. Eng. 11 (31) (2023) 11601–11612, https://doi.org/10.1021/acssuschemeng.3c02436.
[57] Q. Ge, X. Zhu, Z. Yang, Highly conductive and water-swelling resistant anion exchange membrane for alkaline fuel cells, Int. J. Mol. Sci. 20 (14) (2019) 3470, https://doi.org/10.3390/ijms20143470.
[58] T. Mohammadi, S. Chieng, M.S. Kazacos, Water transport study across commercial ion exchange membranes in the vanadium redox flow battery, J. Membr. Sci. 133 (2) (1997) 151–159, https://doi.org/10.1016/S0376-7388(97)00092-6.
[59] E. Moukheiber, G. De Moor, L. Flandin, C. Bas, Investigation of ionomer structure through its dependence on ion exchange capacity (IEC), J. Membr. Sci. 389 (2012) 294–304, https://doi.org/10.1016/j.memsci.2011.10.041.
[60] S. Dharmalingam, V. Kugarajah, V. Elumalai, Proton exchange membrane for microbial fuel cells, PEM fuel Cells, Elsevier (2022) 25–53, https://doi.org/10.1016/B978-0-12-823708-3.00011-0.
[61] L. Wang, S. Rojas-Carbonell, K. Hu, B.P. Setzler, A.R. Motz, M.E. Ueckermann, Y. Yan, Standard operating protocol for ion-exchange capacity of anion exchange membranes, Front. Energy Res. 10 (2022) 887893, https://doi.org/10.3389/fenrg.2022.887893.
[62] M. Eti, N. Hidayati Othman, E. Güler, N. Kabay, Ion exchange membranes for reverse electrodialysis (RED) applications-recent developments, J. Membr. Sci. and Research 7(4) (2021) 260-267. doi: 10.22079/jmsr.2021.534937.1482.
[63] C. Ye, A. Wang, C. Breakwell, R. Tan, C. Grazia Bezzu, E. Hunter-Sellars, D. R. Williams, N.P. Brandon, P.A. Klusener, A.R. Kucernak, Development of efficient aqueous organic redox flow batteries using ion-sieving sulfonated polymer membranes, Nat. Commun. 13 (1) (2022) 3184, https://doi.org/10.1038/s41467-022-30943-y.
[64] V. Soldatov, Potentiometric titration of ion exchangers, React. Funct. Polym. 38 (2–3) (1998) 73–112, https://doi.org/10.1016/S1381-5148(98)00018-2.
[65] R. Yang, S. Zhang, Y. Zhu, A high performance, stable anion exchange membrane for alkaline redox flow batteries, J. Power Sources 594 (2024) 233974, https://doi.org/10.1016/j.jpowsour.2023.233974.

[66] E. Wiedemann, A. Heintz, R. Lichtenthaler, Transport properties of vanadium ions in cation exchange membranes: Determination of diffusion coefficients using a dialysis cell, J. Membr. Sci. 141 (2) (1998) 215–221, https://doi.org/10.1016/S0376-7388(97)00308-6.
[67] J.q. Chen, B.g. Wang, J.c. Yang, Adsorption and diffusion of VO2+ and VO2+ across cation membrane for all-vanadium redox flow battery, Solvent Extr. Ion Exch. 27(2) (2009) 312-327. doi: 10.1080/07366290802674614.
[68] J. Wu, C. Yuan, T. Li, Z. Yuan, H. Zhang, X. Li, Dendrite-free zinc-based battery with high areal capacity via the region-induced deposition effect of turing membrane, J. Am. Chem. Soc. 143 (33) (2021) 13135–13144, https://doi.org/10.1021/jacs.1c04317.
[69] H. Zou, Z. Xu, L. Xiong, J. Wang, H. Fu, J. Cao, M. Ding, X. Wang, C. Jia, An alkaline S/Fe redox flow battery endowed with high volumetric-capacity and long cycle-life, J. Power Sources 591 (2024) 233856, https://doi.org/10.1016/j.jpowsour.2023.233856.
[70] R. Tan, A. Wang, R. Malpass-Evans, R. Williams, E.W. Zhao, T. Liu, C. Ye, X. Zhou, B.P. Darwich, Z. Fan, Hydrophilic microporous membranes for selective ion separation and flow-battery energy storage, Nat. Mater. 19 (2) (2020) 195–202, https://doi.org/10.1038/s41563-019-0536-8.
[71] J. Ye, S. Yu, C. Zheng, T. Sun, J. Liu, H. Li, Advanced hybrid membrane for vanadium redox flow battery created by polytetrafluoroethylene layer and functionalized silicon carbide nanowires, Chem. Eng. J. 427 (2022) 131413, https://doi.org/10.1016/j.cej.2021.131413.
[72] J. Ye, J. Liu, C. Zheng, T. Sun, S. Yu, H. Li, Simple acid etched graphene oxide constructing high-performance sandwich structural hybrid membrane for redox flow battery, Sustain. Mater. Technol. 35 (2023) e00550, https://doi.org/10.1016/j.susmat.2022.e00550.
[73] J. Ye, Y. Cheng, L. Sun, M. Ding, C. Wu, D. Yuan, X. Zhao, C. Xiang, C. Jia, A green SPEEK/lignin composite membrane with high ion selectivity for vanadium redox flow battery, J. Membr. Sci. 572 (2019) 110–118, https://doi.org/10.1016/j.memsci.2018.11.009.
[74] C. Sun, J. Chen, H. Zhang, X. Han, Q. Luo, Investigations on transfer of water and vanadium ions across Nafion membrane in an operating vanadium redox flow battery, J. Power Sources 195 (3) (2010) 890–897, https://doi.org/10.1016/j.jpowsour.2009.08.041.
[75] D. Zhang, Z. Xu, X. Zhang, L. Zhao, Y. Zhao, S. Wang, W. Liu, X. Che, J. Yang, J. Liu, Oriented proton-conductive nanochannels boosting a highly conductive proton-exchange membrane for a vanadium redox flow battery, ACS Appl. Mater. Interfaces 13 (3) (2021) 4051–4061, https://doi.org/10.1021/acsami.0c20847.
[76] X. Teng, J. Dai, J. Su, G. Yin, Modification of Nafion membrane using fluorocarbon surfactant for all vanadium redox flow battery, J. Membr. Sci. 476 (2015) 20–29, https://doi.org/10.1016/j.memsci.2014.11.014.
[77] P. Arévalo-Cid, P. Dias, A. Mendes, J. Azevedo, Redox flow batteries: a new frontier on energy storage, Sust. Energy Fuels. 5 (21) (2021) 5366–5419, https://doi.org/10.1039/D1SE00839K.
[78] I.S. Chae, T. Luo, G.H. Moon, W. Ogieglo, Y.S. Kang, M. Wessling, Ultra-high proton/vanadium selectivity for hydrophobic polymer membranes with intrinsic nanopores for redox flow battery, Adv. Energy Mater. 6 (16) (2016), https://doi.org/10.1002/aenm.201600517.
[79] M. Amjadi, S. Rowshanzamir, S. Peighambardoust, M. Hosseini, M. Eikani, Investigation of physical properties and cell performance of Nafion/TiO2 nanocomposite membranes for high temperature PEM fuel cells, Int. J. Hydrog. Energy 35 (17) (2010) 9252–9260, https://doi.org/10.1016/j.ijhydene.2010.01.005.
[80] B. Jiang, L. Wu, L. Yu, X. Qiu, J. Xi, A comparative study of Nafion series membranes for vanadium redox flow batteries, J. Membr. Sci. 510 (2016) 18–26, https://doi.org/10.1016/j.memsci.2016.03.007.
[81] S. Lu, C. Wu, D. Liang, Q. Tan, Y. Xiang, Layer-by-layer self-assembly of Nafion–[CS–PWA] composite membranes with suppressed vanadium ion crossover for vanadium redox flow battery applications, RSC Adv. 4 (47) (2014) 24831–24837, https://doi.org/10.1039/C4RA01775G.
[82] L. Ding, X. Song, L. Wang, Z. Zhao, Enhancing proton conductivity of polybenzimidazole membranes by introducing sulfonate for vanadium redox flow batteries applications, J. Membr. Sci. 578 (2019) 126–135, https://doi.org/10.1016/j.memsci.2019.02.050.
[83] G.-J. Hwang, H. Ohya, Preparation of cation exchange membrane as a separator for the all-vanadium redox flow battery, J. Membr. Sci. 120 (1) (1996) 55–67, https://doi.org/10.1016/0376-7388(96)00135-4.
[84] S. Sang, Q. Wu, K. Huang, Preparation of zirconium phosphate (ZrP)/Nafion1135 composite membrane and H+/VO2+ transfer property investigation, J. Membr. Sci. 305 (1–2) (2007) 118–124, https://doi.org/10.1016/j.memsci.2007.07.041.
[85] W. Dai, L. Yu, Z. Li, J. Yan, L. Liu, J. Xi, X. Qiu, Sulfonated poly (ether ether ketone)/graphene composite membrane for vanadium redox flow battery, Electrochim. Acta 132 (2014) 200–207, https://doi.org/10.1016/j.electacta.2014.03.156.
[86] L. Xu, M. Dang, F. Yang, F. Lang, B. Li, L. Liang, J. Pang, X.-H. Bu, Rational tuning the proton conductivity and stability of hydrogen-bonded organic frameworks, Inorg. Chem. 63 (38) (2024) 17747–17754, https://doi.org/10.1021/acs.inorgchem.4c02575.
[87] T.-X. Luan, Q. Wang, P. Zhang, W. Li, S. Kong, Y. Feng, S. Yuan, P.-Z. Li, Remarkably enhancing proton conductivity by intrinsic surface sulfonation of a pyrazine-linked covalent organic framework, Sci. China Mater. 67 (1) (2024) 125–133, https://doi.org/10.1007/s40843-023-2685-5.
[88] M. Atiqur Rahman, M.S. Islam, M. Fukuda, J. Yagyu, Z. Feng, Y. Sekine, L. F. Lindoy, J. Ohyama, S. Hayami, High proton conductivity of 3D graphene oxide intercalated with aromatic sulfonic acids, ChemPlusChem 87 (4) (2022) e202200003, https://doi.org/10.1002/cplu.202200003.
[89] Z. Sheng, S. Xiao, G. Zeng, Q. He, Z. Chen, J. Duan, S. Peng, Maximizing flow battery membrane performance via pseudo-nanophase separation enhanced by polymer supramolecular sidechain, J. Membr. Sci. 713 (2025) 123280, https://doi.org/10.1016/j.memsci.2024.123280. Get rights and content.
[90] Y. Xia, X. Hou, X. Chen, F. Mu, Y. Wang, L. Dai, X. Liu, Y. Yu, K. Huang, W. Xing, Membrane with horizontally rigid zeolite nanosheet arrays against zinc dendrites in zinc-based flow battery, Chem. Eng. J. 465 (2023) 142912, https://doi.org/10.1016/j.cej.2023.142912.
[91] L. Su, D. Zhang, S. Peng, X. Wu, Y. Luo, G. He, Orientated graphene oxide/Nafion ultra-thin layer coated composite membranes for vanadium redox flow battery, Int. J. Hydrog. Energy 42 (34) (2017) 21806–21816, https://doi.org/10.1016/j.ijhydene.2017.07.049.
[92] X. Teng, J. Dai, F. Bi, X. Jiang, Y. Song, G. Yin, Ultra-thin polytetrafluoroethene/Nafion/silica membranes prepared with nano SiO2 and its comparison with sol–gel derived one for vanadium redox flow battery, Solid State Ion. 280 (2015) 30–36, https://doi.org/10.1016/j.ssi.2015.08.005.
[93] X. Ling, C. Jia, J. Liu, C. Yan, Preparation and characterization of sulfonated poly (ether sulfone)/sulfonated poly (ether ether ketone) blend membrane for vanadium redox flow battery, J. Membr. Sci. 415 (2012) 306–312, https://doi.org/10.1016/j.memsci.2012.05.014.
[94] J. Dai, X. Teng, Y. Song, J. Ren, Effect of casting solvent and annealing temperature on recast Nafion membranes for vanadium redox flow battery, J. Membr. Sci. 522 (2017) 56–67, https://doi.org/10.1016/j.memsci.2016.09.014.
[95] F. Ai, Z. Wang, N.-C. Lai, Q. Zou, Z. Liang, Y.-C. Lu, Heteropoly acid negolytes for high-power-density aqueous redox flow batteries at low temperatures, Nat. Energy 7 (5) (2022) 417–426, https://doi.org/10.1038/s41560-022-01011-y.
[96] Y. Shi, Z. Wang, Y. Yao, W. Wang, Y.-C. Lu, High-areal-capacity conversion type iron-based hybrid redox flow batteries, Energy Environ. Sci. 14 (12) (2021) 6329–6337, https://doi.org/10.1039/D1EE02258J.
[97] J. Cao, Z. Yuan, X. Li, W. Xu, H. Zhang, Hydrophilic poly (vinylidene fluoride) porous membrane with well connected ion transport networks for vanadium flow battery, J. Power Sources 298 (2015) 228–235, https://doi.org/10.1016/j.jpowsour.2015.08.067.
[98] Z. Yuan, X. Li, Y. Zhao, H. Zhang, Mechanism of polysulfone-based anion exchange membranes degradation in vanadium flow battery, ACS Appl. Mater. Interfaces 7 (34) (2015) 19446–19454, https://doi.org/10.1021/acsami.5b05840.
[99] Z. Yuan, X. Li, J. Hu, W. Xu, J. Cao, H. Zhang, Degradation mechanism of sulfonated poly (ether ether ketone)(SPEEK) ion exchange membranes under vanadium flow battery medium, Phys. Chem. Chem. Phys. 16 (37) (2014) 19841–19847, https://doi.org/10.1039/C4CP03329A.
[100] X. Shi, O.C. Esan, X. Huo, Y. Ma, Z. Pan, L. An, T. Zhao, Polymer electrolyte membranes for vanadium redox flow batteries: fundamentals and applications, Prog. Energy Combust. Sci. 85 (2021) 100926, https://doi.org/10.1016/j.pecs.2021.100926.
[101] Q. Wang, Z. Qu, Z. Jiang, W. Yang, Experimental study on the performance of a vanadium redox flow battery with non-uniformly compressed carbon felt electrode, Appl. Energy 213 (2018) 293–305, https://doi.org/10.1016/j.apenergy.2018.01.047.
[102] N. Zhao, A. Platt, H. Riley, R. Qiao, R. Neagu, Z. Shi, Strategy towards high ion selectivity membranes for all-vanadium redox flow batteries, J. Energy Storage 72 (2023) 108321, https://doi.org/10.1016/j.est.2023.108321.
[103] J. Liao, M. Lu, Y.Q. Chu, J. Wang, Ultra-low vanadium ion diffusion amphoteric ion-exchange membranes for all-vanadium redox flow batteries, J. Power Sources 282 (2015) 241–247, https://doi.org/10.1016/j.jpowsour.2015.02.025.
[104] D. Zhang, Q. Wang, S. Peng, X. Yan, X. Wu, G. He, An interface-strengthened cross-linked graphene oxide/Nafion212 composite membrane for vanadium flow batteries, J. Membr. Sci. 587 (2019) 117189, https://doi.org/10.1016/j.memsci.2019.117189.
[105] R. Niu, L. Kong, L. Zheng, H. Wang, H. Shi, Novel graphitic carbon nitride nanosheets/sulfonated poly (ether ether ketone) acid-base hybrid membrane for vanadium redox flow battery, J. Membr. Sci. 525 (2017) 220–228, https://doi.org/10.1016/j.memsci.2016.10.049.
[106] X.Z. Yuan, C. Song, A. Platt, N. Zhao, H. Wang, H. Li, K. Fatih, D. Jang, A review of all-vanadium redox flow battery durability: Degradation mechanisms and mitigation strategies, Int. J. Energy Res. 43 (13) (2019) 6599–6638, https://doi.org/10.1002/er.4607.
[107] K. Gong, X. Ma, K.M. Conforti, K.J. Kuttler, J.B. Grunewald, K.L. Yeager, M. Z. Bazant, S. Gu, Y. Yan, A zinc–iron redox-flow battery under $100 per kW h of system capital cost, Energy Environ. Sci. 8 (10) (2015) 2941–2945, https://doi.org/10.1039/C5EE02315G.
[108] Y. Zeng, T. Zhao, L. An, X. Zhou, L. Wei, A comparative study of all-vanadium and iron-chromium redox flow batteries for large-scale energy storage, J. Power Sources 300 (2015) 438–443, https://doi.org/10.1016/j.jpowsour.2015.09.100.
[109] F. Wang, F. Ai, Y.-C. Lu, Ion selective membrane for redox flow battery, what's next? Next Energy 1 (3) (2023) 100053 https://doi.org/10.1016/j.nxener.2023.100053.
[110] C. Minke, T. Turek, Materials, system designs and modelling approaches in techno-economic assessment of all-vanadium redox flow batteries–a review, J. Power Sources 376 (2018) 66–81, https://doi.org/10.1016/j.jpowsour.2017.11.058.
[111] V. Viswanathan, A. Crawford, D. Stephenson, S. Kim, W. Wang, B. Li, G. Coffey, E. Thomsen, G. Graff, P. Balducci, Cost and performance model for redox flow

batteries, J. Power Sources 247 (2014) 1040–1051, https://doi.org/10.1016/j.jpowsour.2012.12.023.
[112] A. Trovo, M. Rugna, N. Poli, M. Guarnieri, Prospects for industrial vanadium flow batteries, Ceram. Int. 49 (14) (2023) 24487–24498, https://doi.org/10.1016/j.ceramint.2023.01.165.
[113] C. Minke, T. Turek, Economics of vanadium redox flow battery membranes, J. Power Sources 286 (2015) 247–257, https://doi.org/10.1016/j.jpowsour.2015.03.144.
[114] W. Wang, Q. Luo, B. Li, X. Wei, L. Li, Z. Yang, Recent progress in redox flow battery research and development, Adv. Funct. Mater. 23 (8) (2013) 970–986, https://doi.org/10.1002/adfm.201200694.
[115] R.A. Potash, J.R. McKone, S. Conte, H.D. Abruna, On the benefits of a symmetric redox flow battery, J. Electrochem. Soc. 163 (3) (2015) A338, https://doi.org/10.1149/2.0971602jes.
[116] D. Düerkop, H. Widdecke, C. Schilde, U. Kunz, A. Schmiemann, Polymer membranes for all-vanadium redox flow batteries: a review, Membranes 11 (3) (2021) 214, https://doi.org/10.3390/membranes11030214.
[117] T. Xu, Ion exchange membranes: State of their development and perspective, J. Membr. Sci. 263 (1–2) (2005) 1–29, https://doi.org/10.1016/j.memsci.2005.05.002.
[118] G.-J. Hwang, S.-W. Kim, D.-M. In, D.-Y. Lee, C.-H. Ryu, Application of the commercial ion exchange membranes in the all-vanadium redox flow battery, J. Ind. Eng. Chem. 60 (2018) 360–365, https://doi.org/10.1016/j.jiec.2017.11.023.
[119] H. An, R. Zhang, W. Li, P. Li, H. Qian, H. Yang, Surface-modified approach to fabricate nafion membranes covalently bonded with polyhedral oligosilsesquioxane for vanadium redox flow batteries, ACS Appl. Mater. Interfaces 14 (6) (2022) 7845–7855, https://doi.org/10.1021/acsami.1c20627.
[120] P. Qian, H. Wang, J. Sheng, Y. Zhou, H. Shi, Ultrahigh proton conductive nanofibrous composite membrane with an interpenetrating framework and enhanced acid-base interfacial layers for vanadium redox flow battery, J. Membr. Sci. 647 (2022) 120327, https://doi.org/10.1016/j.memsci.2022.120327.
[121] H.J. Lee, S. Park, H. Kim, Analysis of the effect of MnO2 precipitation on the performance of a vanadium/manganese redox flow battery, J. Electrochem. Soc. 165 (5) (2018) A952, https://doi.org/10.1149/2.0881805jes.
[122] Y. Peng, W.K. Wong, Z. Hu, Y. Cheng, D. Yuan, S.A. Khan, D. Zhao, Room temperature batch and continuous flow synthesis of water-stable covalent organic frameworks (COFs), Chem. Mater. 28 (14) (2016) 5095–5101, https://doi.org/10.1021/acs.chemmater.6b01954.
[123] H. Liu, F. Tian, L. Lei, C. Zhang, Y. Bai, Y. Zhao, L. Dong, Metal-incorporated covalent organic framework membranes via layer-by-layer self-assembly for efficient antibiotic desalination, Desalination (2025) 118537, https://doi.org/10.1016/j.desal.2025.118537.
[124] C. Jia, X. Chen, W. Peng, Q. Yu, D. Zhang, Y. Huang, G. Li, M. Rezakazemi, R. Huang, MOF membranes for enhanced gas separation: materials, mechanisms, and application prospects—a comprehensive survey, Adv. Compos. Hybrid Mater. 7 (6) (2024) 221, https://doi.org/10.1007/s42114-024-01022-1.
[125] W. Fan, X. Zhang, Z. Kang, X. Liu, D. Sun, Isoreticular chemistry within metal–organic frameworks for gas storage and separation, Coord. Chem. Rev. 443 (2021) 213968, https://doi.org/10.1016/j.ccr.2021.213968.
[126] L. Yang, S. Qian, X. Wang, X. Cui, B. Chen, H. Xing, Energy-efficient separation alternatives: metal–organic frameworks and membranes for hydrocarbon separation, Chem. Soc. Rev. 49 (15) (2020) 5359–5406, https://doi.org/10.1039/C9CS00756C.
[127] C. Yang, L. Pan, Q. Jian, Recent advances in sulfonated poly (ether ether ketone) membrane for vanadium redox flow batteries, Future Batteries (2025) 100026, https://doi.org/10.1016/j.fub.2025.100026.
[128] J.-M. García-Martínez, E.P. Collar, Current and future insights in organic–inorganic hybrid materials, Polymers 16 (21) (2024) 3043, https://doi.org/10.3390/polym16213043.
[129] Q. Yan, H. Toghiani, H. Causey, Steady state and dynamic performance of proton exchange membrane fuel cells (PEMFCs) under various operating conditions and load changes, J. Power Sources 161 (1) (2006) 492–502, https://doi.org/10.1016/j.jpowsour.2006.03.077.
[130] X. Chu, H. Zhang, C. Zhang, R. Shao, Z. Huang, H. Lv, S. Liu, L. Liu, N. Li, S. Zhao, Aryl-ether-free polyphenylene-based anion exchange membranes incorporating N-cyclic quaternary ammoniums for enhanced alkaline fuel cell performance, J. Membr. Sci. 715 (2025) 123455, https://doi.org/10.1016/j.memsci.2024.123455.
[131] H. Yang, P. Ding, M. Vagin, V. Gueskine, M. Berggren, I. Engquist, Nanocellulose-based ion-selective membranes for an aqueous organic redox flow battery, Cellul. 31 (18) (2024) 10831–10843, https://doi.org/10.1007/s10570-024-06240-w.
[132] H. Prifti, A. Parasuraman, S. Winardi, T.M. Lim, M. Skyllas-Kazacos, Membranes for redox flow battery applications, Membranes 2 (2) (2012) 275–306, https://doi.org/10.3390/membranes2020275.
[133] J. Winsberg, T. Hagemann, T. Janoschka, M.D. Hager, U.S. Schubert, Redox-flow batteries: from metals to organic redox-active materials, Angew. Chem. Int. Ed. 56 (3) (2017) 686–711, https://doi.org/10.1002/anie.201604925.
[134] Q. Luo, H. Zhang, J. Chen, D. You, C. Sun, Y. Zhang, Preparation and characterization of Nafion/SPEEK layered composite membrane and its application in vanadium redox flow battery, J. Membr. Sci. 325 (2) (2008) 553–558, https://doi.org/10.1016/j.memsci.2008.08.025.
[135] M. Vijayakumar, M. Bhuvaneswari, P. Nachimuthu, B. Schwenzer, S. Kim, Z. Yang, J. Liu, G.L. Graff, S. Thevuthasan, J. Hu, Spectroscopic investigations of the fouling process on Nafion membranes in vanadium redox flow batteries, J. Membr. Sci. 366 (1–2) (2011) 325–334, https://doi.org/10.1016/j.memsci.2010.10.018.
[136] S. Kim, T.B. Tighe, B. Schwenzer, J. Yan, J. Zhang, J. Liu, Z. Yang, M.A. Hickner, Chemical and mechanical degradation of sulfonated poly (sulfone) membranes in vanadium redox flow batteries, J. Appl. Electrochem. 41 (2011) 1201–1213, https://doi.org/10.1007/s10800-011-0313-0.
[137] D. Chen, M.A. Hickner, V 5+ degradation of sulfonated Radel membranes for vanadium redox flow batteries, Phys. Chem. Chem. Phys. 15 (27) (2013) 11299–11305, https://doi.org/10.1039/C3CP52035H.
[138] K.F. Hagesteijn, S. Jiang, B.P. Ladewig, A review of the synthesis and characterization of anion exchange membranes, J. Mater. Sci. 53 (16) (2018) 11131–11150, https://doi.org/10.1007/s10853-018-2409-y.
[139] B. Hu, C. DeBruler, Z. Rhodes, T.L. Liu, Long-cycling aqueous organic redox flow battery (AORFB) toward sustainable and safe energy storage, J. Am. Chem. Soc. 139 (3) (2017) 1207–1214, https://doi.org/10.1021/jacs.6b10984.
[140] Y. Li, Y. Liu, Z. Xu, Z. Yang, Poly (phenylene oxide)-based ion-exchange membranes for aqueous organic redox flow battery, Ind. Eng. Chem. Res. 58 (25) (2019) 10707–10712, https://doi.org/10.1021/acs.iecr.9b01377.
[141] J. Qiu, M. Zhai, J. Chen, Y. Wang, J. Peng, L. Xu, J. Li, G. Wei, Performance of vanadium redox flow battery with a novel amphoteric ion exchange membrane synthesized by two-step grafting method, J. Membr. Sci. 342 (1–2) (2009) 215–220, https://doi.org/10.1016/j.memsci.2009.06.043.
[142] J. Ran, L. Wu, Y. He, Z. Yang, Y. Wang, C. Jiang, L. Ge, E. Bakangura, T. Xu, Ion exchange membranes: New developments and applications, J. Membr. Sci. 522 (2017) 267–291, https://doi.org/10.1016/j.memsci.2016.09.033.
[143] J. Thomas, M.E. Thomas, S. Thomas, A. Schechter, F. Grynszpan, A perspective into recent progress on the tailored cationic group-based polymeric anion exchange membranes intended for electrochemical energy applications, Mater. Today Chem. 35 (2024) 101866, https://doi.org/10.1016/j.mtchem.2023.101866.
[144] Y. Cui, X. Chen, Y. Wang, J. Peng, L. Zhao, J. Du, M. Zhai, Amphoteric ion exchange membranes prepared by preirradiation-induced emulsion graft copolymerization for vanadium redox flow battery, Polymers 11 (9) (2019) 1482, https://doi.org/10.3390/polym11091482.
[145] H. Wang, X. Li, X. Zhuang, B. Cheng, W. Wang, W. Kang, L. Shi, H. Li, Modification of Nafion membrane with biofunctional SiO2 nanofiber for proton exchange membrane fuel cells, J. Power Sources 340 (2017) 201–209, https://doi.org/10.1016/j.jpowsour.2016.11.072.
[146] J. Li, X. Chen, J. Liao, Y. Li, J. Mu, Y. Xu, Y. Du, H. Ruan, X. Xu, J. Shen, The endowment of monovalent anion selectivity and antifouling property to cross-linked ion-exchange membranes by constructing amphoteric structure, Sep. Purif. Technol. 328 (2024) 125104, https://doi.org/10.1016/j.seppur.2023.125104.
[147] W. Dai, Y. Shen, Z. Li, L. Yu, J. Xi, X. Qiu, SPEEK/Graphene oxide nanocomposite membranes with superior cyclability for highly efficient vanadium redox flow battery, J. Mater. Chem. A2 (31) (2014) 12423–12432, https://doi.org/10.1039/C4TA02124J.
[148] C. Jia, Y. Cheng, X. Ling, G. Wei, J. Liu, C. Yan, Sulfonated poly (ether ether ketone)/functionalized carbon nanotube composite membrane for vanadium redox flow battery applications, Electrochim. Acta 153 (2015) 44–48, https://doi.org/10.1016/j.electacta.2014.11.123.
[149] S.I. Hossain, M.A. Aziz, D. Han, P. Selvam, S. Shanmugam, Fabrication of SPAEK–cerium zirconium oxide nanotube composite membrane with outstanding performance and durability for vanadium redox flow batteries, J. Mater. Chem. A6 (41) (2018) 20205–20213, https://doi.org/10.1039/C8TA08349E.
[150] Y. Zhang, H. Wang, W. Yu, H. Shi, Structure and properties of sulfonated poly (ether ether ketone) hybrid membrane with polyaniline-chains-modified graphene oxide and its application for vanadium redox flow battery, ChemistrySelect 3 (32) (2018) 9249–9258, https://doi.org/10.1002/slct.201801548.
[151] Y. Ahn, D. Kim, Ultra-low vanadium ion permeable electrolyte membrane for vanadium redox flow battery by pore filling of PTFE substrate, Energy Storage Mater. 31 (2020) 105–114, https://doi.org/10.1016/j.ensm.2020.06.035.
[152] X. Lou, B. Lu, M. He, Y. Yu, X. Zhu, F. Peng, C. Qin, M. Ding, C. Jia, Functionalized carbon black modified sulfonated polyether ether ketone membrane for highly stable vanadium redox flow battery, J. Membr. Sci. 643 (2022) 120015, https://doi.org/10.1016/j.memsci.2021.120015.
[153] J. Li, J. Liu, W. Xu, J. Long, W. Huang, Y. Zhang, L. Chu, Highly ion-selective sulfonated polyimide membranes with covalent self-crosslinking and branching structures for vanadium redox flow battery, Chem. Eng. J. 437 (2022) 135414, https://doi.org/10.1016/j.cej.2022.135414.
[154] W. Chen, B. Pang, X. Yan, X. Jiang, F. Cui, X. Wu, G. He, Oxidized black phosphorus nanosheets/sulfonated poly (ether ether ketone) composite membrane for vanadium redox flow battery, J. Membr. Sci. 644 (2022) 120084, https://doi.org/10.1016/j.memsci.2021.120084.
[155] M.S. Cha, H.Y. Jeong, H.Y. Shin, S.H. Hong, T.-H. Kim, S.-G. Oh, J.Y. Lee, Y. T. Hong, Crosslinked anion exchange membranes with primary diamine-based crosslinkers for vanadium redox flow battery application, J. Power Sources 363 (2017) 78–86, https://doi.org/10.1016/j.jpowsour.2017.07.068.
[156] Y. Ma, L. Li, L. Ma, N.A. Qaisrani, S. Gong, P. Li, F. Zhang, G. He, Cyclodextrin templated nanoporous anion exchange membrane for vanadium flow battery application, J. Membr. Sci. 586 (2019) 98–105, https://doi.org/10.1016/j.memsci.2019.05.055.
[157] J. Si, Y. Lv, S. Lu, Y. Xiang, Microscopic phase-segregated quaternary ammonia polysulfone membrane for vanadium redox flow batteries, J. Power Sources 428 (2019) 88–92, https://doi.org/10.1016/j.jpowsour.2019.04.100.

[158] M.S. Cha, S.W. Jo, S.H. Han, S.H. Hong, S. So, T.-H. Kim, S.-G. Oh, Y.T. Hong, J. Y. Lee, Ether-free polymeric anion exchange materials with extremely low vanadium ion permeability and outstanding cell performance for vanadium redox flow battery (VRFB) application, J. Power Sources 413 (2019) 158–166, https://doi.org/10.1016/j.jpowsour.2018.12.036.
[159] W. Xu, J. Long, J. Liu, H. Luo, H. Duan, Y. Zhang, J. Li, X. Qi, L. Chu, A novel porous polyimide membrane with ultrahigh chemical stability for application in vanadium redox flow battery, Chem. Eng. J. 428 (2022) 131203, https://doi.org/10.1016/j.cej.2021.131203.
[160] X. Che, W. Tang, J. Dong, D. Aili, J. Yang, Anion exchange membranes based on long side-chain quaternary ammonium-functionalized poly (arylene piperidinium) s for vanadium redox flow batteries, Sci. China Mater. 65 (3) (2022) 683–694, https://doi.org/10.1007/s40843-021-1786-0.
[161] A.K. Singh, P. Sharma, K. Singh, V.K. Shahi, Improved performance of vanadium redox flow battery with tuneable alkyl spacer based cross-linked anion exchange membranes, J. Power Sources 520 (2022) 230856, https://doi.org/10.1016/j.jpowsour.2021.230856.
[162] J. Qiu, J. Zhang, J. Chen, J. Peng, L. Xu, M. Zhai, J. Li, G. Wei, Amphoteric ion exchange membrane synthesized by radiation-induced graft copolymerization of styrene and dimethylaminoethyl methacrylate into PVDF film for vanadium redox flow battery applications, J. Membr. Sci. 334 (1–2) (2009) 9–15, https://doi.org/10.1016/j.memsci.2009.02.009.
[163] S. Liu, L. Wang, Y. Ding, B. Liu, X. Han, Y. Song, Novel sulfonated poly (ether ether keton)/polyetherimide acid-base blend membranes for vanadium redox flow battery applications, Electrochim. Acta 130 (2014) 90–96, https://doi.org/10.1016/j.electacta.2014.02.144.
[164] L. Cao, Q. Sun, Y. Gao, L. Liu, H. Shi, Novel acid-base hybrid membrane based on amine-functionalized reduced graphene oxide and sulfonated polyimide for vanadium redox flow battery, Electrochim. Acta 158 (2015) 24–34, https://doi.org/10.1016/j.electacta.2015.01.159.
[165] S. Liu, L. Wang, D. Li, B. Liu, J. Wang, Y. Song, Novel amphoteric ion exchange membranes by blending sulfonated poly (ether ether ketone)/quaternized poly (ether imide) for vanadium redox flow battery applications, J. Mater. Chem. A3 (34) (2015) 17590–17597, https://doi.org/10.1039/C5TA04351D.
[166] S. Liu, D. Li, L. Wang, H. Yang, X. Han, B. Liu, Ethylenediamine-functionalized graphene oxide incorporated acid-base ion exchange membranes for vanadium redox flow battery, Electrochim. Acta 230 (2017) 204–211, https://doi.org/10.1016/j.electacta.2017.01.170.
[167] D. Chen, X. Chen, L. Ding, X. Li, Advanced acid-base blend ion exchange membranes with high performance for vanadium flow battery application, J. Membr. Sci. 553 (2018) 25–31, https://doi.org/10.1016/j.memsci.2018.02.039.
[168] J. Dai, Y. Dong, C. Yu, Y. Liu, X. Teng, A novel Nafion-g-PSBMA membrane prepared by grafting zwitterionic SBMA onto Nafion via SI-ATRP for vanadium redox flow battery application, J. Membr. Sci. 554 (2018) 324–330, https://doi.org/10.1016/j.memsci.2018.03.017.
[169] W. Lu, Z. Yuan, M. Li, X. Li, H. Zhang, I. Vankelecom, Solvent-induced rearrangement of ion-transport channels: a way to create advanced porous membranes for vanadium flow batteries, Adv. Funct. Mater. 27 (4) (2017) 1604587, https://doi.org/10.1002/adfm.201604587.
[170] H. Zhang, H. Zhang, X. Li, Z. Mai, J. Zhang, Nanofiltration (NF) membranes: the next generation separators for all vanadium redox flow batteries (VRBs)? Energy Environ. Sci. 4 (5) (2011) 1676–1679, https://doi.org/10.1039/C1EE01117K.
[171] H. Dou, M. Xu, B. Wang, Z. Zhang, G. Wen, Y. Zheng, D. Luo, L. Zhao, A. Yu, L. Zhang, Microporous framework membranes for precise molecule/ion separations, Chem. Soc. Rev. 50 (2) (2021) 986–1029, https://doi.org/10.1039/D0CS00552E.
[172] B. Zdravkov, J. Čermák, M. Šefara, J. Janků, Pore classification in the characterization of porous materials: a perspective, Open Chem. 5 (2) (2007) 385–395, https://doi.org/10.2478/s11532-007-0017-9.
[173] J.-X. Jiang, A.I. Cooper, Microporous organic polymers: design, synthesis, and function, Functional metal-organic frameworks: Gas storage, separation and catalysis (2010) 1-33. doi: 10.1007/128_2009_5.
[174] P. Aptel, J. Armor, R. Audinos, R.W. Baker, R. Bakish, G. Belfort, B. Bikson, R. G. Brown, M. Bryk, J.J. Burke, Terminology for membranes and membrane processes (IUPAC Recommendations 1996), J. Membr. Sci. 120 (2) (1996) 149–159, https://doi.org/10.1016/0376-7388(96)82861-4.
[175] X. Zhou, T. Zhao, L. An, Y. Zeng, L. Wei, Modeling of ion transport through a porous separator in vanadium redox flow batteries, J. Power Sources 327 (2016) 67–76, https://doi.org/10.1016/j.jpowsour.2016.07.046.
[176] Y. Li, H. Zhang, H. Zhang, J. Cao, W. Xu, X. Li, Hydrophilic porous poly (sulfone) membranes modified by UV-initiated polymerization for vanadium flow battery application, J. Membr. Sci. 454 (2014) 478–487, https://doi.org/10.1016/j.memsci.2013.12.015.
[177] Z. Yuan, X. Zhu, M. Li, W. Lu, X. Li, H. Zhang, A highly ion-selective zeolite flake layer on porous membranes for flow battery applications, Angew. Chem. 128 (9) (2016) 3110–3114, https://doi.org/10.1002/ange.201510849.
[178] M.A.A. Shahmirzadi, S.S. Hosseini, G. Ruan, N. Tan, Tailoring PES nanofiltration membranes through systematic investigations of prominent design, fabrication and operational parameters, RSC Adv. 5 (61) (2015) 49080–49097, https://doi.org/10.1039/C5RA05985B.
[179] N.W. Ockwig, O. Delgado-Friedrichs, M. O'Keeffe, O.M. Yaghi, Reticular chemistry: occurrence and taxonomy of nets and grammar for the design of frameworks, Acc. Chem. Res. 38 (3) (2005) 176–182, https://doi.org/10.1021/ar020022l.
[180] O.M. Yaghi, Reticular chemistry construction, properties, and precision reactions of frameworks, ACS Publications (2016) 15507–15509, https://doi.org/10.1021/jacs.6b11821.
[181] O.M. Yaghi, M. O'Keeffe, N.W. Ockwig, H.K. Chae, M. Eddaoudi, J. Kim, Reticular synthesis and the design of new materials, Nature 423 (6941) (2003) 705–714, https://doi.org/10.1038/nature01650.
[182] M. Rubio-Martinez, C. Avci-Camur, A.W. Thornton, I. Imaz, D. Maspoch, M. R. Hill, New synthetic routes towards MOF production at scale, Chem. Soc. Rev. 46 (11) (2017) 3453–3480, https://doi.org/10.1039/C7CS00109F.
[183] P.Z. Moghadam, A. Li, S.B. Wiggin, A. Tao, A.G. Maloney, P.A. Wood, S.C. Ward, D. Fairen-Jimenez, Development of a Cambridge Structural Database subset: a collection of metal–organic frameworks for past, present, and future, Chem. Mater. 29 (7) (2017) 2618–2625, https://doi.org/10.1021/acs.chemmater.7b00441.
[184] R.-B. Lin, S. Xiang, W. Zhou, B. Chen, Microporous metal-organic framework materials for gas separation, Chem 6 (2) (2020) 337–363, https://doi.org/10.1016/j.chempr.2019.10.012.
[185] F. Ahmadijokani, S. Tajahmadi, A. Bahi, H. Molavi, M. Rezakazemi, F. Ko, T. M. Aminabhavi, M. Arjmand, Ethylenediamine-functionalized Zr-based MOF for efficient removal of heavy metal ions from water, Chemosphere 264 (2021) 128466, https://doi.org/10.1016/j.chemosphere.2020.128466.
[186] T. Islamoglu, S. Goswami, Z. Li, A.J. Howarth, O.K. Farha, J.T. Hupp, Postsynthetic tuning of metal–organic frameworks for targeted applications, Acc. Chem. Res. 50 (4) (2017) 805–813, https://doi.org/10.1021/acs.accounts.6b00577.
[187] Y. Sun, UiO-66 metal-organic framework membranes: structural engineering for separation applications, Membranes 15 (1) (2025) 8, https://doi.org/10.3390/membranes15010008.
[188] Q. Chen, Y. Tang, Y.M. Ding, H.Y. Jiang, Z.B. Zhang, W.X. Li, M.L. Liu, S.P. Sun, Synergistic construction of sub-nanometer channel membranes through MOF–polymer composites: strategies and nanofiltration applications, Polymers 16 (2024) 1653, https://doi.org/10.3390/polym16121653.
[189] Z. Xu, C. Liu, L. Xiao, Q. Meng, G. Zhang, Metal-organic frameworks-based mixed matrix pervaporation membranes for recovery of organics, Adv. Membr. 4 (2024) 100092, https://doi.org/10.1016/j.advmem.2024.100092.
[190] N.H. Kwon, S. Han, J. Kim, E.S. Cho, Super proton conductivity through control of hydrogen-bonding networks in flexible metal–organic frameworks, Small 19 (32) (2023) 2301122, https://doi.org/10.1002/smll.202301122.
[191] S. Liu, X. Sang, L. Wang, J. Zhang, J. Song, B. Han, Incorporation of metal-organic framework in polymer membrane enhances vanadium flow battery performance, Electrochim. Acta 257 (2017) 243–249, https://doi.org/10.1016/j.electacta.2017.10.084.
[192] S. Ge, K. Wei, W. Peng, R. Huang, E. Akinlabi, H. Xia, M.W. Shahzad, X. Zhang, B. B. Xu, J. Jiang, A comprehensive review of covalent organic frameworks (COFs) and their derivatives in environmental pollution control, Chem. Soc. Rev. (2024), https://doi.org/10.1039/D4CS00521J.
[193] J. Zhou, Y. Wang, Selective swelling of block copolymers: an upscalable greener process to ultrafiltration membranes? Macromolecules 53 (1) (2019) 5–17, https://doi.org/10.1021/acs.macromol.9b01747.
[194] Z. Wang, S. Zhang, Y. Chen, Z. Zhang, S. Ma, Covalent organic frameworks for separation applications, Chem. Soc. Rev. 49 (3) (2020) 708–735, https://doi.org/10.1039/C9CS00827F.
[195] J. Liu, M. Zhang, N. Wang, C. Wang, L. Ma, Research progress of covalent organic framework materials in catalysis, Acta Chim. Sin. 78 (4) (2020) 311, https://doi.org/10.6023/A19120426.
[196] W.K. Haug, E.M. Moscarello, E.R. Wolfson, P.L. McGrier, The luminescent and photophysical properties of covalent organic frameworks, Chem. Soc. Rev. 49 (3) (2020) 839–864, https://doi.org/10.1039/C9CS00807A.
[197] H. Wang, Z. Zeng, P. Xu, L. Li, G. Zeng, R. Xiao, Z. Tang, D. Huang, L. Tang, C. Lai, Recent progress in covalent organic framework thin films: fabrications, applications and perspectives, Chem. Soc. Rev. 48 (2) (2019) 488–516, https://doi.org/10.1039/C8CS00376A.
[198] X. Liu, D. Huang, C. Lai, G. Zeng, L. Qin, H. Wang, H. Yi, B. Li, S. Liu, M. Zhang, Recent advances in covalent organic frameworks (COFs) as a smart sensing material, Chem. Soc. Rev. 48 (20) (2019) 5266–5302, https://doi.org/10.1039/C9CS00299E.
[199] C.Y. Lin, D. Zhang, Z. Zhao, Z. Xia, Covalent organic framework electrocatalysts for clean energy conversion, Adv. Mater. 30 (5) (2018) 1703646, https://doi.org/10.1002/adma.201703646.
[200] K. Dey, M. Pal, K.C. Rout, S. Kunjattu H, A. Das, R. Mukherjee, U.K. Kharul, R. Banerjee, Selective molecular separation by interfacially crystallized covalent organic framework thin films, J. Am. Chem. Soc. 139(37) (2017) 13083-13091. doi: 10.1021/jacs.7b06640.
[201] S. Maiti, S.S. Islam, S. Bose, Covalent organic framework assisted interlocked graphene oxide based thin-film composite membrane for effective water remediation, Environ. Sci.: Water Res. Technol. 9(1) (2023) 249-264. doi: 10.1039/D2EW00545J.
[202] G. Li, K. Zhang, T. Tsuru, Two-dimensional covalent organic framework (COF) membranes fabricated via the assembly of exfoliated COF nanosheets, ACS Appl. Mater. Interfaces 9 (10) (2017) 8433–8436, https://doi.org/10.1021/acsami.6b15752.
[203] M. Fang, C. Montoro, M. Semsarilar, Metal and covalent organic frameworks for membrane applications, Membranes 10 (5) (2020) 107, https://doi.org/10.3390/membranes10050107.

[204] H.B. Park, J. Kamcev, L.M. Robeson, M. Elimelech, B.D. Freeman, Maximizing the right stuff: the trade-off between membrane permeability and selectivity, Science 356 (6343) (2017) eaab0530, https://doi.org/10.1126/science.aab0530.
[205] D. Shi, X. Yu, W. Fan, V. Wee, D. Zhao, Polycrystalline zeolite and metal-organic framework membranes for molecular separations, Coord. Chem. Rev. 437 (2021) 213794, https://doi.org/10.1016/j.ccr.2021.213794.
[206] Y. Wang, Nondestructive creation of ordered nanopores by selective swelling of block copolymers: toward homoporous membranes, Acc. Chem. Res. 49 (7) (2016) 1401–1408, https://doi.org/10.1021/acs.accounts.6b00233.
[207] N.M. Chola, P.P. Bavdane, R.K. Nagarale, "SPEEK-COF" composite cation exchange membrane for Zn-I2 redox flow battery, J. Electrochem. Soc. 169 (10) (2022) 100542, https://doi.org/10.1149/1945-7111/ac99a3.
[208] X. Zhou, T. Zhao, L. An, L. Wei, C. Zhang, The use of polybenzimidazole membranes in vanadium redox flow batteries leading to increased coulombic efficiency and cycling performance, Electrochim. Acta 153 (2015) 492–498, https://doi.org/10.1016/j.electacta.2014.11.185.
[209] X. Che, H. Zhao, X. Ren, D. Zhang, H. Wei, J. Liu, X. Zhang, J. Yang, Porous polybenzimidazole membranes with high ion selectivity for the vanadium redox flow battery, J. Membr. Sci. 611 (2020) 118359, https://doi.org/10.1016/j.memsci.2020.118359.
[210] Y. Wan, J. Sun, H. Jiang, X. Fan, T. Zhao, A highly-efficient composite polybenzimidazole membrane for vanadium redox flow battery, J. Power Sources 489 (2021) 229502, https://doi.org/10.1016/j.jpowsour.2021.229502.
[211] Y. Wan, J. Sun, Q. Jian, X. Fan, T. Zhao, A detachable sandwiched polybenzimidazole-based membrane for high-performance aqueous redox flow batteries, J. Power Sources 526 (2022) 231139, https://doi.org/10.1016/j.jpowsour.2022.231139.
[212] Z. Li, W. Dai, L. Yu, L. Liu, J. Xi, X. Qiu, L. Chen, Properties investigation of sulfonated poly (ether ether ketone)/polyacrylonitrile acid–base blend membrane for vanadium redox flow battery application, ACS Appl. Mater. Interfaces 6 (21) (2014) 18885–18893, https://doi.org/10.1021/am5047125.
[213] J. Xi, Z. Li, L. Yu, B. Yin, L. Wang, L. Liu, X. Qiu, L. Chen, Effect of degree of sulfonation and casting solvent on sulfonated poly (ether ether ketone) membrane for vanadium redox flow battery, J. Power Sources 285 (2015) 195–204, https://doi.org/10.1016/j.jpowsour.2015.03.104.
[214] S. Liu, L. Wang, B. Zhang, B. Liu, J. Wang, Y. Song, Novel sulfonated polyimide/polyvinyl alcohol blend membranes for vanadium redox flow battery applications, J. Mater. Chem. A3 (5) (2015) 2072–2081, https://doi.org/10.1039/C4TA05504G.
[215] D. Chen, S. Wang, M. Xiao, Y. Meng, Synthesis and characterization of novel sulfonated poly (arylene thioether) ionomers for vanadium redox flow battery applications, Energy Environ. Sci. 3 (5) (2010) 622–628, https://doi.org/10.1039/B917117G.
[216] C. Luan, D. Zhang, Z. Liu, X. Zhang, Y. Zhang, Z. Yu, Y. Zhang, W. Xu, J. Liu, C. Yan, Advanced hybrid polybenzimidazole membrane enabled by a "linker" of metal-organic framework for high-performance vanadium flow battery, Chem. Eng. J. 461 (2023) 142032, https://doi.org/10.1016/j.cej.2023.142032.
[217] D. Liang, S. Wang, W. Ma, D. Wang, G. Liu, F. Liu, Y. Cui, X. Wang, Z. Yong, Z. Wang, A low vanadium permeability sulfonated polybenzimidazole membrane with a metal-organic framework for vanadium redox flow batteries, Electrochim. Acta 405 (2022) 139795, https://doi.org/10.1016/j.electacta.2021.139795.
[218] S. Zhai, Z. Lu, Y. Ai, X. Liu, Q. Wang, J. Lin, S. He, M. Tian, L. Chen, Highly selective proton exchange membranes for vanadium redox flow batteries enabled by the incorporation of water-insoluble phosphotungstic acid-metal organic framework nanohybrids, J. Membr. Sci. 645 (2022) 120214, https://doi.org/10.1016/j.memsci.2021.120214.
[219] Y. Lu, S. Lin, H. Cao, Y. Xia, Y. Xia, L. Xin, K. Qu, D. Zhang, Y. Yu, K. Huang, Efficient proton-selective hybrid membrane embedded with polydopamine modified MOF-808 for vanadium flow battery, J. Membr. Sci. 671 (2023) 121347, https://doi.org/10.1016/j.memsci.2023.121347.
[220] L. Xin, D. Zhang, K. Qu, Y. Lu, Y. Wang, K. Huang, Z. Wang, W. Jin, Z. Xu, Zr-MOF-enabled controllable ion sieving and proton conductivity in flow battery membrane, Adv. Funct. Mater. 31 (42) (2021) 2104629, https://doi.org/10.1002/adfm.202104629.
[221] H. Cao, Y. Xia, Y. Lu, Y. Wu, Y. Xia, X. Hou, Y. Wang, G. Liu, K. Huang, Z. Xu, MOF-801 polycrystalline membrane with sub-10 nm polymeric assembly layer for ion sieving and flow battery storage, AIChE J 68 (6) (2022) e17657, https://doi.org/10.1002/aic.17657.
[222] S. Zhai, X. Jia, Z. Lu, Y. Ai, X. Liu, J. Lin, S. He, Q. Wang, L. Chen, Highly ion selective composite proton exchange membranes for vanadium redox flow batteries by the incorporation of UiO-66-NH2 threaded with ion conducting polymers, J. Membr. Sci. 662 (2022) 121003, https://doi.org/10.1016/j.memsci.2022.121003.
[223] L. Xiao, Y. Xia, Y. Yu, H. Cao, Y. Lu, D. Zhang, K. Huang, Z. Xu, Usability of unstable metal organic framework enabled by carbonization within flow battery membrane under harsh environment, J. Membr. Sci. 671 (2023) 121349, https://doi.org/10.1016/j.memsci.2023.121349.
[224] D. Zhang, L. Xin, Y. Xia, L. Dai, K. Qu, K. Huang, Y. Fan, Z. Xu, Advanced Nafion hybrid membranes with fast proton transport channels toward high-performance vanadium redox flow battery, J. Membr. Sci. 624 (2021) 119047, https://doi.org/10.1016/j.memsci.2020.119047.
[225] X.B. Yang, L. Zhao, K. Goh, X.L. Sui, L.H. Meng, Z.B. Wang, Ultra-high ion selectivity of a modified nafion composite membrane for vanadium redox flow battery by incorporation of phosphotungstic acid coupled UiO-66-NH2, ChemistrySelect 4 (15) (2019) 4633–4641, https://doi.org/10.1002/slct.201900888.
[226] Q. Gao, L. Zhang, H. Zhang, D. Zhang, W., Xiao, Preparation and performance of UIO-66-NH2 enhanced proton exchange membranes for vanadium redox flow batteries, J. Solid State Electrochem. (2024) 1–11, https://doi.org/10.1007/s10008-024-05923-5.
[227] H.J. Choi, C. Youn, S.C. Kim, D. Jeong, S.N. Lim, D.R. Chang, J.W. Bae, J. Park, Nafion/functionalized metal–organic framework composite membrane for vanadium redox flow battery, Microporous Mesoporous Mater. 341 (2022) 112054, https://doi.org/10.1016/j.micromeso.2022.112054.
[228] P. Sharma, R. Goswami, S. Neogi, V.K. Shahi, Devising ultra-robust mixed-matrix membrane separators using functionalized MOF–poly (phenylene oxide) for high-performance vanadium redox flow batteries, J. Mater. Chem. A10 (20) (2022) 11150–11162, https://doi.org/10.1039/D1TA10715A.
[229] S. Peng, L. Zhang, C. Zhang, Y. Ding, X. Guo, G. He, G. Yu, Gradient-distributed metal–organic framework–based porous membranes for nonaqueous redox flow batteries, Adv. Energy Mater. 8 (33) (2018) 1802533, https://doi.org/10.1002/aenm.201802533.
[230] J. Yuan, C. Zhang, T. Liu, Y. Zhen, Z.-Z. Pan, Y. Li, Two-dimensional metal-organic framework nanosheets-modified porous separator for non-aqueous redox flow batteries, J. Membr. Sci. 612 (2020) 118463, https://doi.org/10.1016/j.memsci.2020.118463.
[231] J. Yuan, C. Zhang, Q. Qiu, Z.-Z. Pan, L. Fan, Y. Zhao, Y. Li, Highly selective metal-organic framework-based (MOF-5) separator for non-aqueous redox flow battery, Chem. Eng. J. 433 (2022) 133564, https://doi.org/10.1016/j.cej.2021.133564.
[232] Z. Yuan, Y. Duan, H. Zhang, X. Li, H. Zhang, I. Vankelecom, Advanced porous membranes with ultra-high selectivity and stability for vanadium flow batteries, Energy Environ. Sci. 9 (2) (2016) 441–447, https://doi.org/10.1039/C5EE02896E.
[233] Y. Chen, P. Xiong, S. Xiao, Y. Zhu, S. Peng, G. He, Ion conductive mechanisms and redox flow battery applications of polybenzimidazole-based membranes, Energy Storage Mater. 45 (2022) 595–617, https://doi.org/10.1016/j.ensm.2021.12.012.
[234] M. Sadeghi, M.A. Semsarzadeh, H. Moadel, Enhancement of the gas separation properties of polybenzimidazole (PBI) membrane by incorporation of silica nano particles, J. Membr. Sci. 331 (1–2) (2009) 21–30, https://doi.org/10.1016/j.memsci.2008.12.073.
[235] Y.-N. Chang, J.-Y. Lai, Y.-L. Liu, Polybenzimidazole (PBI)-functionalized silica nanoparticles modified PBI nanocomposite membranes for proton exchange membranes fuel cells, J. Membr. Sci. 403 (2012) 1–7, https://doi.org/10.1016/j.memsci.2012.01.043.
[236] Y.-L. Liu, Preparation and properties of nanocomposite membranes of polybenzimidazole/sulfonated silica nanoparticles for proton exchange membranes, J. Membr. Sci. 332 (1–2) (2009) 121–128, https://doi.org/10.1016/j.memsci.2009.01.045.
[237] G. Nawn, G. Pace, S. Lavina, K. Vezzù, E. Negro, F. Bertasi, S. Polizzi, V. Di Noto, Nanocomposite membranes based on polybenzimidazole and ZrO2 for high-temperature proton exchange membrane fuel cells, ChemSusChem 8 (8) (2015) 1381–1393, https://doi.org/10.1002/cssc.201403049.
[238] L. Hu, Y. Du, L. Gao, M. Di, N. Zhang, Y. Pan, X. Yan, B. An, G. He, Nanoscale solid superacid-coupled polybenzimidazole membrane with high ion selectivity for flow batteries, ACS Sustain. Chem. Eng. 8 (44) (2020) 16493–16502, https://doi.org/10.1021/acssuschemeng.0c05359.
[239] N. Üregen, K. Pehlivanoğlu, Y. Özdemir, Y. Devrim, Development of polybenzimidazole/graphene oxide composite membranes for high temperature PEM fuel cells, Int. J. Hydrog. Energy 42 (4) (2017) 2636–2647, https://doi.org/10.1016/j.ijhydene.2016.07.009.
[240] P. Zhang, W. Li, L. Wang, C. Gong, J. Ding, C. Huang, X. Zhang, S. Zhang, L. Wang, W. Bu, Polydopamine-modified sulfonated polyhedral oligomeric silsesquioxane: an appealing nanofiller to address the trade-off between conductivity and stabilities for proton exchange membrane, J. Membr. Sci. 596 (2020) 117734, https://doi.org/10.1016/j.memsci.2019.117734.
[241] M. Di, L. Hu, L. Gao, X. Yan, W. Zheng, Y. Dai, X. Jiang, X. Wu, G. He, Covalent organic framework (COF) constructed proton permselective membranes for acid supporting redox flow batteries, Chem. Eng. J. 399 (2020) 125833, https://doi.org/10.1016/j.cej.2020.125833.
[242] M. Di, X. Sun, L. Hu, L. Gao, J. Liu, X. Yan, X. Wu, X. Jiang, G. He, Hollow COF selective layer based flexible composite membranes constructed by an integrated "casting-precipitation-evaporation" strategy, Adv. Funct. Mater. 32 (22) (2022) 2111594, https://doi.org/10.1002/adfm.202111594.
[243] J. Wang, W. Xu, F. Xu, L. Dai, Y. Wu, Y. Wang, S. Li, Z. Xu, A polybenzimidazole-covalent organic framework hybrid membrane with highly efficient proton-selective transport channels for vanadium redox flow battery, J. Membr. Sci. 695 (2024) 122470, https://doi.org/10.1016/j.memsci.2024.122470.
[244] G. Xie, F. Cui, H. Zhao, Z. Fan, S. Liu, B. Pang, X. Yan, R. Du, C. Liu, G. He, Free-standing COF nanofiber in ion conductive membrane to improve efficiency of vanadium redox flow battery, J. Membr. Sci. 708 (2024) 123052, https://doi.org/10.1016/j.memsci.2024.123052.
[245] A. Li, G. Wang, X. Wei, F. Li, M. Zhang, J. Zhang, J. Chen, R. Wang, Highly selective sulfonated poly (ether ether ketone)/polyvinylpyrrolidone hybrid membranes for vanadium redox flow batteries, J. Mater. Sci. 55 (2020) 16822–16835, https://doi.org/10.1007/s10853-020-05228-8.
[246] J. Li, Y. Zhang, S. Zhang, X. Huang, Sulfonated polyimide/s-MoS2 composite membrane with high proton selectivity and good stability for vanadium redox flow battery, J. Membr. Sci. 490 (2015) 179–189, https://doi.org/10.1016/j.memsci.2015.04.053.

[247] G. Palanisamy, T.H. Oh, TiO2 containing hybrid composite polymer membranes for vanadium redox flow batteries, Polymers 14 (8) (2022) 1617, https://doi.org/10.3390/polym14081617.
[248] J. Li, F. Xu, Y. Chen, Y. Han, B. Lin, Sulfonated poly (ether ether ketone)/sulfonated covalent organic framework composite membranes with enhanced performance for application in vanadium redox flow batteries, ACS Appl. Energy Mater. 5 (12) (2022) 15856–15863, https://doi.org/10.1021/acsaem.2c03397.
[249] X. Zhao, P. Pachfule, A. Thomas, Covalent organic frameworks (COFs) for electrochemical applications, Chem. Soc. Rev. 50 (2021) 6871–6913, https://doi.org/10.1039/D0CS01569E.
[250] Y. Wu, Y. Wang, D. Zhang, F. Xu, L. Dai, K. Qu, H. Cao, Y. Xia, S. Li, K. Huang, Z. Xu, Crystallizing self-standing covalent organic framework membranes for ultrafast proton transport in flow batteries, e202313571, Angew. Chem. Int. Ed. 62 (2023), https://doi.org/10.1002/ange.202313571.
[251] W. Xu, Y. Wang, Y. Wu, F. Xu, L. Dai, K. Qu, J. Wang, J. Wu, L. Lei, S. Li, Sub-2-nm channels within covalent triazine framework enable fast proton-selective transport in flow battery membrane, Adv. Funct. Mater. 33 (21) (2023) 2300138, https://doi.org/10.1002/adfm.202300138.
[252] Y. Afzal, S. Ren, H. Wang, S. Ma, Q. Yuan, M.B. Zhao, X. Wadud, Q. Liang, G. Pan, Z. He, Jiang, Highly proton-conductive and stable sulfonated covalent organic framework hybrid membrane for vanadium redox flow battery, J. Membr. Sci. 722 (2025) 123863, https://doi.org/10.1016/j.memsci.2025.123863.
[253] W. Xu, J. Xu, Z. Yi, J. Ding, S. Li, Y. Wang, Z. Xu, Zwitterionic channels within covalent organic frameworks facilitate proton-selective transport for flow battery membrane, Chem. Eng. Sci. 299 (2024) 120468, https://doi.org/10.1016/j.ces.2024.120468.
[254] H. Liu, M. Liu, Y. Zhang, H. Sun, C. Ding, P. Qian, Y. Zhang, Ultrahigh ion selectivity composite membrane contained cationic covalent organic nanosheets for vanadium redox flow battery, J. Membr. Sci. 713 (2025) 123314, https://doi.org/10.1016/j.memsci.2024.123314.
[255] Y. Zhang, H. Liu, M. Liu, X. Li, Y. Zhang, H. Sun, H. Shi, Y. Feng, Enhanced selectivity of SPEEK membrane incorporated covalent organic nanosheet crosslinked graphene oxide for vanadium redox flow battery, J. Membr. Sci. 714 (2025) 123410, https://doi.org/10.1016/j.memsci.2024.123410.
[256] B. Liu, Y. Jiang, H. Wang, J. Ge, H. Shi, Sulfonated poly (ether ether ketone) hybrid membranes with amphoteric graphene oxide nanosheets as interfacial reinforcement for vanadium redox flow battery, Energy Fuels 34 (2) (2020) 2452–2461, https://doi.org/10.1021/acs.energyfuels.9b03924.
[257] Y. Zhang, H. Wang, P. Qian, Y. Zhou, J. Shi, H. Shi, Sulfonated poly (ether ether ketone)/amine-functionalized graphene oxide hybrid membrane with various chain lengths for vanadium redox flow battery: a comparative study, J. Membr. Sci. 610 (2020) 118232, https://doi.org/10.1016/j.memsci.2020.118232.
[258] Y. Zhang, H. Wang, B. Liu, J. Shi, J. Zhang, H. Shi, An ultra-high ion selective hybrid proton exchange membrane incorporated with zwitterion-decorated graphene oxide for vanadium redox flow batteries, J. Mater. Chem. A7 (20) (2019) 12669–12680, https://doi.org/10.1039/C9TA01891C.
[259] J. Sheng, L. Li, H. Wang, L. Zhang, S. Jiang, H. Shi, An ultrahigh conductivity and efficiency of SPEEK-based hybrid proton exchange membrane containing amphoteric GO-VIPS nanofillers for vanadium flow battery, J. Membr. Sci. 669 (2023) 121326, https://doi.org/10.1016/j.memsci.2022.121326.
[260] X. Meng, Q. Peng, L. Peng, Y. Wang, X. Zhang, T. Wu, C. Cong, H. Ye, Q. Zhou, In situ growth of covalent organic framework on graphene oxide nanosheet enable proton-selective transport in flow battery membrane, J. Power Sources 609 (2024) 234690, https://doi.org/10.1016/j.jpowsour.2024.234690.
[261] J. Sun, D. Shi, H. Zhong, X. Li, H. Zhang, Investigations on the self-discharge process in vanadium flow battery, J. Power Sources 294 (2015) 562–568, https://doi.org/10.1016/j.jpowsour.2015.06.123.
[262] S. Jeong, L.-H. Kim, Y. Kwon, S. Kim, Effect of nafion membrane thickness on performance of vanadium redox flow battery, Korean J. Chem. Eng. 31 (2014) 2081–2087, https://doi.org/10.1007/s11814-014-0157-5.
[263] L. Cao, H. Wu, Y. Cao, C. Fan, R. Zhao, X. He, P. Yang, B. Shi, X. You, Z. Jiang, Weakly humidity-dependent proton-conducting COF membranes, Adv. Mater. 32 (52) (2020) 2005565, https://doi.org/10.1002/adma.202005565.
[264] Y. Peng, G. Xu, Z. Hu, Y. Cheng, C. Chi, D. Yuan, H. Cheng, D. Zhao, Mechanoassisted synthesis of sulfonated covalent organic frameworks with high intrinsic proton conductivity, ACS Appl. Mater. Interfaces 8 (28) (2016) 18505–18512, https://doi.org/10.1021/acsami.6b06189.
[265] S. Chandra, T. Kundu, K. Dey, M. Addicoat, T. Heine, R. Banerjee, Interplaying intrinsic and extrinsic proton conductivities in covalent organic frameworks, Chem. Mater. 28 (5) (2016) 1489–1494, https://doi.org/10.1021/acs.chemmater.5b04947.
[266] Y. Peng, Z. Hu, Y. Gao, D. Yuan, Z. Kang, Y. Qian, N. Yan, D. Zhao, Synthesis of a sulfonated two-dimensional covalent organic framework as an efficient solid acid catalyst for biobased chemical conversion, ChemSusChem 8 (19) (2015) 3208–3212, https://doi.org/10.1002/cssc.201500755.
[267] B. Pang, R. Du, W. Chen, F. Cui, N. Wang, H. Zhao, G. Xie, L. Tiantian, G. He, X. Wu, Self-supporting sulfonated covalent organic framework as a highly selective continuous membrane for vanadium flow battery, Energy Storage Mater. 67 (2024) 103293, https://doi.org/10.1016/j.ensm.2024.103293.
[268] M.L. Liu, Y. Chen, C. Hu, C.X. Zhang, Z.J. Fu, Z. Xu, Y.M. Lee, S.P. Sun, Microporous membrane with ionized sub-nanochannels enabling highly selective monovalent and divalent anion separation, Nat. Commun. 15 (2024) 7271, https://doi.org/10.1038/s41467-024-51540-1.
[269] Y. Chen, S. Li, X. Pei, J. Zhou, X. Feng, S. Zhang, Y. Cheng, H. Li, R. Han, B. Wang, A solvent-free hot-pressing method for preparing metal–organic-framework coatings, Angew. Chem. Int. Ed.55(10) (2016) 3419–3423, https://doi.org/10.1002/anie.201511063.